FutureWater

TA-9144 NEP

Climate Risk Adaptation Assessment for Dudhkoshi HEP, Nepal

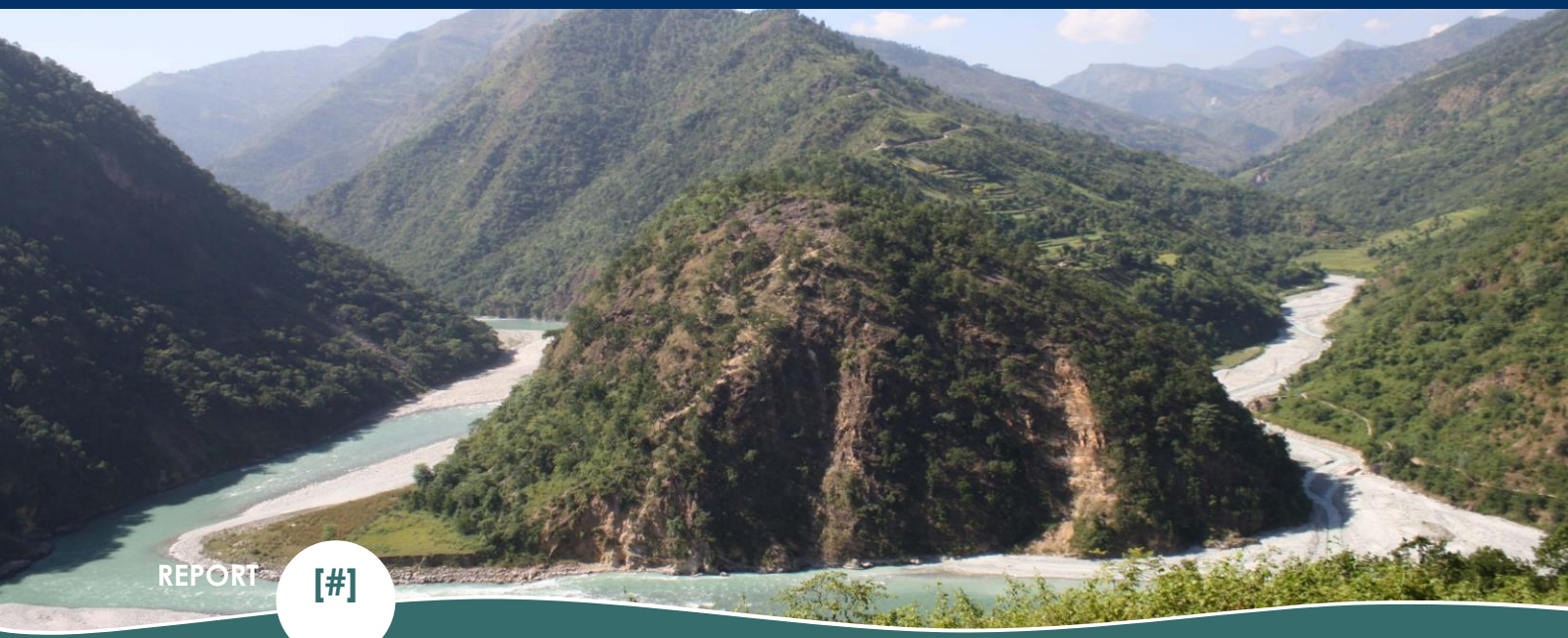

REPORT [#]

CLIENT **Asian Development Bank**

AUTHORS **Sonu Khanal**

DATE **July 2021**

Climate Risk Adaptation Assessment for Dudhkoshi HEP, Nepal

TA-9144 NEP

FutureWater Report [#]

Client
Asian Development Bank

Authors
Sonu khanal – Hydrologist and Climate Change Expert (s.khanal@futurewater.nl)

Date
22 July 2021

Executive Summary

This Climate Risk Assessment (CRA) evaluates the greenhouse gas (GHG) emissions, potential climate sensitivities and risks of the Dudhkoshi Storage Hydroelectric Project (DKSHEP) and identifies climate adaptation activities. The report presents an assessment of historic trends in relevant climate-related variables and analyses future climate projections for the project. Based on these projections, an assessment is presented of the **climate risks**, considering **current vulnerabilities** and projections in the related climate variables. Risks are classified and **climate adaptation** activities are proposed for the project.

The trend analysis was performed based on historic climate data from a state-of-the-art global reanalysis dataset, which is a dataset that blends ground-based observations, satellite-based observations and modelled data (**ERA5**). Trends were analyzed for the project areas specifically the region upstream of the main dam and the project region till the main powerhouse. The future climate change analysis was done based on the **NASA-NEX** ensemble of downscaled General Circulation Models (GCMs). The consideration based on the full ensemble for a medium stabilization scenario (**RCP4.5**) and a business-as-usual scenario (**RCP8.5**) allows for the inclusion of the uncertainty in future climate in the assessment. The carbon emission and climate model analysis yields the following conclusions for the project area:

- The DKSHEP will **reduce 923,264 tCO2 every year** compared to the baseline condition.
- The **annual daily maximum temperature is expected to increase** on average by about 1.2 and 1.3 degrees under the RCP 4.5 scenario for T1 (2015–2045) and T2 (2065–2095) time horizon and 2.4 and 3.9 degrees under the RCP 8.5 scenario for the T1 and T2 time horizon.
- Extremes related to temperatures (e.g. **warm spells, extremely warm days**) are **likely to increase in frequency and intensity**.
- On average the **precipitation is expected to increase** by 9.1 and 9.3% for the T1 and T2 time horizon under the RCP4.5 scenario; 22.8 and 37.4% for the T1 and T2 time horizon under the RCP8.5 scenario.
- The GCMs show **a large range of uncertainty for seasonal changes** under both RCP 4.5 and RCP 8.5.
- Precipitation extremes are likely to increase in frequency and intensity. **Maximum 1-day precipitation is expected to increase** by about 9% for both the T1 and T2 time horizon under the RCP4.5 scenario; 20 and 31% for the T1 and T2 time horizon under the RCP8.5 scenario.
- There is no significant change in the number of consecutive dry days per year. However, the model **uncertainty increases** over the end of the century time horizon.

Considering the type of climate hazards and risks in the project area, and the area-specific climate change projections, overall, the most serious threat comes from the expected increase in precipitation and temperature extremes. Due to the increase in magnitude and frequency of precipitation, it is very likely that **erosion** and **landslide** activity will increase in the future. In addition, while the hazard exposure is constricted to upstream parts of the project area, the expected increase in **extreme precipitation events may cascade** and lead to **more frequent and powerful flooding** events over the larger regions. **Seismic activity** and warming-induced **GLOF** events in the upstream part of DKSHEP may have a significant impact on the project infrastructure. Higher **extreme discharges** may also lead to **more frequent landslides** and **more powerful mudflows**, posing a serious risk of **damaging reservoir** and **transmission towers** which may lead to power outages.

Heat related stresses may put significant strain on the electricity system, leading to system faults, reduced power supply and power outages.

For adaptation and climate proofing the main recommendation is to use a **full ensemble of future projections** rather than three as currently used in the detailed design report. Including more GCM outputs in the analysis will help to **quantify the uncertainty and the upper bound** of the probable maximum flood. This is highly relevant to the DKSHEP as there are many instances in the Himalayan region, such as the **Melamchi flood** in June 2021, the **Chamoli flood** in February 2021, the **Kedarnath flood** in June 2013, and the **Bhotekoshi flood** in June 2016, which resulted in significant damage to the critical water resources infrastructures, especially hydropower, and the livelihood of the communities downstream. The second high-priority recommendation is to **increase the flood passage capacity through the reservoir**. The extreme events in the recent past have increased significantly and it's highly likely that more extremes are on the way. The third recommendation is to **increase the sediment flushing capacity of the reservoir**. The project region is highly vulnerable to seismic, GLOF and landslide activity. All of these catastrophic events are associated with the transport of large amounts and sediments. Sediment concentration under the normal dry and wet conditions will not be representative of extreme conditions. A number of catastrophic and cascading GLOF and landslide events in a single monsoon season may fill the water storage capacity of the reservoir so it is highly recommended to increase the sediment flushing capacity to cope with unprecedented situations. The final recommendation is to **implement bioengineering techniques, nature-based solutions and an early warning system** for the mitigation of flood and landslide-related hazards in the project region.

The downscaled climate models used in this study have a spatial resolution of about 25 km, whereas climate change signals may vary strongly over short distances and particularly in mountainous terrain. There is often also a large spread in the climate model projections. Therefore, the full ensemble of models has been analyzed and the uncertainty range is displayed in all figures in this report.

Content

Tables

Figures

1 Introduction

1.1 Background

Nepal is the world's second richest country in inland water resources with as many as 6000 rivers rivulets, and tributaries (**Figure 1**), and possesses about 2.27% of the world's freshwater resources (CBS, 2005). The total run-off per year from Nepal, including run-off from the Tibetan catchment, is estimated to be about 225 billion cubic meters (WECS, 2011). Within relatively short lateral extension topographic elevation varies from 60masl to 8848 masl, providing a steep topographic gradient for potential hydropower generation (**Figure 2**). Nepal's gross hydropower potential is estimated to be about 72,500 MW, 32,700 MW of which is techno-economically possible (WECS, 2019). Nepal can harness its abundance of water to meet not just its own electricity needs, but also serve energy-hungry neighbors like Bangladesh and India. However, the actual electricity generation from hydropower in Nepal is currently 1260 MW from 109 major hydropower plants and a number of small and micro hydropower plants (DOED, 2021). The total available energy in the system is 7,741 GWH of which 2,991 GWh power is purchased from Independent Power Producers (IPPs) within Nepal (NEA, 2020b). Out of the total available energy, Nepal Electricity Authority (NEA) generation contributed 39.02%, whereas those imported from India and domestic IPPs accounted for 22.33% and 38.64% respectively (NEA, 2020b).

The Koshi basin alone constitutes 39% (27,800 MW) of the total gross hydropower potential of Nepal (WECS, 2019). The Dudhkoshi subbasin alone has the potential to generate 3,657 MW (**Figure 3** and **Table 1**). ADB is supporting NEA for the updated feasibility and detailed design of the Dudhkoshi Storage Hydroelectric Project (DKSHEP). The installed capacity of the DKSHEP project is 635 MW and is proposed to be built in the Dudhkoshi River originating from Solukhumbu district and bordering Khotang and Okhaldhunga districts in Province no. 1 of Nepal. ELC Electroconsult S.p.A. (Italy) in association with NEWJEC Inc. (Japan) has submitted the detailed feasibility, investigations, environmental and social impact study, and engineering design to NEA and ADB.

ADB experts identified the need for a detailed Climate Risk and Adaptation (CRA) assessment for the DKSHEP to understand the risk posed by the changing climate on hydropower and the environment. Therefore, the objective of this Climate Risk and Adaptation Assessment (CRA) is to assess the vulnerability of the project components to future climate change and recommend adaptation options for climate-proofing the design. Therefore, this CRA covers both type 2 adaptation, related to system change and resilience building, as well as type 1 adaptation related to climate-proofing (Watkiss et al., 2020).

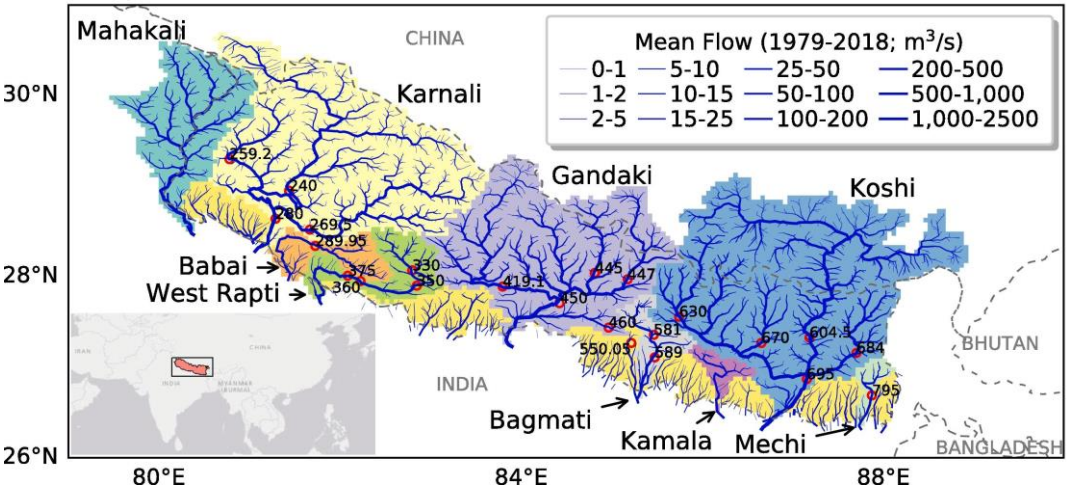

Figure 1. The river basins of Nepal and the location of the basins are indicated in the lower left corner. The background color coding indicates the spatial extent of the basins. Blue lines with varying widths show the spatial distribution of the long-term mean (1979–2018) river discharge at ~ 5 km grids. Red circles mark the location of hydrological gauging stations; the numbers indicate the station IDs used in the database of the Department of Hydrology and Meteorology (DHM), Nepal. (Source: Shin, Pokhrel, Talchabhadel, & Panthi, (2021))[1]

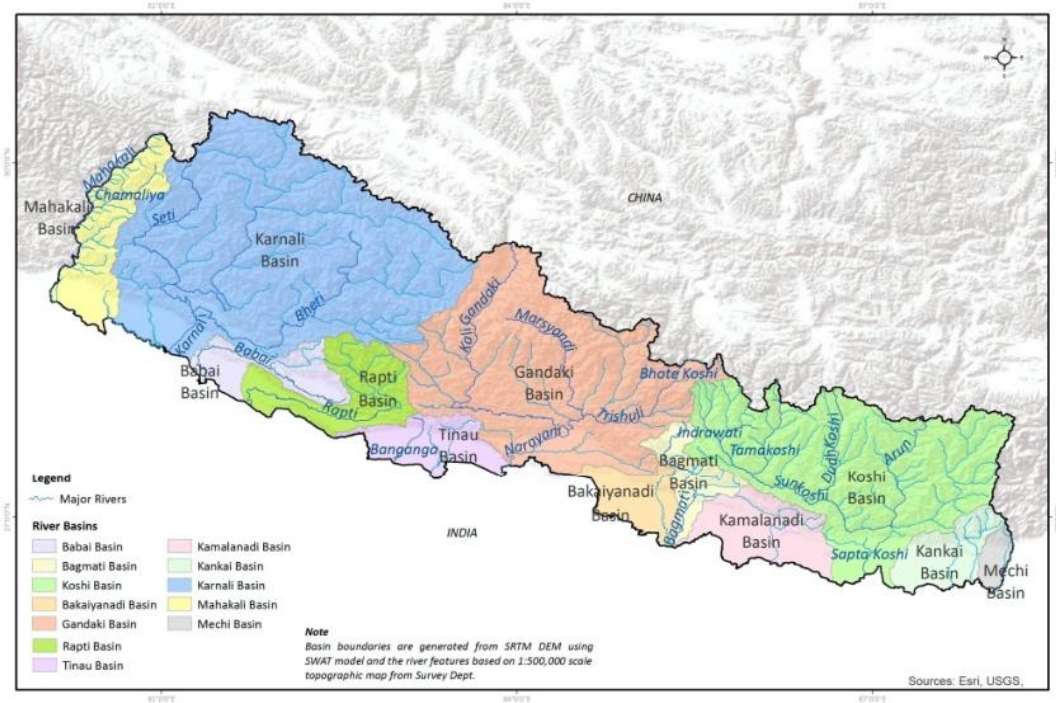

Figure 2. Major rivers and basins in Nepal (Source: WECS, (2019)).

[1] The designations employed on the map presented do not imply the expression of any opinion whatsoever on the part of FutureWater concerning the legal status of any country, territory, city or area or of its authorities, or concerning the delimitation of its frontiers or boundaries. The maps used in this report are derived from published reports and journal articles and are properly referenced.

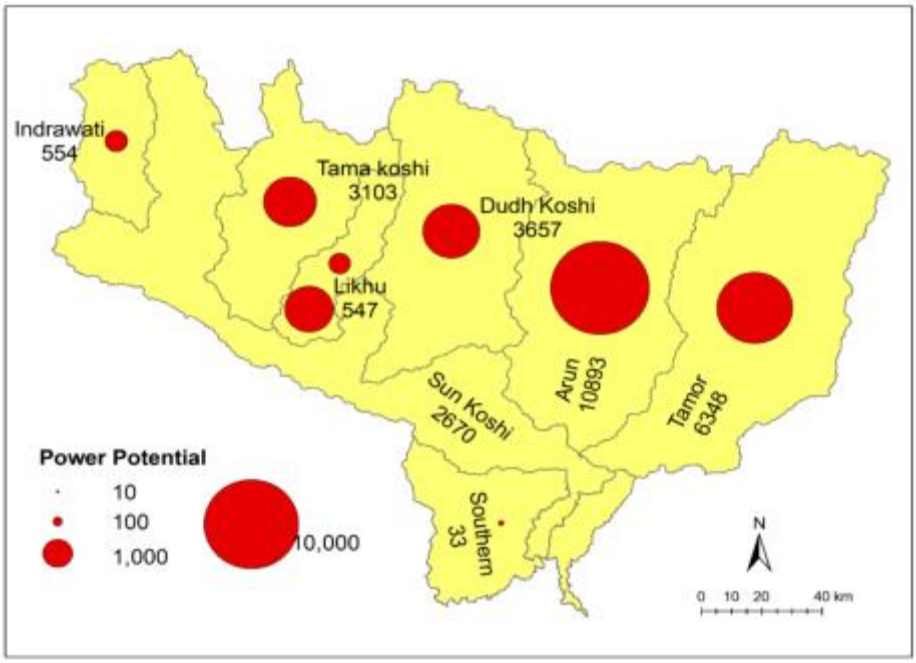

Figure 3. The gross hydropower potential of different tributaries of the Koshi River basin (Source: WECS, (2019)).

Table 1. Gross Hydropower Potential of major tributaries in the Koshi Basin (Source: WECS, (2019)).

SN	Tributary Basin	Power Potential (MW)	% of Basin Potential
1	Indrawati	554	1.99
2	Likhu	547	1.97
3	Arun	10,893	39.18
4	Dudhkoshi	3,657	13.15
5	Sunkoshi	2,670	9.60
6	Tamakoshi	3,103	11.16
7	Tamor	6,348	22.83
8	Southern	33	0.12
	Total	**27805**	**100**

1.2 Project description

DKSHEP is a storage type of hydropower project which addresses the prevailing power and energy deficit during the dry season in Nepal (NEA, 2020). The project is proposed to be built in the Dudhkoshi River which flows through province 1 of Nepal. The base cost of the Project at present-day price levels is estimated to be 1,531 MUSD. The net present value is estimated to be about 280 million USD with 9.6% internal rate of return. The proposed dam is located close to 'Rabuwa' village on the left bank of the Dudhkoshi River. The total installed capacity of 635 MW comprising a powerhouse with an installed capacity of 600 MW located near Sunkoshi river with a 13.3 km long headrace tunnel and a surface powerhouse of capacity 35 MW located in the right abutment at dam toe to generate energy from the downstream release of the environmental flow is envisaged in the project (**Figure 5)**. A 220 m high concrete face rockfill dam with a 630m long crest at elevation 648m asl located on the Dudhkoshi River in a gorge nearly one km downstream of the confluence between the Dudhkoshi River and Thotne Khola. An underground powerhouse with an installed capacity of 600 MW located near Sunkoshi river

with a 13.3 km long headrace tunnel and a surface powerhouse with an installed capacity of 35 MW located in the right abutment immediately downstream of the dam site to generate energy from the downstream release of the environmental flow is proposed. A combined spillway (gated and labyrinth overflow) is proposed on the left abutment of the dam. An emergency spillway (fuse gates) at the left side of the main spillway approach canal has been proposed to ensure the safety of the dam in the worst case when all radial gates are out of operation. The total storage capacity of the reservoir is 1,581 Mm^3 out of which the live storage capacity is 1,342 Mm^3 and the dam body volume is about 26.7 million m^3.

The annual energy production will be 3,443 GWh per year, with an average energy production of 1,358 GWh in the dry season and 2,084 GWh in the wet season. The power generated from the project is planned to be transmitted by a double circuit 400 KV transmission line connecting to Dhalekbar. Compared to similar projects, DKSHEP will produce more energy in terms of cost and installed capacity with minimal social impact. The project is proposed to be implemented and fully commissioned in 7 years period. The financial arrangement and land acquisition of the project are planned to be completed by 2023. The construction of the project is expected to commence at the start of 2024 and be complete by the end of 2030. However, due to COVID, some delays are foreseen in these activities.

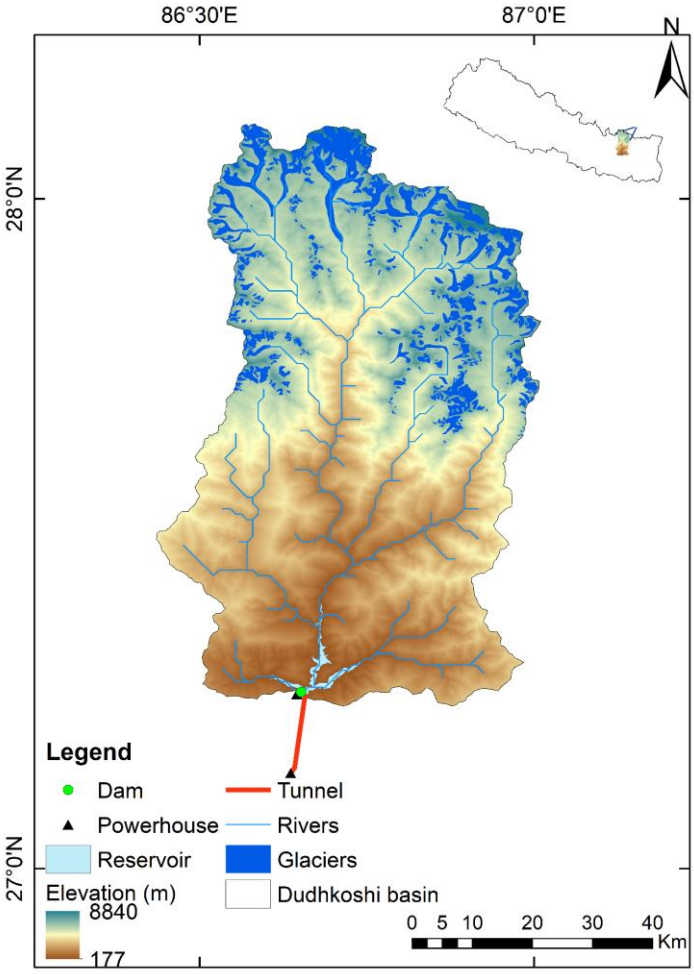

Figure 4. Dudhkoshi basin boundary (delineated at the dam location) and other components of DKSHEP. Randolph glacier inventory v6 is used for the glacier extent (RGI Consortium, 2017). The Hydroshed river network (30 arc seconds) is used for the river network (Lehner & Grill, 2013).

1.3 Scope of work

This climate risk and adaptation assessment (CRA) assesses historic trends in relevant climate-related variables and analyses climate projections for the DKSHEP (**Figure 4**). Based on these projections, an assessment is presented of the current and future climate risks and vulnerabilities relating to the proposed project activities and recommendations will be presented for climate adaptation measures.

1.3.1 Objectives of the assignment

Nepal's power sector predominantly relies on hydropower generation. Hydropower is vulnerable to climate change and natural disasters caused by climate change. An understanding of the future impact of climate change on hydropower assets and their performance is important for the successful implementation of hydropower projects. A CRA is required for DKSHEP to ensure the project addresses climate change mitigation and adaptation in accordance with ADB's requirements. Based on an initial climate risk screening assessment of the project, the project is likely to be affected by future changes in climate conditions and their impacts including temperature increase, precipitation increase, flood, glacial lake outburst flood (GLOF), and landslide risk. This CRA will provide a detailed and focused risk and vulnerability assessment that will identify and, to the extent possible quantify risks to the project from climate change and variability and provide corresponding adaptation measures. Additionally, this CRA will also quantify the carbon footprint of the project. Outputs of this CRA will be used to finalize the detailed design, ensuring that the proposed investment is climate-proofed to the extent feasible.

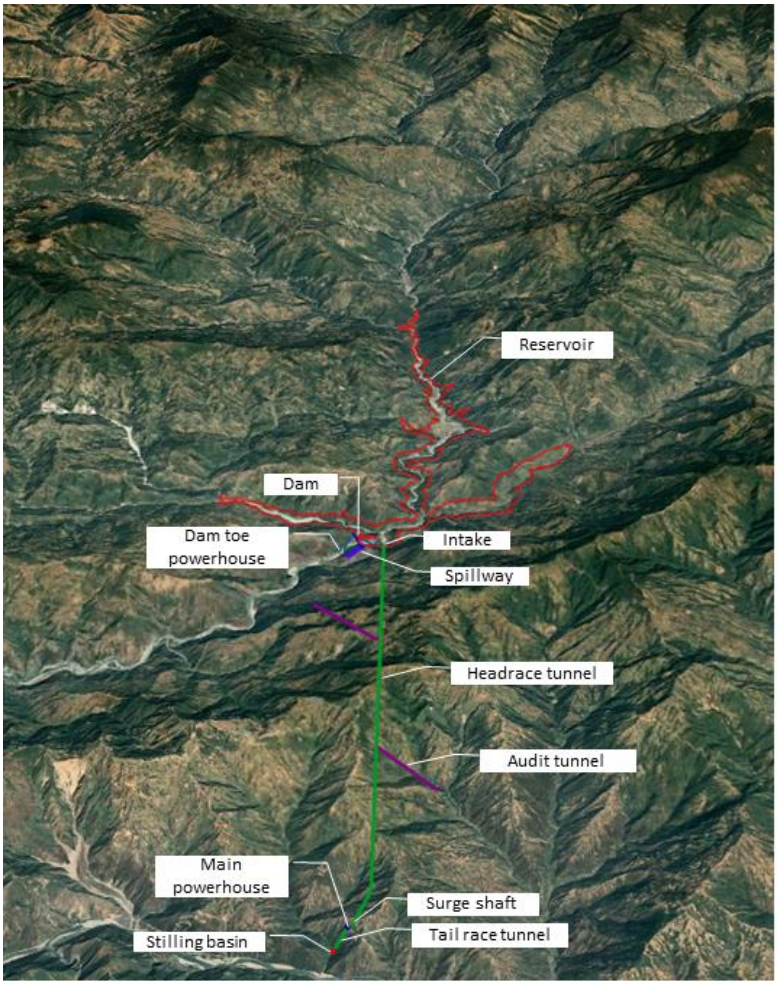

Figure 5. General layout and key component of the Dudhkoshi Storage Hydroelectric Project (DKSHEP).

2 Methodology

2.1 Climate risk assessment guidelines

Since 2014, the ADB requires that all investment projects consider climate and disaster risk and incorporate adaptation measures in projects at-risk from geo-physical and climate change impacts. This is consistent with the ADB's commitment to scale up support for adaptation and climate resilience in project design and implementation, articulated in the Midterm Review of Strategy 2020: Meeting the Challenges of a Transforming Asia and Pacific (ADB, 2014a), in the Climate Change Operational Framework 2017–2030: Enhancing Actions for Low Greenhouse Gas Emissions and Climate-Resilient Development (ADB, 2017), and in the Climate Risk Management in ADB Projects guidelines (2014b).

Climate risk management (CRM) is a mandatory part of project development. Climate risk screening is applied to all ADB investments, with a more detailed CRA undertaken for projects that are assessed to be at medium or high risk. The principal objective of a CRA is to identify those components of the project that may be at risk of failure, damage and/or deterioration, reduction, interruption, and/or decreased reliability of service delivery from natural hazards, extreme climatic events or significant changes to baseline climate design values (ADB, 2011, 2014 and 2017). Adaptation measures consistent with the risk assessment serve to improve the resilience of the infrastructure to the impacts of climate change and geo-physical hazards, to protect communities, and provide a safeguard so that infrastructure services are available when they are needed most (**Figure 6**). As part of this process, the nature and relative levels of risk are evaluated and determined to establish appropriate actions for each proposed investment to help minimize climate change-associated risk.

Earlier the terminology "Climate risk and vulnerability Assessment (CRVA)" was used. However, since vulnerability is part of the risk, ADB now recommended using the term "Climate Risk and Adaptation Assessment (CRA)". The CRA process embodies the recognition that many of the future impacts of climate change are fundamentally uncertain and that project risk management procedures must be robust to a range of uncertainty. The CRA, therefore, includes a technical and economic appraisal of adaptation options for the project design.

ADB has developed specific guidelines regarding CRAs. These guidelines mentioned that the main characteristics of a CRA are (i) to characterize climate risks to a project by identifying both the nature and likely magnitude of climate change impacts on the project, and the specific features of the project that make it vulnerable to these impacts. (ii) To identify the underlying causes of a system's vulnerability to climate change, and (iii) to ensure that adaptation measures are locally beneficial, sustainable, and economically efficient.

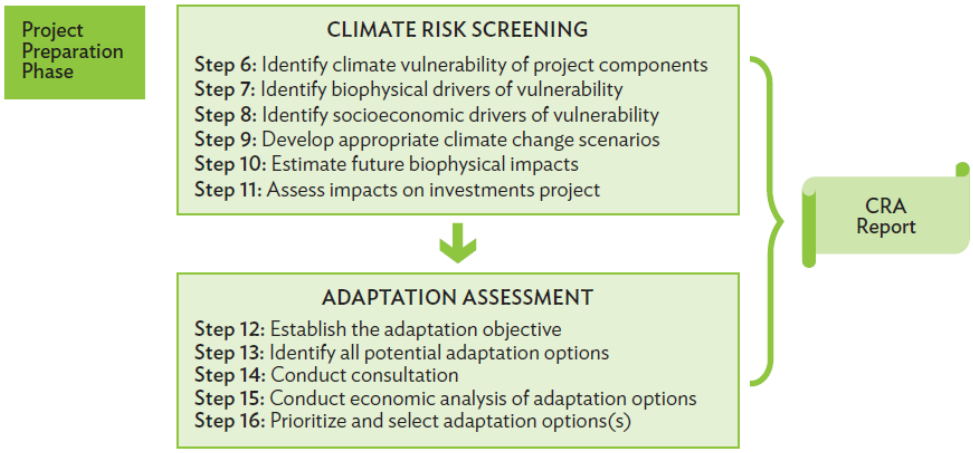

Figure 6. Climate Risk and Adaptation Assessment components. (Source: ADB, (2015a))

CRAs use a variety of definitions relating to risk and climate change. In this study the following definitions are used (adapted from IPCC, 2014), with links between concepts shown in **Figure 7**:

- Exposure: The presence of people, livelihoods, species or ecosystems, environmental functions, services, and resources, infrastructure, or economic, social, or cultural assets in places and settings that could be adversely affected by climate change and variability.
- Sensitivity: The degree to which a system, asset, or species may be affected, either adversely or beneficially, when exposed to climate change and variability.
- Potential impact: The potential effects of hazards on human or natural assets and systems. These potential effects, which are determined by both exposure and sensitivity, may be beneficial or harmful.
- Adaptive capacity: The ability of systems, institutions, humans, and other organisms to adjust to potential damage, to take advantage of opportunities, or to respond to consequences of hazards.
- Vulnerability: The extent to which a system is susceptible to, or unable to cope with, adverse effects of climate change, including climate variability and extremes. It depends not only on a system's exposure and sensitivity but also on its adaptive capacity.
- Likelihood: A general concept relating to the chance of an event occurring. Generally expressed as a probability or frequency.
- Risk: A combination of the chance or probability of an event occurring, and the impact or consequence associated with that event if it occurs.

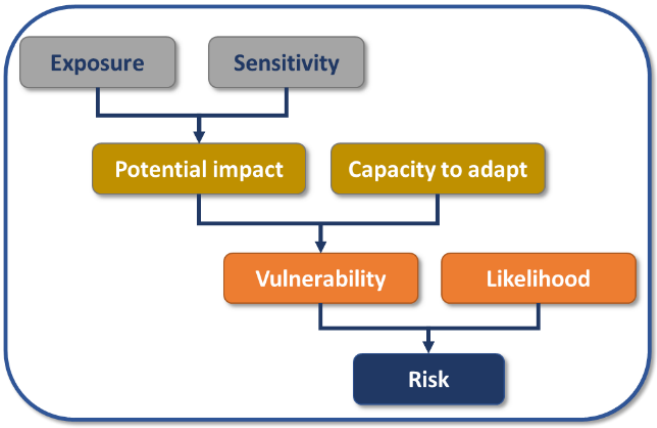

Figure 7. Climate Risk components. (Source: http://www.ukcip.org.uk).

2.2 'Top-down' vs 'bottom-up'

Many recent studies make a distinction between climate scenario-driven impact assessment approaches, often referred to as "top-down" and vulnerability-oriented approaches, often called "bottom-up" (**Figure 8**). The ADB guidelines are less restrictive and recognize that both approaches can work and can be conducted in parallel:

While current good practice in adaptation emphasizes risk management, and increasing recognition of the fundamental uncertainty of future climate discourages the overinterpretation of model-generated climate projections, impact and vulnerability assessments should be understood as complementary processes in project climate risk management, and they can be conducted in parallel:

- An impact assessment is useful in narrowing and illuminating the potential range of future conditions with which project designers must be concerned.
- A vulnerability assessment provides an understanding of how robust the project and specific project components are to depart from design assumptions and identifies critical thresholds of vulnerability past which the project fails to perform as designed.

In summary, the main difference between the top-down and the bottom-up approach is in the use of GCM projections. The top-down approach is a constraint (limited) to the GCM projections, while the bottom-up approach considers a range of potential changes in climate. **Figure 9** summarizes in one graph a typical example of the result of a bottom-up approach.

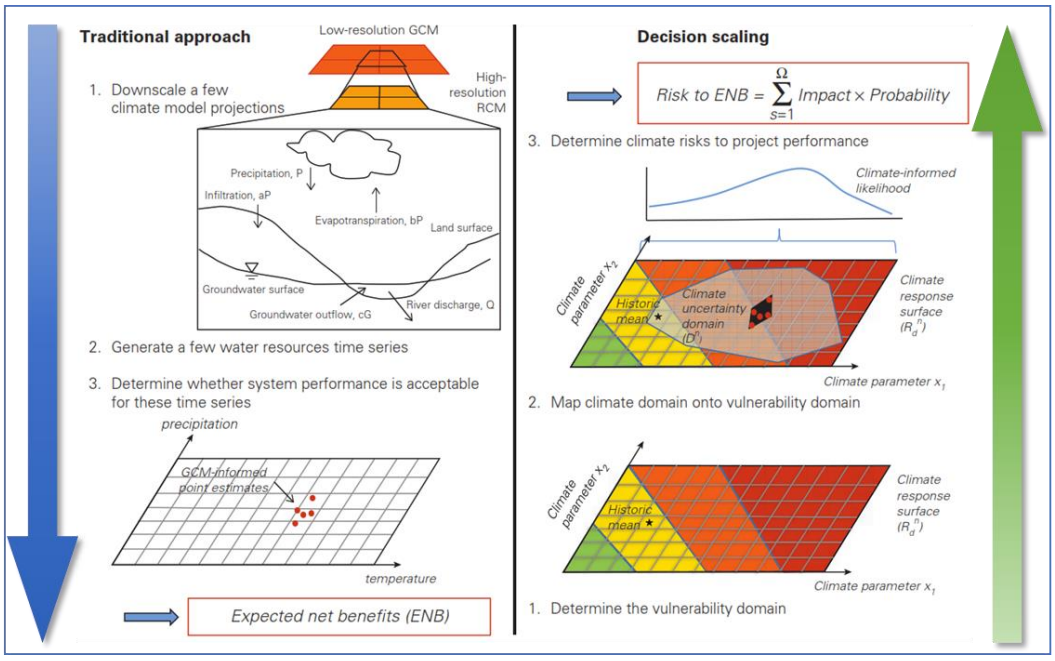

Figure 8. Schematic comparison of decision scaling (right) with traditional approach (left) to Climate Change Risk Assessment. (Based on World Bank, 2015)

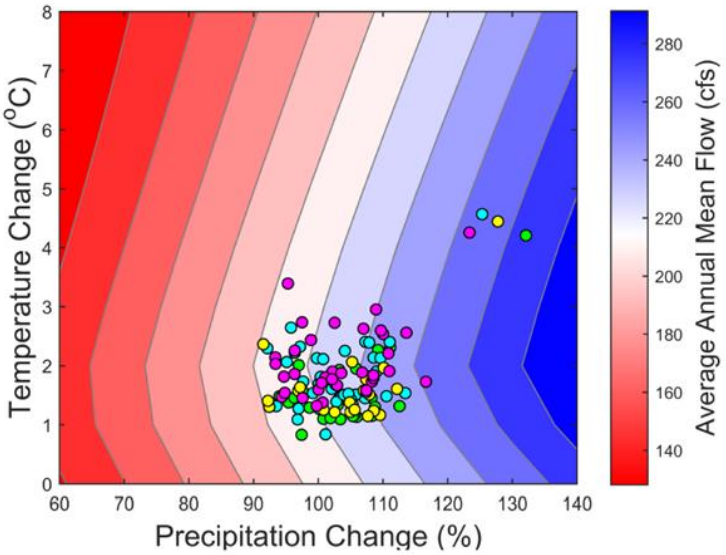

Figure 9. Example of the outcome of a "bottom-up" CRA approach (example from Nepal study on hydropower): response function of mean annual streamflow under changes in precipitation (x-axis) and temperature (y-axis). Colored circles represent mean climate change projections for 2050 from a multi-model ensemble of GCMs (RCP2.6 - green; RCP4.5 - blue; RCP6.0 - yellow; RCP8.5 - purple).

2.3 Approach to CRA

The approach towards the development of the CRA is described in this section, while the specific details regarding methodologies and results are presented in the subsequent chapters. Overall, the CRA will consist of the following steps:

1) Analysis of historic climate events
2) Projections of future climate change
3) Impact and vulnerability of climate change on DKSHEP project reservoir and its components
4) Adaptation options and recommendations for the planned project components

2.3.1 Analysis of historic climate events

A credible and acceptable CRA assessment starts with analyzing historic observations of climate-related events and performing a trend analysis. Obviously, trends, or the absence of trends, do not imply that future changes will follow those historic trends. Any statistical trend analysis should be accompanied by an understanding of the underlying physical processes. Analysis of historic climate events should go beyond looking at weather parameters (e.g. temperature and wind) and should include parameters that might have been influenced by historic weather conditions. Given the climate risks and vulnerabilities associated with components of the energy sector in general and specific to this project (hydropower in mountainous terrain), the following climate parameters and hazards were prioritized:

1. Precipitation and temperature
2. Extreme precipitation, related to extreme runoff and flooding events including flash floods, and landslide, erosion and glacial lake outburst floods (GLOF) risks
3. Drought hazards
4. Heatwave hazards

Other hazards such as cyclonic activities and storminess are not included in this report as the risk level is too low for the scope of this report[1].

2.3.2 Projections of future climates

Projections of future climates are provided by GCMs (Global Circulation Models). The Intergovernmental Panel on Climate Change (IPCC) is a credible body on climate change projections. The IPCC is an intergovernmental body under the auspices of the United Nations "dedicated to the task of providing the world with an objective, scientific view of climate change and its political and economic impacts". The IPCC does not carry out its original research, nor does it do the work of monitoring climate or related phenomena itself. The IPCC bases its assessment on the published literature, which includes peer-reviewed and non-peer-reviewed sources.

An important source of the climate projections to date is the results from the Coupled Model Intercomparison Project Phase 5 (CMIP5) activities. CMIP5 has led to a standard set of model simulations and a (more or less) uniform output. Since the downscaling and local adjustment of GCMs is needed, NASA has developed the so-called NEX-GDDP (NASA Earth Exchange Global Daily Downscaled Projections) (NASA, 2015). The dataset is provided to assist in conducting studies of climate change impacts at local to regional scales and to enhance public understanding of possible future global climate patterns at the spatial scale of individual towns, cities, and watersheds.

The NASA-NEX-GDDP consists of 21 GCM outputs for two RCPs (4.5 and 8.5) for a historic period (1950-2005) and the future (2006-2100). For the CRA these data are used for two purposes. First, the projections are analyzed using a set of indicators ranging from more direct ones (e.g. change in temperature) to more meaningful integrated and advanced indicators (e.g. monthly maximum consecutive 5-day precipitation). Second, the NASA-NEX-GDDP is used in the bottom-up approach of the impact and vulnerability assessment. As described later in this report, the projections of future climate vary strongly per climate model, forming one important dimension of future climate uncertainty. It is key to consider this uncertainty by including an ensemble of climate models in the analysis. Based on the range (uncertainty) in the projections, a confidence threshold can be used to benchmark infrastructural developments in the context of future climate change.

2.3.3 Impact and vulnerability of climate change

A standardized approach to climate change impact and vulnerability assessment does not exist. There is however a clear trend in CRAs to move from climate projections (GCM) focus to a vulnerability-oriented approach. This change started by the aforementioned often non-consistent projections of GCMs (especially in precipitation) and at the same time the desire to put stakeholders' perspectives back into the analysis. This distinction between climate scenario-driven impact assessment approaches is often referred to as "top-down", while the vulnerability-oriented approach is referred to as "bottom-up." The ADB guidelines are less restrictive and recognize that both approaches are complementary and can even be conducted in parallel. In this CRA we combine the approaches and present the full scope of possible futures in terms of climate change, but for the final chapters on vulnerability and adaptation options, we take the perspective from the designers to come up with actionable recommendations.

2.3.4 Adaptation options and recommendations for design

Adaptation policy design requires considerations in time-horizon ("when"), spatial ("where"), and decision-level ("how") terms: in fact, there is a need to assess the location of current and future impacts; to identify people, resources, sectors at risk; to gather information about the timeframe of

[1] https://thinkhazard.org/en/report/175-nepal/CY

impacts; to define and implement appropriate adaptation actions at appropriate levels of decision-making.

ADB has developed some specific guidelines regarding CRAs that are used as a source:

- Climate risk management in ADB projects (ADB, 2014)
- Climate Risk and Adaptation in the Electric Power Sector (ADB, 2012)
- Guidelines for Climate Proofing Investment in the Energy Sector (ADB, 2013)
- Guidelines for Climate Proofing Investment in the Transport Sector: Road Infrastructure Projects
- Guidelines for Climate Proofing Investment in the Water Sector: Water Supply and Sanitation (ADB, 2016)

For the project, some potential climate adaptation options are outlined. These options are based on the detailed study described in this report. A close collaboration between the CRA team and the other teams working on the project will lead to a more specific list of recommendations for adaptation and design, and some of the recommendations may require further specification and investigation per project site.

3 Historic Climate Trends

An essential step in developing a credible and acceptable Climate risk and adaptation Assessment (CRA) is to look at historic observations of climate and to perform trend analyses. This can reveal whether trends in climate variables can already be observed based on historic data. Trends, or the absence of trends, do not imply that future changes will follow historic patterns. Any statistical trend analysis should be accompanied by an understanding of the underlying physical processes and future projections using GCMs.

3.1 Global climate reanalysis dataset

Reanalysis of past weather (model) data provides a clear picture of past weather. Through a variety of methods of observations from various instruments (in situ, remote sensing, models) are assimilated onto a regularly spaced grid of data. Placing all instrument observations onto a regularly spaced grid makes comparing the actual observations with other gridded datasets easier. In addition to putting observations onto a grid, reanalysis also holds the gridding model constant keeping the historical record uninfluenced by artificial factors. Reanalysis helps ensure a level playing field for all instruments throughout the historical record.

ERA5 and ERA5-Land Reanalysis Data

ERA5 is the fifth generation European Centre for Medium-Range Weather Forecasts (ECMWF) reanalysis for the global climate and weather for the past 4 to 7 decades. Currently data is available from 1951 until near-present. Reanalysis combines observations from different sources into globally complete fields using the laws of physics with the method of data assimilation (4D-Var in the case of ERA5). ERA5 provides hourly estimates for many atmospheric, ocean-wave and land-surface quantities and fluxes.

ERA5-land is a reanalysis dataset at an enhanced resolution compared to ERA5. ERA5-land has been produced by replaying the land component of the ECMWF ERA5 climate reanalysis. Currently data is available from 1981 until near-present. Reanalysis combines model data with observations from across the world into a globally complete and consistent dataset using the laws of physics. Reanalysis produces data that goes several decades back in time, providing a uniform and accurate description of the climate of the past.

Source: ECMWF

For this, the ERA5-land reanalysis product from the ECMWF is used to analyze historical trends in temperature and precipitation, and derived indicators, for the project area. This product is used as it provides a global, spatially gridded time series of several climate variables at resolutions of 31km and sub-daily (3hr) timescales. The dataset is fully operational (updated every month) and runs from 1981 to the near present. From this dataset, spatially averaged time series of precipitation and temperature are extracted for the project area at daily, weekly, and yearly timescales for the entire period that the dataset covers. This allows for the analysis of annual and seasonal trends in historical climates alongside extremes.

3.2 Temperature trends

Historical data on temperature shows that average annual temperatures are around 5.1 ºC for the upstream part of the Dudhkoshi dam (**Figure 10**). Fairly large intra-annual variations in temperature are evident, with average daily temperatures ranging from around -10 to 15 ºC (**Figure 11**). Analysis of temperature data shows that temperatures have increased by ~ 1.2 ºC between 1981–2020 **(Figure 10**). This trend is extracted from the yearly average temperature time series and has medium statistical significance. A clear seasonality is evident in Figure 12, with high average monthly temperatures (~ 12 ºC) prevailing during pre-monsoon and monsoon seasons (April – September).

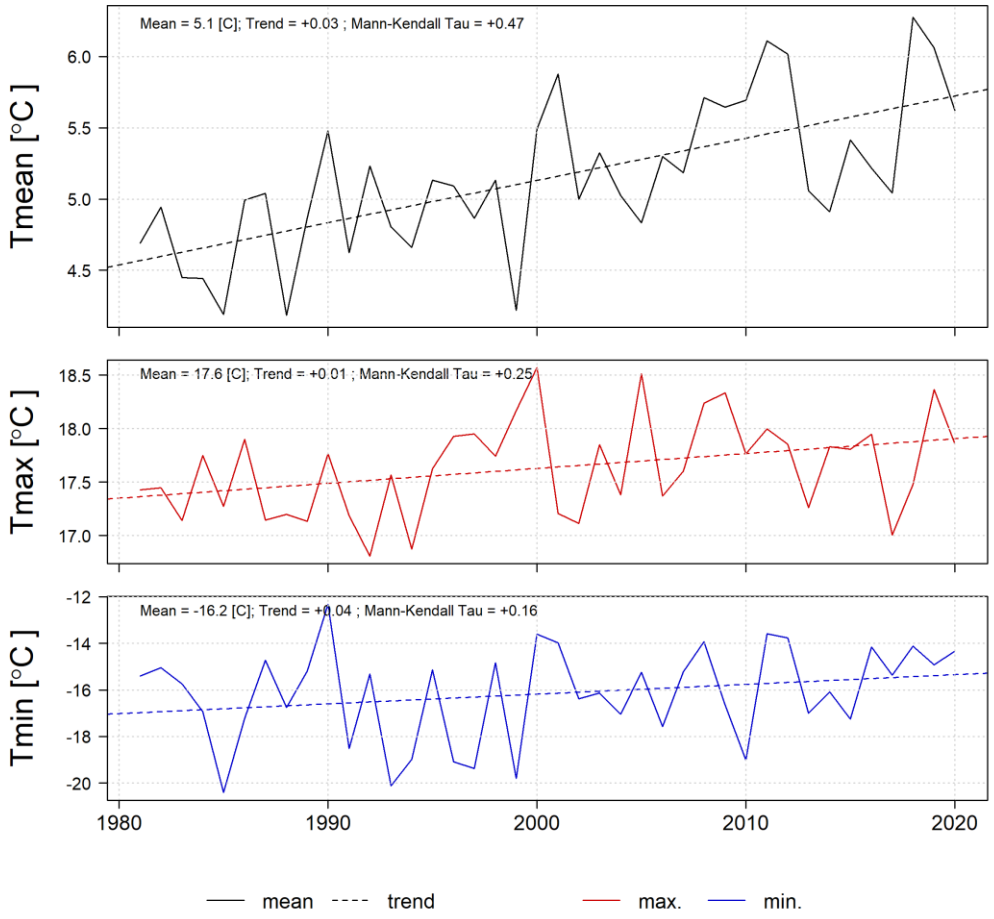

Figure 10. Average, maximum, and minimum daily temperatures per year from ERA5-land dataset with a trendline. Mann Kendall Tau value indicates the strength of the monotonic trend (increase or decrease) in a time series, with a value of 1 indicating a strong significant trend and -1 indicating no trend.

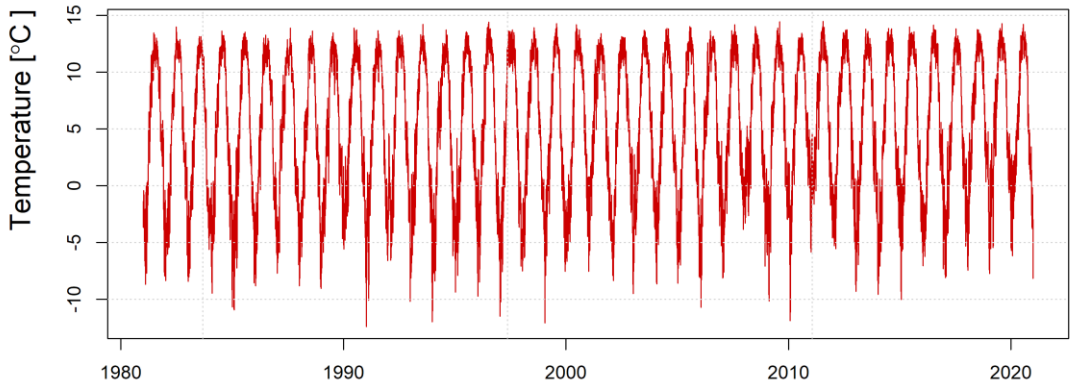

Figure 11. The daily average temperature from ERA5-land dataset

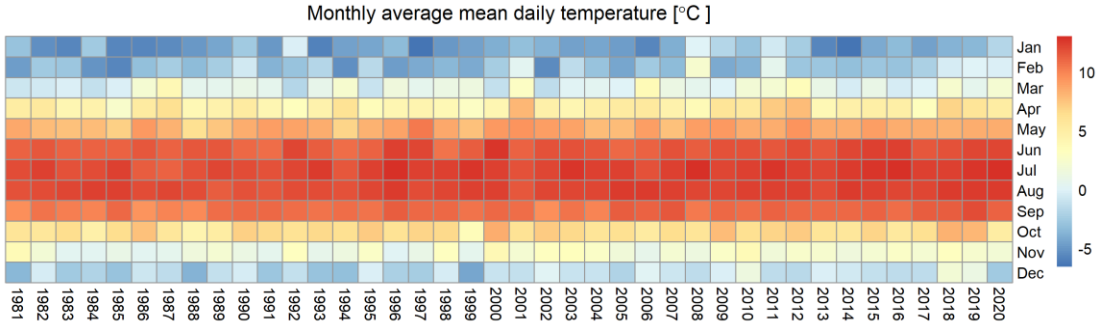

Figure 12. Seasonality in mean temperature from ERA-5 land dataset for the project area

3.3 Precipitation trends

Historical ERA5-land data on precipitation shows that the average total annual precipitation is around 2460 mm on average for the project area (**Figure 13 top)**. There is a large annual precipitation variability (minimum of ~2000 mm to a maximum of ~3000 mm) in the region. However, the exact figures may have some uncertainty due to possible biases in the precipitation data of ERA5 compared to stations over High Mountain Asia (S. Khanal et al., 2021). The true amounts of precipitation over the High Mountains of Asia are highly uncertain in general (W W Immerzeel et al., 2015). Rain gauges are usually situated in the valleys because of accessibility, whereas the majority of precipitation falls at high altitudes due to orographic effects. Besides, precipitation gauges usually under-catch snowfall. Remote sensing precipitation products on the other hand underestimate snowfall. Work analyzing glacier mass balances and observed discharge in the upper Indus in the western Himalayas and Karakoram indicates that station-based precipitation products may underestimate the total amount of precipitation by up to 50% (W W Immerzeel et al., 2015; Walter Willem Immerzeel et al., 2012). The use of a numerical weather model-based reanalysis product, like ERA5-land, which takes the orographic effect into account, maybe the better alternative.

A trend (~11 mm per year) of increasing total annual rainfall is evident for the historical period, but with significant interannual variability. Most of the rainfall occurs during the Monsoon period in June, July, and August. The pre and post-monsoon periods from November until February are very dry (**Figure 14**). The interannual variation, high precipitation in the rainy season and low precipitation in the winter season, is also evident from daily precipitation plots (**Figure 15)**. The daily maximum precipitation for individual years (**Figure 13 bottom**), which is an indicator of extreme precipitation, does not indicate a clear increasing trend.

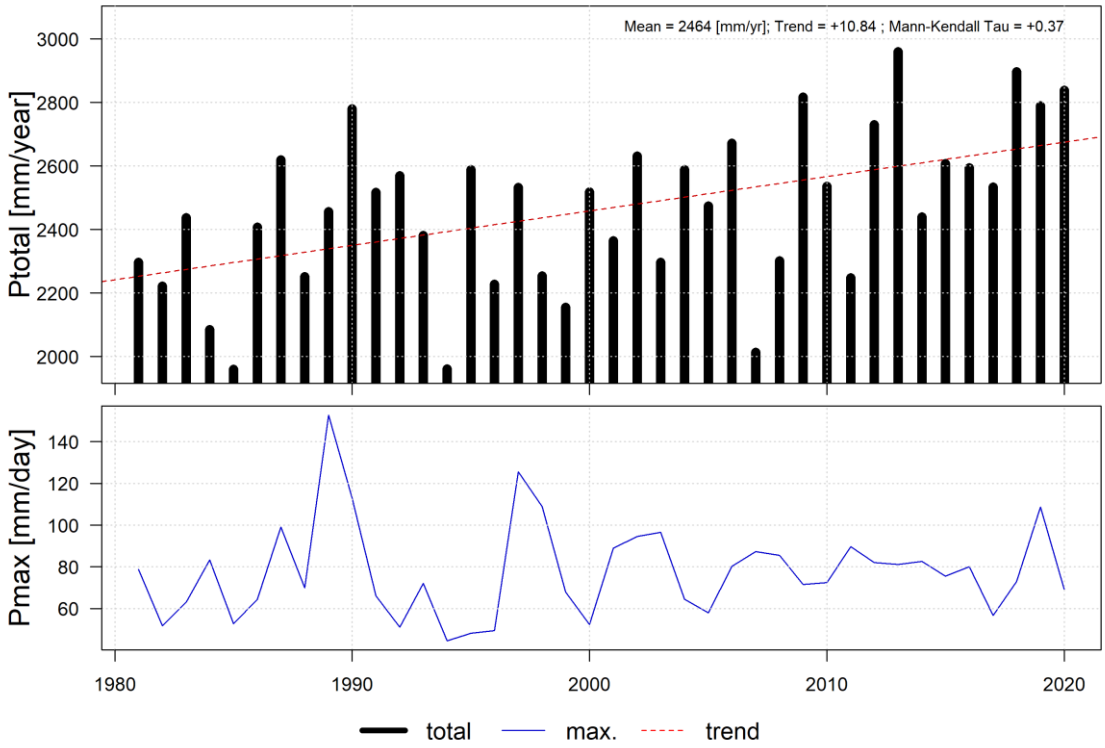

Figure 13. Total yearly and maximum one-day precipitation from ERA5-land dataset with a trendline. Mann Kendall Tau value indicates the strength of the monotonic trend (increase or decrease) in a time series, with a value of 1 indicating a strong significant trend and -1 indicating no trend.

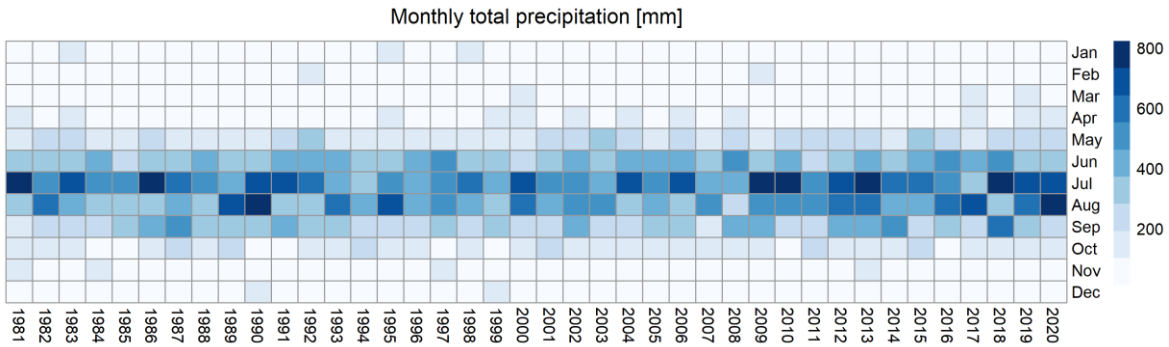

Figure 14. Seasonality of precipitation from ERA-5 dataset for the project area.

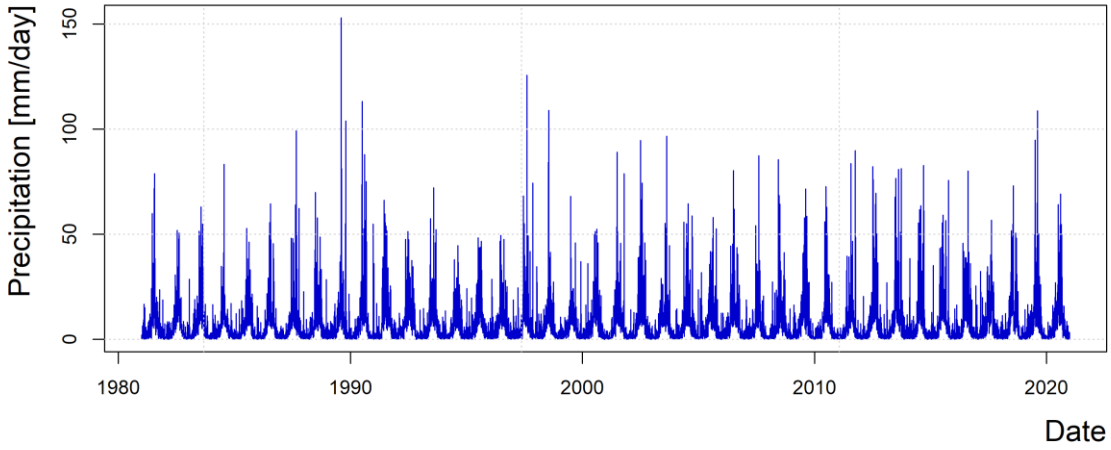

Figure 15. Daily precipitation from the ERA5-land dataset

4 Future Climate Projections

4.1 Methodology

4.1.1 Climate Model Ensemble

For this CRA, the NASA-NEX (NASA, 2015) data is used to analyze future climate trends. This dataset is used to provide an analysis of trends in terms of temperature and precipitation, and derived climate change indicators. This product is used as it provides spatially gridded time series of temperature and precipitation derived from an ensemble of 21 General Circulation Models with global coverage (see **Table 2** for descriptions of models). Data is available at downscaled resolutions of ~25 km and daily time series, covering "historical" (1950 – 2005) and "future" (2006 – 2100) periods and varying emissions scenarios or Representative Concentration Pathways (RCP 4.5, 8.5), which are sufficient for the scale of the project.

From this dataset, spatially averaged time series of precipitation and temperature are extracted for the project area at daily, weekly, and yearly timescales for the entire period that the dataset covers. This allows for the analysis of annual and seasonal trends in future climate in terms of climatic means as well as extremes.

Table 2. Climate models included in the NASA-NEX dataset.

Model	***Research center***	***Country***	***Resolution (Original)***		***Resolution (NASA-NEX)***	
			Lat (°)	**Lon (°)**	**Lat (°)**	**Lon (°)**
BCC-CSM1-1	GCESS	PRC	2.79	2.81	0.25	0.25
BNU-ESM	NSF-DOE-NCAR	PRC	2.79	2.81	0.25	0.25
CanESM2	LASG-CESS	Canada	2.79	2.81	0.25	0.25
CCSM4	NSF-DOE-NCAR	USA	0.94	1.25	0.25	0.25
CESM1-BGC	NSF-DOE-NCAR	USA	0.94	1.25	0.25	0.25
CNRM-CM5	CSIRO-QCCCE	France	1.40	1.41	0.25	0.25
CSIRO-MK3-6-0	CCCma	Australia	1.87	1.88	0.25	0.25
GFDL-CM3	NOAAGFDL	USA	2.00	2.50	0.25	0.25
GFDL-ESM2G	NOAAGFDL	USA	2.02	2.00	0.25	0.25
GFDL-ESM2M	NOAAGFDL	USA	2.02	2.50	0.25	0.25
INMCM4	IPSL	Russia	1.50	2.00	0.25	0.25
IPSL-CM5A-LR	IPSL	France	1.89	3.75	0.25	0.25
IPSL-CM5A-MR	MIROC	France	1.27	2.50	0.25	0.25
MIROC5	MPI-M	Japan	1.40	1.41	0.25	0.25
MIROC-ESM	MIROC	Japan	2.79	2.81	0.25	0.25
MIROC-ESM-CHEM	MIROC	Japan	2.79	2.81	0.25	0.25
MPI-ESM-LR	MPI-M	Germany	1.87	1.88	0.25	0.25

MPI-ESM-MR	MRI	Germany	1.87	1.88	0.25	0.25
MRI-CGCM3	NICAM	Japan	1.12	1.13	0.25	0.25
NorESM1-M	NorESM1-M	Norway	1.89	2.50	0.25	0.25

4.1.2 Scenarios and future horizons

Two RCP scenarios are analyzed to provide a range of future projections to be considered in project design. RCP4.5 represents a “stabilization scenario” in which greenhouse gas emissions peak around 2040 and are then reduced. Although often used as ‘business as usual’, the RCP8.5 is above the business-as-usual emission scenarios and designed as a worst-case scenario. We include this scenario as an upper limit to the possible future climate. These scenarios are selected as they represent an envelope of likely changes in climate and hence cover a plausible range of possible future changes in temperature and precipitation relating to project implementation. Note that RCP2.6, which covers most optimistic scenarios, including scenarios where global temperature increase is limited to 1.5 °C with respect to preindustrial levels, is not included. Since already more than 1 °C global temperature increase is realized, and considerable emissions are already committed to, this scenario is very unlikely, and therefore not suitable for robust climate change adaptation purposes.

Alongside the two RCP scenarios, projections are evaluated at the following time horizons:
- Reference period [1990]: 1975 – 2005
- Near-future (T1) [2030]: 2015 – 2045
- Distant-future (T2) [2080]: 2065 – 2095

These periods were selected as appropriate for the project as they are relevant to the lifetime of the project infrastructure as well as the existing hydropower infrastructure, and therefore cover a realistic range of climate changes that are likely to affect project functioning. A 30-year window was selected as appropriate for deriving average climate changes, effectively considering interannual variations in temperature and precipitation, and robust comparison (**Table 3**).

Table 3. Summary of RCP scenarios and future time horizons used in this CRA

RCP Scenarios	***Time horizons***	***Model projections***
Historical	1990 (1975-2005)	21
RCP45	2030 (2015-2045) T1	21
	2085 (2065-2095) T2	21
RCP85	2030 (2015-2045) T1	21
	2085 (2065-2095) T2	21

4.1.3 Climate Extremes Indices

To determine future trends in extreme climate events, CLIMDEX[1] indicators are used. These represent a standardized, peer-reviewed way of representing extremes in climate data and are widely used in climate analyses. They are derived from daily temperature and precipitation data. These are produced through processing the NASA-NEX dataset with Climate Data Operator (CDO) software. This takes as input spatially gridded daily time series and returns yearly series of CLIMDEX indices. This process is useful as it effectively reduces the amount of data analysis needed whilst retaining the ability to represent extremes within data in a comparable way.

[1] https://www.climdex.org/learn/

To this end, the indices described here are considered the most relevant out of the 27 available. The Rx1day (annual maximum 1-day precipitation), CWD (consecutive wet days), and PRCPTOT (annual total precipitation on wet days) indexes are representatives of future trends in extreme precipitation and therefore likely to be a good measure of potential impacts related to flooding, slope instability, erosion and extreme snowfall on project components (see **Table 4**). CDD (consecutive dry days) is important as it provides a useful indication of trends in meteorological drought, which may impact hydropower generation. TX_X (annual maximum of daily maximum temperature), TN_N (annual minimum of daily minimum temperature), and ID (number of icing days) variables are good predictors of extreme temperature, which may have negative effects on project components through freezing (and heavy snowfall if combined with precipitation) and extreme heat events.

Table 4. CLIMDEX Precipitation Indices used in the project

Index name	***Description***	***Unit***
Rx1day	Annual maximum 1-day precipitation	mm
CDD	Annual maximum consecutive dry days: annual maximum length of dry spells, sequences of days where daily precipitation is less than 1mm per day.	days
TXx	Annual maximum of daily maximum temperature	Celsius
TNn	Annual minimum of daily minimum temperature	Celsius

4.2 Climate projections for the project area

4.2.1 Average trends in temperature and precipitation

In terms of climate trends, the climate model ensemble projects an increase in mean temperature for the project area throughout the end of the century (**Figure 16**). It is also clear that the RCP 8.5 scenario projects a higher temperature increase compared to RCP 4.5 scenario. For the near-future (2015-2045), delta changes (calculated with reference period) in temperature are in the range of around 1 – 2 °C compared to 1.5 – 4°C for the distant-future (2065-2095) (**Figure 19**).

The future trend for precipitation is less clear but, overall, the climate model ensemble projects an increase in mean precipitation for the project area till the end of the century (**Figure 17)**. A large spread in model predictions is evident, with some models predicting (much) higher future increases in precipitation than others. For the near-future horizon (T1), changes in precipitation in the range of around 10% are projected by the climate model ensemble, for the distant-future horizon (T2), this increases to around 20 – 25%, with a larger spread in model projections and higher divergence between emissions pathway RCP 4.5 and RCP 8.5 (**Figure 19**). The magnitude of projected precipitation is higher in this study (**Figure 17)** compared to the detailed design report which was based on outputs of 3 GCM (**Figure 18**).

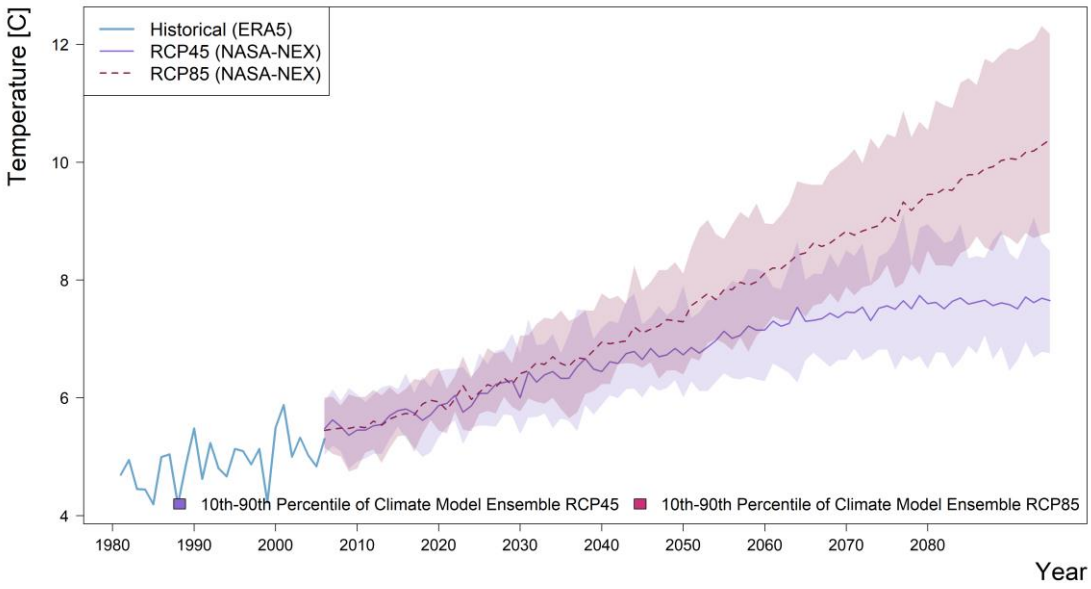

Figure 16. Time series of mean yearly temperature constructed using ERA5-land dataset for the historical period (1979-2019), and NASA NEX (per model bias corrected to ERA5-land) for the future period. *Shaded areas show the 10th and 90th percentiles in the spread of model predictions (uncertainty in the future climate).*

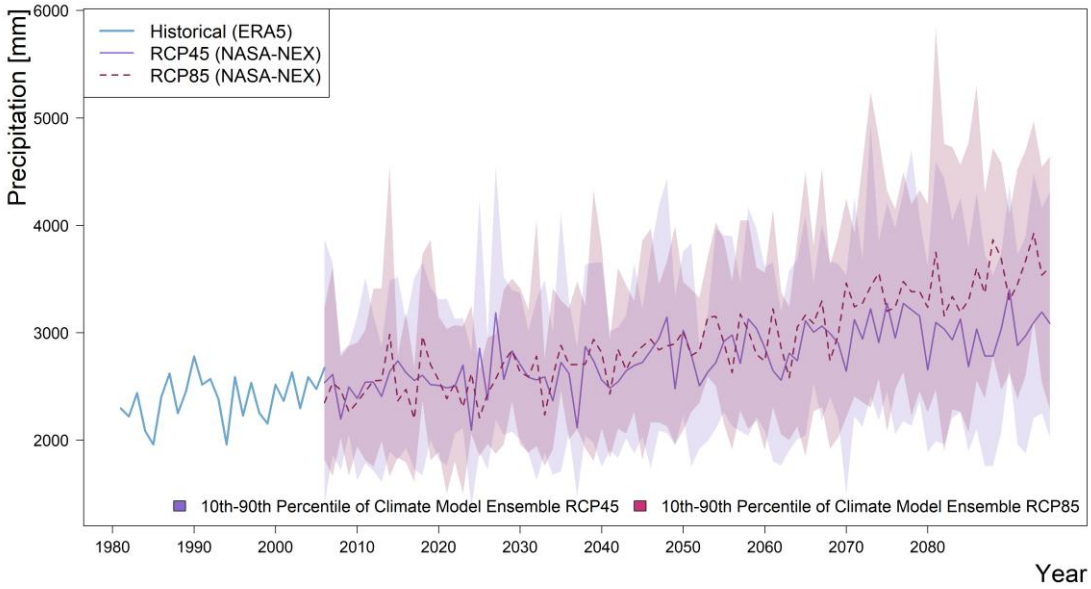

Figure 17. Time series of total yearly precipitation constructed using ERA5-land dataset for the historical period (1979-2019), and NASA NEX (per model bias-corrected) for the future period. *Shaded areas show the 10th and 90th percentiles in the spread of model predictions (uncertainty in the future climate).*

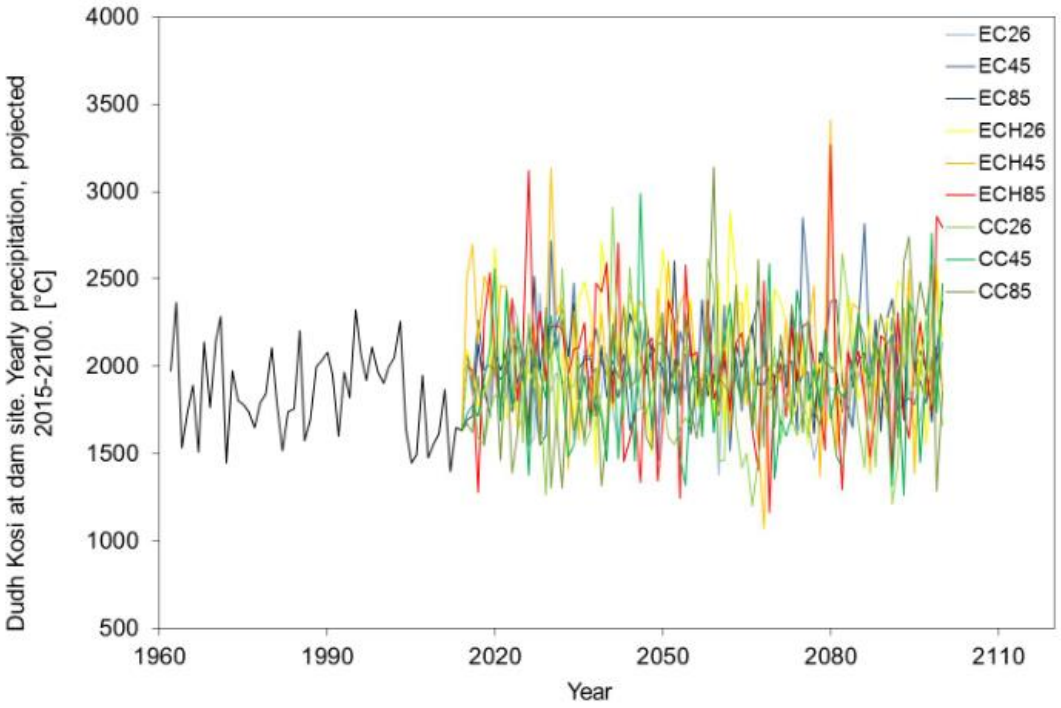

Figure 18. DudhKoshi river near the dam site. Projected mean yearly precipitation, 2015-2100. The projections were based on ECHAM6 (European Centre HAmburg Model, version 6), CCSM4 (Community Climate System Model, version 4), and EC-Earth (European Consortium Earth system model, version 2.3) (Source: Dudhkoshi SHEP - Detailed Design - Vol. 02 - Hydrological and Meteorological Report - Jan 2020).

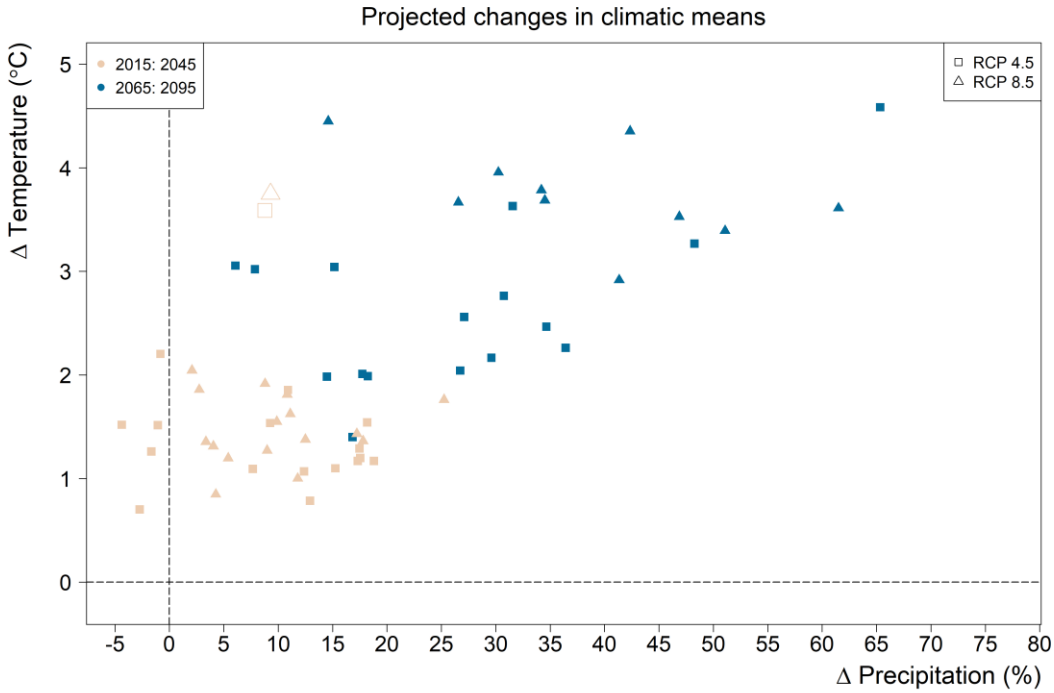

Figure 19. Average temperature and precipitation changes in the project area. These indicate the difference (Δ) between historical (1975-2005) and future (2015-2045; 2065:2095) time horizons for the two RCP scenarios.

4.2.2 Seasonality

In terms of seasonality, the climate model ensemble projects a general increase in both minimum and maximum temperatures for all months (**Figure 20**). A greater increase in temperatures is predicted in the distant-future (2065-2095) timescale and under the higher RCP 8.5 scenario. However, the models do not suggest a greater increase in temperature during the warmer months (May-September), which indicates that a change toward a more extreme seasonality in terms of temperature is not expected.

The GCM ensemble results suggest an increase in precipitation, especially in the monsoon season from May-August (**Figure 21**). This trend is more extreme under the RCP 8.5 scenario compared to RCP4.5. This result must, however, be considered uncertain due to the variation shown in model predictions for precipitation. The amount of precipitation is projected to remain fairly stable during pre- and post-Monsoon months, though a slight decrease in precipitation is foreseen for the distant-future horizon (2065-2095) for both RCP scenarios.

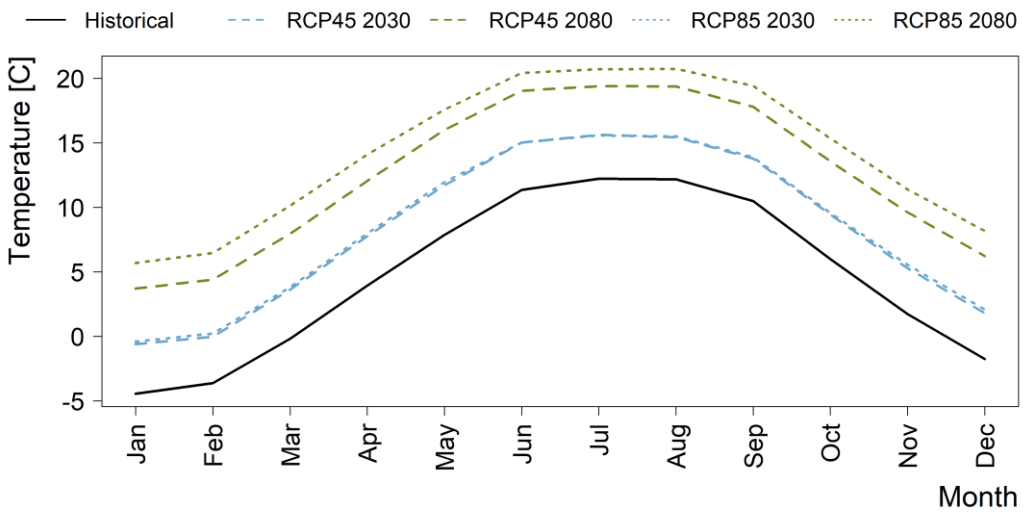

Figure 20. Average maximum daily temperature per month for historical (1975-2005) and future (2015-2045; 2065:2095) time horizons under the two RCP scenarios

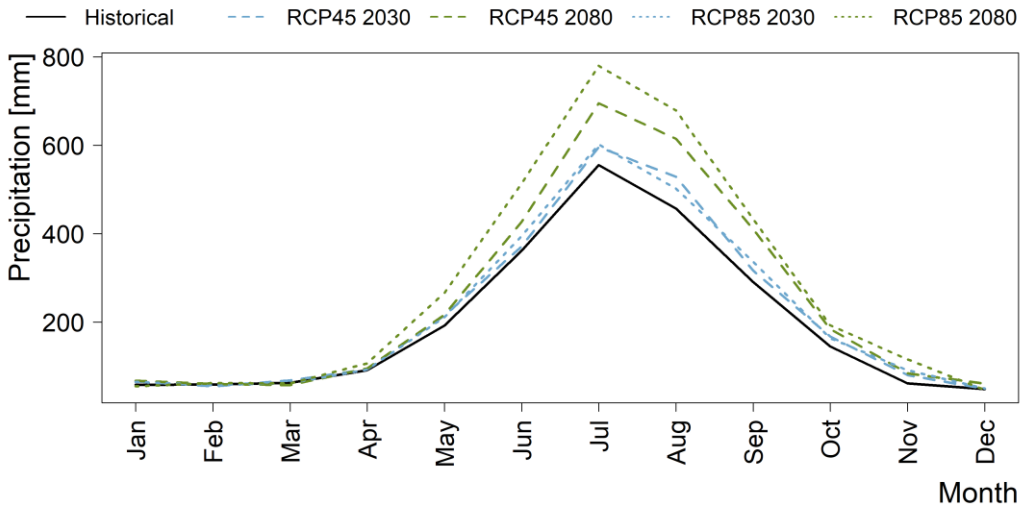

Figure 21. Average total monthly precipitation per month for historical (1975-2005) and future (2015-2045; 2065:2095) time horizons under the two RCP scenarios

4.2.3 Trends in Climate Extremes

Temperature-related extremes

When extreme trends are considered, a large level of variation is evident in climate model projections. This is expected since climate models are inherently limited in terms of predicting trends in extremes due to the stochastic nature of these events. The annual daily maximum temperature is expected to increase on average by about 1.2 and 2.4 degrees under RCP 4.5 scenario for T1 and T2 time horizon and 2.4 and 3.9 degrees under RCP 8.5 scenario for T2 and T2 time horizon (**Figure 22**). Similar changes were found for the annual daily minimum temperature (**Figure 23**). The uncertainty range of future temperature is larger for RCP 8.5 compared to RCP 4.5. The climate model ensemble does, however, show a clear trend of increasing extreme temperatures under both RCP scenarios and time horizons (**Figure 22** and **Figure 23**), suggesting an increase in the likelihood of heatwaves in the area. These processes are certain to affect seasonal water storage and seasonal patterns of discharge, particularly in the high-elevation sections of river basins.

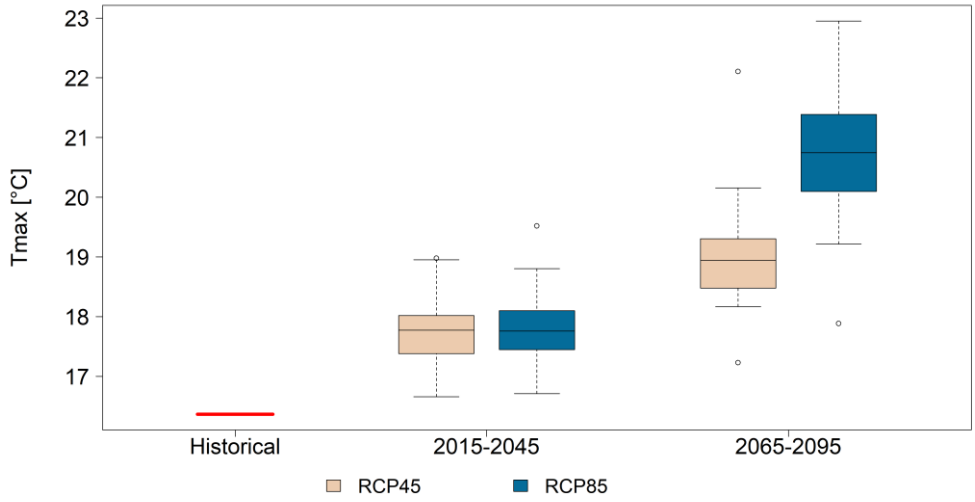

Figure 22. Boxplots indicating the spread in climate model predictions of maximum daily temperature per year (TXx) for the historical and future time periods under two RCP scenarios.

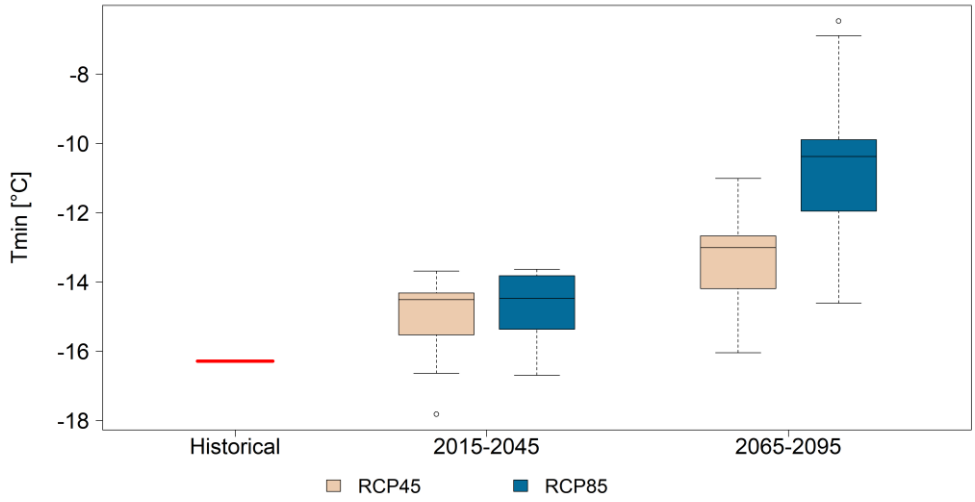

Figure 23. Boxplots indicating the spread in climate model predictions of minimum daily temperature per year (TNn) for the historical and future time periods under two RCP scenarios.

Precipitation-related extremes

The climate model ensemble shows a clear trend of increasing extreme precipitation events under both RCP scenarios and time horizons (**Figure 24** and **Table 5**), suggesting also an increase in intense precipitation-associated risks (flash flooding, soil erosion) in the future for the project area.

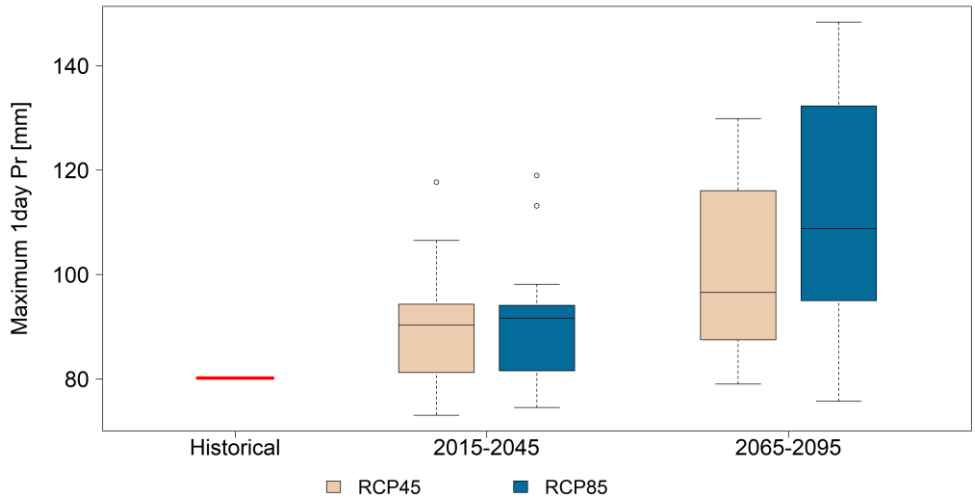

Figure 24. Boxplots indicating the spread in climate model predictions of yearly maximum 1-day precipitation sum (Rx1day, in mm/day) for the historical and future time periods under two RCP scenarios.

Table 5. Predicted change (%) in yearly maximum 1-day precipitation sum (Rx1day) for the full climate model (GCM) ensemble.

		bcc-csm1-1	BNU-ESM	CanESM2	CCSM4	CESM1-BGC	CNRM-CM5	CSIRO-Mk3-6-0	GFDL-CM3	GFDL-ESM2G	GFDL-ESM2M	inmcm4	IPSL-CM5A-LR	IPSL-CM5A-MR	MIROC-ESM-CHEM	MIROC-ESM	MIROC5	MPI-ESM-LR	MPI-ESM-MR	MRI-CGCM3	NorESM1-M
Rx1day (%)	2030_RCP45	8%	25%	20%	9%	-4%	-8%	10%	0%	12%	7%	0%	21%	14%	5%	13%	11%	2%	-8%	36%	10%
	2080_RCP45	26%	33%	41%	22%	12%	7%	17%	39%	32%	20%	-4%	43%	36%	17%	16%	11%	-4%	5%	29%	5%
	2030_RCP85	16%	9%	12%	12%	7%	-6%	12%	-1%	11%	4%	-2%	35%	10%	4%	14%	4%	4%	-7%	26%	10%
	2080_RCP85	35%	47%	54%	29%	15%	14%	14%	51%	57%	33%	9%	71%	47%	24%	37%	21%	3%	-8%	41%	33%

Table 6. Summary table showing statistics regarding spread in climate model (GCM) ensemble predictions for future changes (%) in max annual 1-day precipitation in the project area

	Average (%)	*25th perc (%)*	*75th perc. (%)*	*GCMs dryer*	*GCMs wetter*
2030_RCP45	9%	1%	14%	5	15
2080_RCP45	20%	8%	33%	2	18
2030_RCP85	9%	4%	12%	4	16
2080_RCP85	31%	14%	47%	1	19

A return period analysis for extreme precipitation events was conducted. For this, the third quartile (75th percentile) of climate model ensemble predictions of yearly maximum 1-day precipitation events (Rx1day) were taken, which ADB frequently considers for robust climate change adaptation. Then the Gumbel extreme distribution is fitted to the 75th percentile value of the projections in the GCM model

ensemble distribution, to assess the design precipitation events at different return periods for each time horizon and RCP scenario. The relative changes (delta values) are then imposed on the historical reanalysis (ERA-5) data to allow for the projection of absolute values for 1-day precipitation events (**Figure 25, Table 7 and Table 8**). Considering different return periods, in general, the statement can be made that the precipitation amounts for events with that return period increase by 17-23% for the T1 time horizon and 43-58% for the T2 time horizon with respect to the historical period according to the 75th percentile value of the climate model ensembles. In addition, **Table 6** indicates for the maximum 1-day precipitation sums that the 75th percentile value of the ensemble indicates a 12-14% increase for the T1 time horizon and a 33-47% increase for the T2 time horizon.

This analysis shows for the project area that under climate change, the intensity of the most severe precipitation events predicted by the climate model ensemble will increase, with the largest increases occurring at the more distant time horizon (2080) and more extreme emissions scenario (RCP8.5). This likely signifies an increase in intense precipitation-associated risks (flooding, erosion, landslides) in the future for the project area. These and other impacts of climate change, including seasonal reductions in flow, more unpredictable flow patterns, and changes in rates of sediment transport can potentially decrease the reliability of hydropower generation, particularly for systems with limited storage or run-of-river facilities which are common in Nepal. The loss of buffering capacity (due to rising temperatures) increases the susceptibility to both extreme runoff (due to increasingly frequent extreme rainfall events) and prolonged low flows. These adverse impacts may be exacerbated due to increasingly frequent and severe extreme precipitation events.

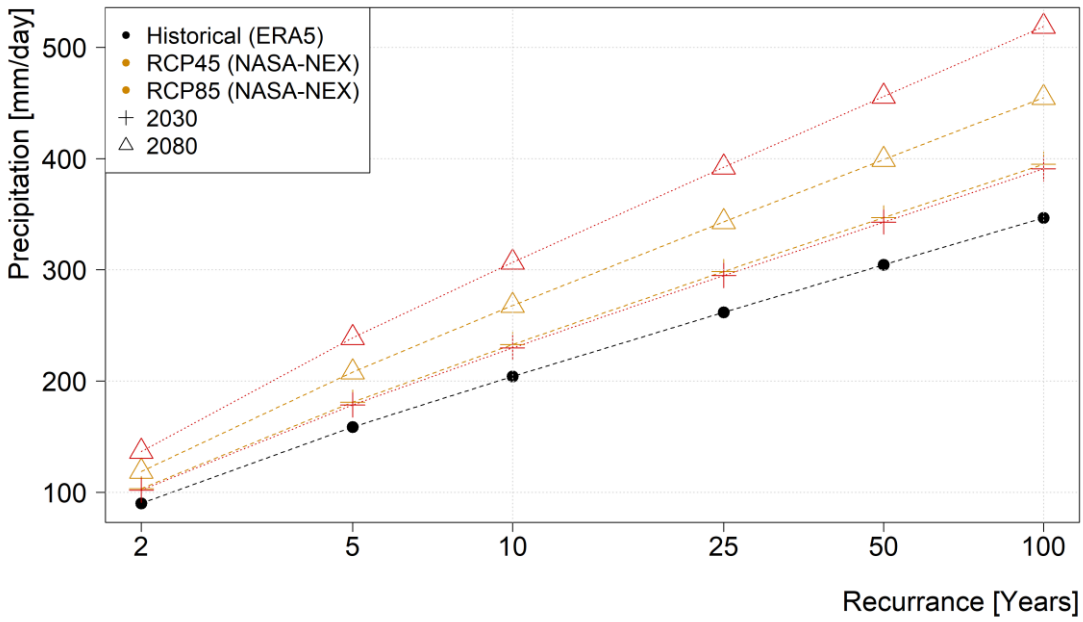

Figure 25. Recurrence intervals of daily precipitation for 5 scenarios (at 75th percentile of model projections): ERA5 (1975-2005); 2030-RCP45; 2080-RCP45; 2030-RCP85; 2080-RCP85

Table 7. Absolute intensity (mm/day) of precipitation events at different return periods under a variety of emissions scenarios (at 75th percentile of model projections) and time horizons.

	Return Period [years]					
	2	**5**	**10**	**25**	**50**	**100**
Historical daily maximum precipitation [mm/day]						
ERA5	90	159	204	262	305	347
*Future (**75th percentile of climate model ensemble predictions**) daily maximum [mm/day]*						
RCP45 2030	103	181	233	298	347	395
RCP45 2080	119	208	268	343	399	455
RCP85 2030	102	179	230	295	343	391
RCP85 2080	137	239	307	392	456	519

Table 8. Predicted change (%) in the intensity of precipitation events at different return periods under a variety of emissions scenarios and time horizons

	Return Period [years]					
	2	**5**	**10**	**25**	**50**	**100**
Historical daily maximum precipitation [mm]						
ERA5	90	159	204	262	305	347
Change in daily max. precipitation [%], format = **median (25th, 75th percentile** *of GCM ensemble)*						
RCP45 2030	7 (-3, 23)	9 (-2, 21)	10 (-2, 21)	10 (-2, 21)	10 (2, 22)	9.6 (-2, 22)
RCP45 2080	21 (5 ,48)	21 (4, 45)	21 (4, 44)	21 (4, 43)	21 (4, 43)	20 (3, 43)
RCP85 2030	9 (0, 18)	10 (0, 17)	10 (0, 17)	10 (0, 17)	10 (0, 17)	10 (0, 17)
RCP85 2080	33 (14, 58)	31 (12, 56)	31 (11, 55)	31 (11, 55)	31 (11, 54)	31 (11, 54)

There is no significant change in the number of consecutive dry days per year (**Figure 26)**. This indicates that on average more prolonged meteorological droughts are not necessarily expected, although the model uncertainty increases over the end of the century time horizon. However, taking into account also the loss of the water buffering capacity of snow and ice (see section 5.1.1), hydrological droughts are likely to become more frequent.

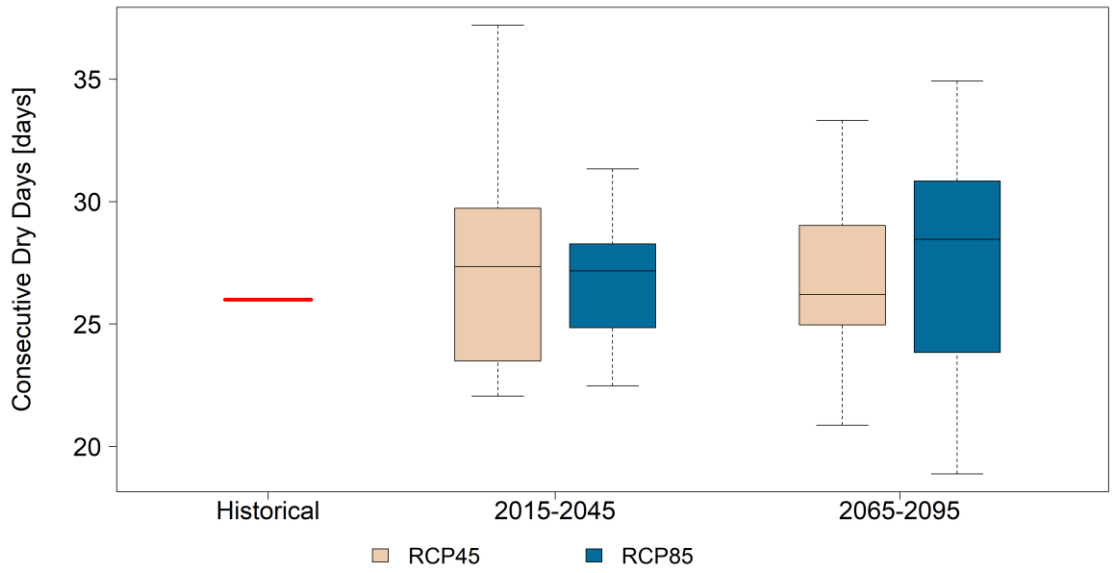

Figure 26. Boxplots indicating the spread in climate model predictions of consecutive dry days per year (CDD) for the historical and future time periods under two RCP scenarios.

4.3 Summary tables and return period analysis

The combination of 21 GCMs, two RCPs and two time-horizons leads to a total of 84 (21 x 2 x 2) projections for the future. **Table 9** shows detailed results for all 84 projections of changes in mean annual temperature and total annual precipitation. Delta values indicate the difference between historical (1975-2005) and future (T1; T2) time horizons for the two RCP scenarios. This shows consistency between GCMs in terms of projecting a warmer future climate in the project area (especially for the longer-term horizon) but indicates the large uncertainty in the future precipitation. The authors of the detailed design report, based on the results of 3 GCM, found that the largest increase occurs consistently under the warmest scenarios (i.e. at 2100 under RCP8.5, +13.3%, and +17.3% with Ec-Earth, and CCSM4, respectively). The authors also found only under RCP8.5 of ECHAM6 at 2050 precipitation decreases (-0,7%). On average, precipitation would increase by +5.7% and by 7% in 2050, and 2100, respectively. However, this study reports a maximum 35% increase in precipitation for T1 under RCP4.5 and a 69% increase for 2065-2095 under RCP4.5 when compared to the base period (1975-2005) (**Table 9)**. The change in precipitation is even higher under RCP8.5 scenarios, 28% and 81% for the T1 and T2 horizon. On average the precipitation is expected to increase by 9.1 and 9.3% for T1 and T2 under RCP4.5 and 22.8 and 37.4% for T1 and T2 under RCP8.5 scenario.

Table 10 and **Table 11** show the main statistics (median, 10th percentile and 90th percentile) of the changes in precipitation and temperature, respectively. It also includes the number of GCMs that are showing a positive versus negative change for precipitation, and the number of GCMs that are predicting a change above 2ºC and 4ºC. In summary, all GCMs predict a hotter future, with most predictions lying between 2 and 4ºC. There is no clear consensus in precipitation predictions, but a slight majority of GCMs predict a drier future under the RCP45 scenario.

Also here, when considering the 75th percentile value of the projections as a benchmark for robust climate change adaptation, the statement can be made that wetter conditions with 13% (T1) and 22-49% (T2) increases should be anticipated.

Table 9. Average climate change (delta values) in total annual precipitation and mean annual temperature predicted by the full climate model (GCM) ensemble.

		bcc-csm1-1	BNU-ESM	CanESM2	CCSM4	CESM1-BGC	CNRM-CM5	CSIRO-Mk3-6-0	GFDL-CM3	GFDL-ESM2G	GFDL-ESM2M	inmcm4	IPSL-CM5A-LR	IPSL-CM5A-MR	MIROC-ESM-CHEM	MIROC-ESM	MIROC5	MPI-ESM-LR	MPI-ESM-MR	MRI-CGCM3	NorESM1-M
Precip (%)	2030_RCP45	12%	17%	9%	14%	11%	12%	-4%	1%	21%	9%	-4%	17%	11%	-5%	0%	17%	-1%	-2%	35%	12%
	2080_RCP45	17%	33%	33%	27%	23%	36%	2%	69%	15%	23%	13%	46%	32%	13%	9%	30%	-7%	2%	20%	21%
	2030_RCP85	11%	8%	10%	9%	15%	11%	1%	4%	4%	20%	2%	24%	10%	0%	13%	9%	4%	-7%	28%	10%
	2080_RCP85	35%	39%	47%	30%	30%	50%	12%	81%	59%	49%	41%	76%	45%	20%	24%	30%	4%	-5%	48%	33%
Tavg (oC)	2030_RCP45	1.01	1.22	1.41	0.97	1.07	0.72	1.20	2.15	1.06	0.98	0.54	1.31	1.77	1.53	1.30	1.09	1.37	1.10	0.76	1.12
	2080_RCP45	1.80	2.48	2.61	1.94	1.94	2.06	2.80	4.37	1.92	1.73	1.29	2.90	3.49	2.84	3.03	2.45	2.47	2.25	1.89	2.03
	2030_RCP85	1.19	1.58	1.81	1.24	1.27	0.94	1.13	1.94	1.25	1.30	0.71	1.56	1.73	1.87	1.34	1.19	1.56	1.39	0.86	1.14
	2080_RCP85	3.29	3.78	4.43	3.56	3.51	3.08	3.77	5.59	3.32	3.03	2.32	4.74	5.48	5.21	4.56	3.29	4.30	4.14	3.00	3.50

Table 10. Summary table showing statistics regarding spread in Climate Model (GCM) ensemble predictions for future changes in mean annual precipitation in the project area

	Median (%)	*25th Perc. (%)*	*75th Perc. (%)*	*GCMs dryer*	*GCMs wetter*
2030_RCP45	9%	-1%	16%	6	14
2080_RCP45	23%	13%	32%	1	19
2030_RCP85	9%	4%	13%	2	18
2080_RCP85	37%	25%	49%	1	19

Table 11. Summary table showing statistics regarding spread in Climate Model (GCM) ensemble predictions for future changes in mean annual temperature in the project area

	Median (ºC)	*25th Perc. (ºC)*	*75th Perc. (ºC)*	*GCMs > 2ºC*	*GCMs > 4ºC*
2030_RCP45	+1.2	+1.0	+1.4	1	0
2080_RCP45	+2.4	+1.9	+2.8	13	1
2030_RCP85	+1.3	+1.2	+1.6	0	0
2080_RCP85	+3.9	+3.3	+4.5	20	8

Note that although the projections presented here are based on spatially downscaled data, there still is a scale gap between the used climate projections, based on a scale around 25 km, and the specific sites. In particular in a mountainous country like Nepal, with high climatic variability over short horizontal and vertical distances, site-specific projections may deviate.

5 Climate Risks and Vulnerabilities

Nepal is one of the most vulnerable countries to natural disasters (WB and ADB, 2021; WHO, 2015). Globally, it is ranked fourth, eleventh, and thirtieth in terms of vulnerability to climate change, earthquake, and flood risks respectively. Among the natural hazards, earthquakes and hydrometeorological events cause the largest economic losses, but also hydrometeorological extremes cause increasingly severe economic damage.

This chapter assesses the principal climate vulnerabilities for the proposed hydropower project. Then, based on the likely changes in the related climate indicators described in the preceding chapters, climate risks are evaluated and scored. This assessment indicates the extent to which the key climate risks pose a threat to the project areas. Vulnerability in this context refers to the extent to which the hydropower project (including its socio-economic characteristics) is unable to cope with hazardous climatic events and trends.

5.1 Climate change impacts for hydrology and hydropower

5.1.1 Future impacts for glaciers and snow

Mountains serve as water towers. Their key hydrological feature is to store water as snow and ice, which is released to flow downstream more gradually than direct rainfall-runoff (W. W. Immerzeel et al., 2020). The fact that mountain ranges in High Mountain Asia (HMA) are the highest on Earth combined with monsoon-dominated precipitation regimes (implying large amounts of precipitation), makes the amount of water generated in those mountain ranges particularly large (Bookhagen & Burbank, 2010; Viviroli et al., 2003). In particular, glaciers have a strong modulating effect on the flows, ensuring a constant water supply during droughts (Pritchard, 2019).

Because of its large areas and volumes of snow and glacier ice, HMA is also referred to as the “Asian Water Tower”, or the “Third Pole” (Walter W Immerzeel, 2010). However, due to the increase in temperature, the glaciers in the central Himalayas are retreating rapidly, with a mass loss of -0.4 mw.e. yr^{-1} **(**meters water equivalent per year) between 1970 and 2010 (Bolch et al., 2019). Similar trends were found in other scientific studies (Brun et al., 2017; Shean et al., 2020).

Modeling simulations at the HMA scale indicate for the Central Himalaya where Dudhkoshi is located (see **Figure 27**) that ice mass loss towards the end of the century varies from 40% to 90% loss, depending on the climate scenario (Kraaijenbrink et al., 2017) (**Figure 27**). Another modelling study (Rounce et al., 2020) showed similar results for the Eastern Himalayas.

Snow melt is an important contributor to flows in Nepal (Lutz et al., 2014). Snow cover monitoring on a regional scale has started only recently. With the availability of satellite data, near real-time spatial maps of snow cover have become available. However, long-term trends in snow cover cannot be established since these analyses cover a maximum of ten years. Most of the available studies are based on MODIS satellite products. They do not show clear general temporal changes in the snow-covered area over the whole HMA region. There is a large inter-annual variation in snow cover and an increasing trend from west to east for HMA from 2000 until 2008 (W.W. Immerzeel et al., 2009). Future simulations of snow cover show overall decreases, with the magnitude of decline mostly related to the temperature scenarios (Lutz et al., 2014; René R Wijngaard et al., 2017).

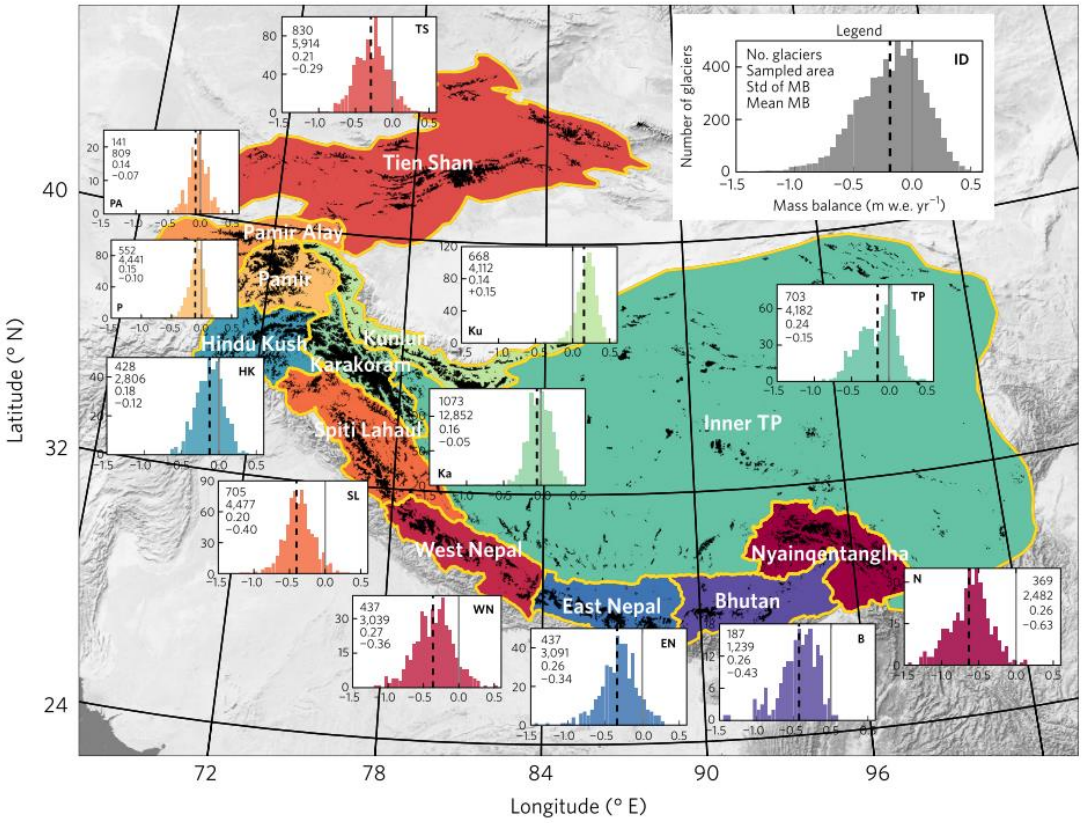

Figure 27. Remote sensing derived geodetic mass balance for High Mountain Asia (2000–2016). For each region, the distribution of glacier-wide mass balance for every individual glacier (>2km2) is represented in histograms of the number of glaciers (y-axis) as a function of MB (x-axis in mw.e. yr−1). The black dashed line represents the area-weighted mean. The numbers denote the total number of individual glaciers (first), the corresponding total area (in km2, second), the standard deviation of their mass balances (in mw.e. yr−1, third) and the area-weighted average mass balance (in mw.e. yr−1, fourth). Initials of the respective regions are repeated in bold. (Source: Brun et al., (2017)).

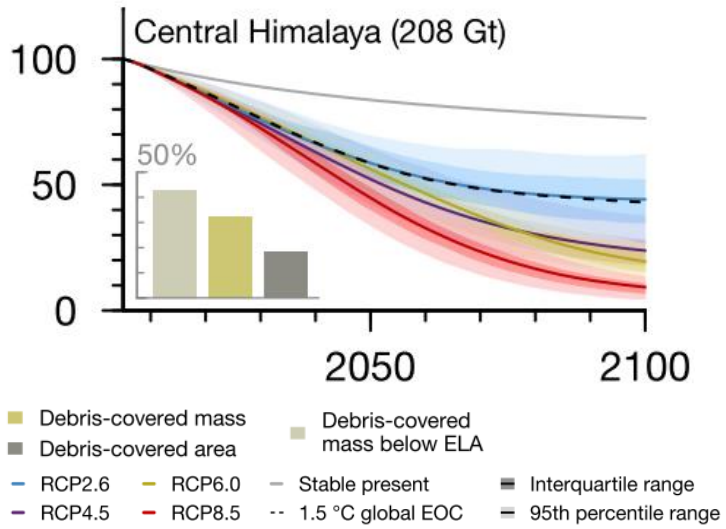

Figure 28. Projected ice mass loss for the Eastern Himalaya for 4 RCP scenarios, stable present climate, and a 1.5 °C global temperature increase scenario. The y-axis indicates the remaining ice mass compared to 2005 as baseline. (Source: Kraaijenbrink et al. (2017)).

5.1.2 Future impacts for hydrological flows and hydropower generation

Global warming is expected to increase flood risk by altering the distribution, variability, and intensity of hydrometeorological events (Hirabayashi et al., 2013). Climate change impacts flow in various ways by affecting different water balance components. The input of water changes with precipitation changes. Changes in glaciers and snow cover alter the buffering capacity of the hydrological system. How this affects the stream flow depends strongly on the role of glacier melt and snow melt in the stream flow composition (Lutz et al., 2014). Climate change impacts glaciated catchments at different time scales (IPCC, 2019a) (**Figure 29**). Changes at the yearly and decadal time scale are of interest for changes in hydropower generation. Glaciated catchments first witness an increase in meltwater generation with increasing temperature. When glaciers have lost a significant amount of their mass, the meltwater generation starts to decline. This concept is commonly referred to as 'peak water' (Huss & Hock, 2018). The time when peak water is reached strongly depends on the degree of glaciation of a catchment. For the Central Himalaya where Dudhkoshi is located, this is generally expected around 2060, albeit with a large uncertainty band (Huss & Hock, 2018). Changes in total flows however depend mostly on the precipitation projections, which mostly project increasing precipitation for Nepal (Lutz et al., 2014). With declining glacier mass and snow cover, the hydrograph will become more erratic when the hydrological system shifts towards a more rainfall-dominated system. This can imply more frequent hydrologic droughts and periods of low flows outside the monsoon season, as well as more frequent extremely high flows or floods during the monsoon season.

To mitigate the destructive potential of floods and maximize water availability for human consumption, an estimated 2.8 million dams have been constructed globally (Boulange et al., 2021). Storage-based hydroelectric projects are economically profitable due to their multifunctional nature and are thus well adapted to the challenges of the changing hydrometeorological extremes as compared to the runoff river hydroelectric projects. The accumulation of large volumes of water during the erratic monsoon season will make flood management a crucial part of hydropower plants in this region. However, damming of a continuous supply of water has further effects on local ecologies due to flooded vegetation, changing water depth and chemical composition, and effects on siltation.

Hydropower infrastructure is designed to operate at flows between a design minimum and maximum. The projected changes in flows can indicate a longer flow duration outside the turbine's design range, and therefore less generation during the low flow season when generation is at present already at its minimum. A study into future changes in extreme flows in three of South Asia's river basins, including Nepal, shows this effect Wijngaard et al., (2017). This study indicates changes in the discharge level of events with a present 50-year return period to increase in Nepal by around 40 to 180%, strongly depending on the scenario (**Figure 30**).

The strong increase in extreme flows not only indicates more flows at the high tail of the distribution outside the turbine range but also significantly increases the risk of damage to hydropower infrastructure due to floods. Wijngaard et al., (2017) also did a detailed assessment of flow changes at several representative locations in Nepal. Flows in these locations are constituted by approximately 25-30% snow melt and glacier melt. For these locations, present and future flow duration curves are shown in **Figure 31.** These figures reveal the flows, in general, will increase in the future. Interestingly, the low flows are projected to increase as per the ensemble mean. However, the uncertainty range indicates that low flows could also decrease, depending on the climate scenario, in particular for the RCP4.5 climate scenario. Also, in the middle of the distribution, likely near the optimum for hydropower generation, the projections are uncertain. The exact impacts of these projections for hydropower generation depend on the operational ranges of the turbines. Note also that these projections are based on a large river basin scale study covering the upper Indus, upper Ganges, and upper Brahmaputra river basins at a spatial scale of 5x5 km, and may therefore lack reliability at smaller scales, like the current application. Detailed hydrological modelling for exact existing or envisioned

hydropower infrastructure sites would be required to provide better insights. As a general conclusion, in particular, the projections for the increase in magnitude and frequency of extreme flow events in the upper tail of the distributions substantiate the rationale of incorporating uncertainty explicitly in the design of the hydropower infrastructure.

The authors of the detailed design used Poly-hydro, a semi-distributed cell-based hydro-glaciological model, for the detailed hydrological assessment. The study used a 300-meter resolution spatial resolution at the daily time step for this purpose. This study quantifies higher interannual variability compared to the annual averages (**Figure 32**). However, the diurnal variation of melt components is not simulated in such daily scale models. Daily timestep models underestimate the flood peak values and thus overall variation. Also, extreme flood estimation requires a cascade of sub-daily hydrological and hydraulic modeling for accurate estimates. Moreover, the seasonal variation is calculated based on limited, i.e. 3 GCM outputs, and thus the results do not represent the full distribution of projected future climate change. This might have some implications on the probable maximum design flood estimates used by the authors of the detailed design report.

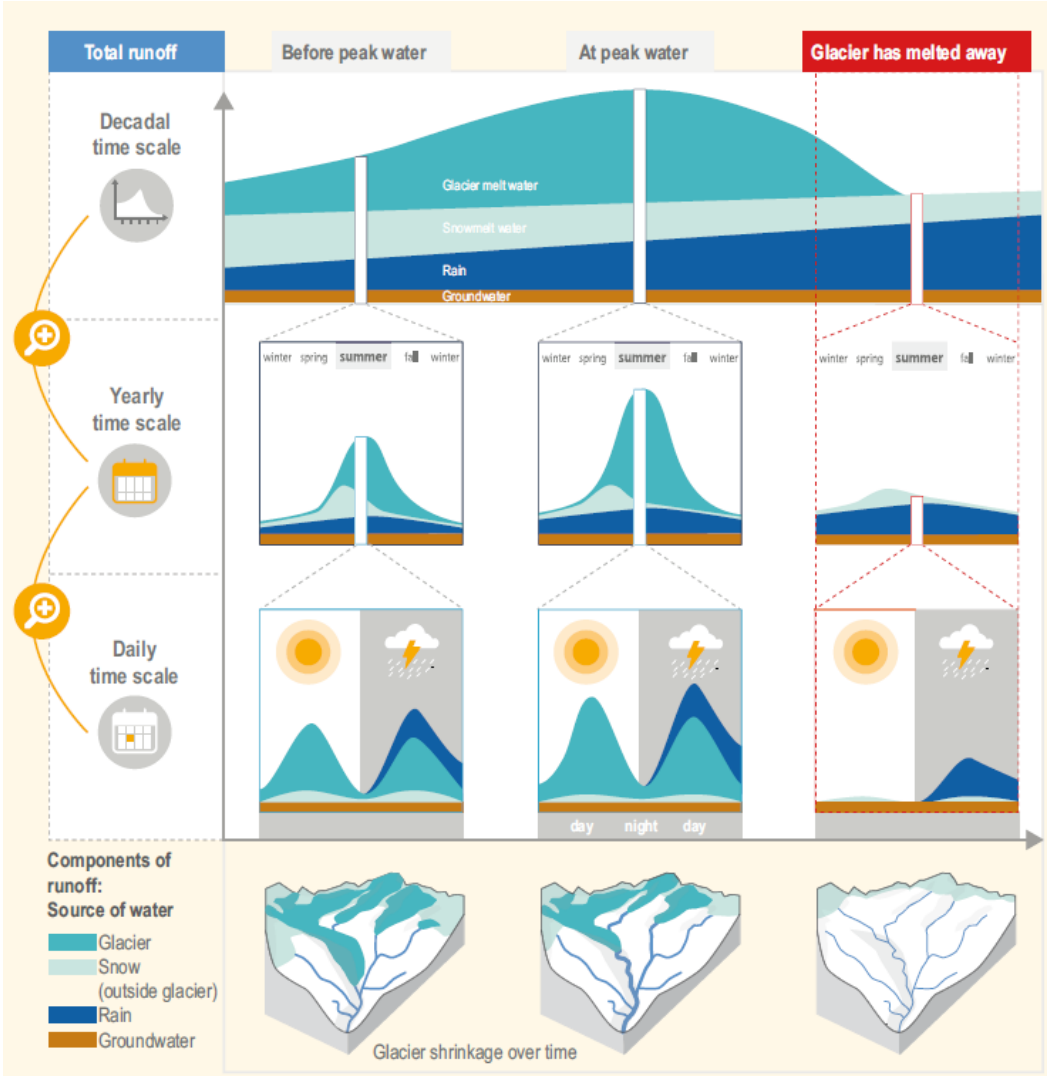

Figure 29. A simplified overview of changes in runoff from a river basin with large (e.g., >50%) glacier cover as the glaciers shrink, showing the relative amounts of water from different sources – glaciers, snow (outside the glacier), rain and groundwater. Three different time scales are shown: annual runoff

from the entire basin (upper panel); runoff variations over one year (middle panel) and variations during a sunny and then a rainy summer day (lower panel). Note that seasonal and daily runoff variations are different before, during, and after peak flow. The glacier's initial negative annual mass budget becomes more negative over time until eventually, the glacier has melted away. This is a simplified figure so permafrost is not addressed specifically and the exact partitioning between the different sources of water will vary between river basins. (Source: Hock et al., (2019))

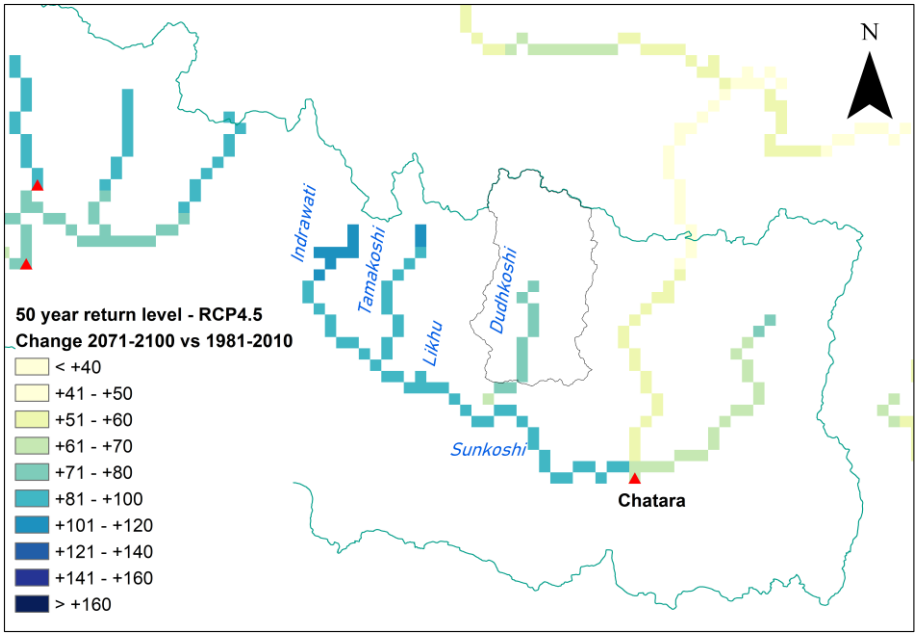

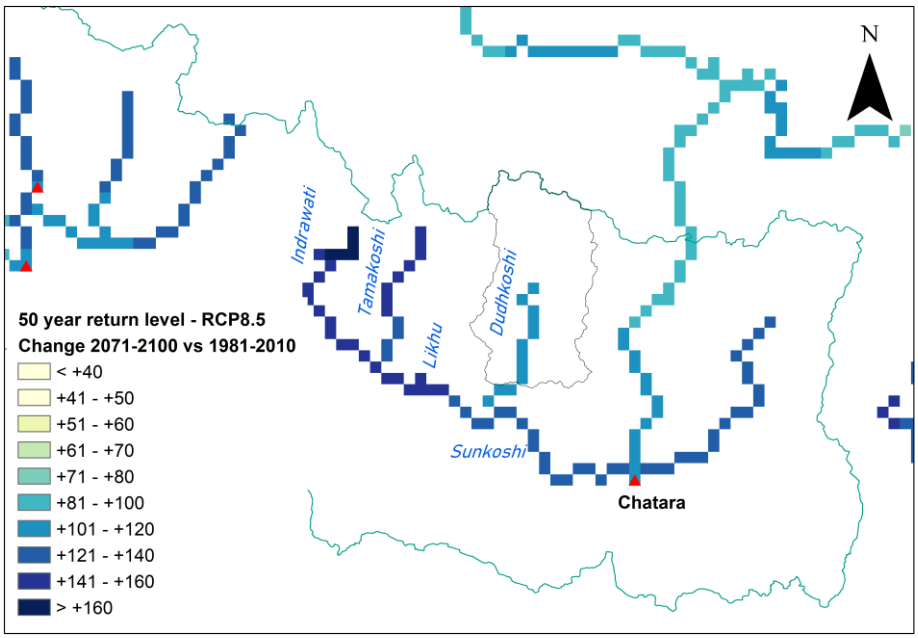

Figure 30. Relative changes in 50-year return period discharge level. Maps showing the mean relative changes in 50-year return period discharge levels (%) at the end of the 21st century (2071–2100) under RCP4.5 (top) and RCP8.5 (bottom). Maps show the ensemble mean projections. Red triangles indicate locations where flow duration curves described in this section have been established. The grey boundary represents the catchment area upstream of the prsoposed DKSHEP dam (Data source: Wijngaard et al., (2017)).

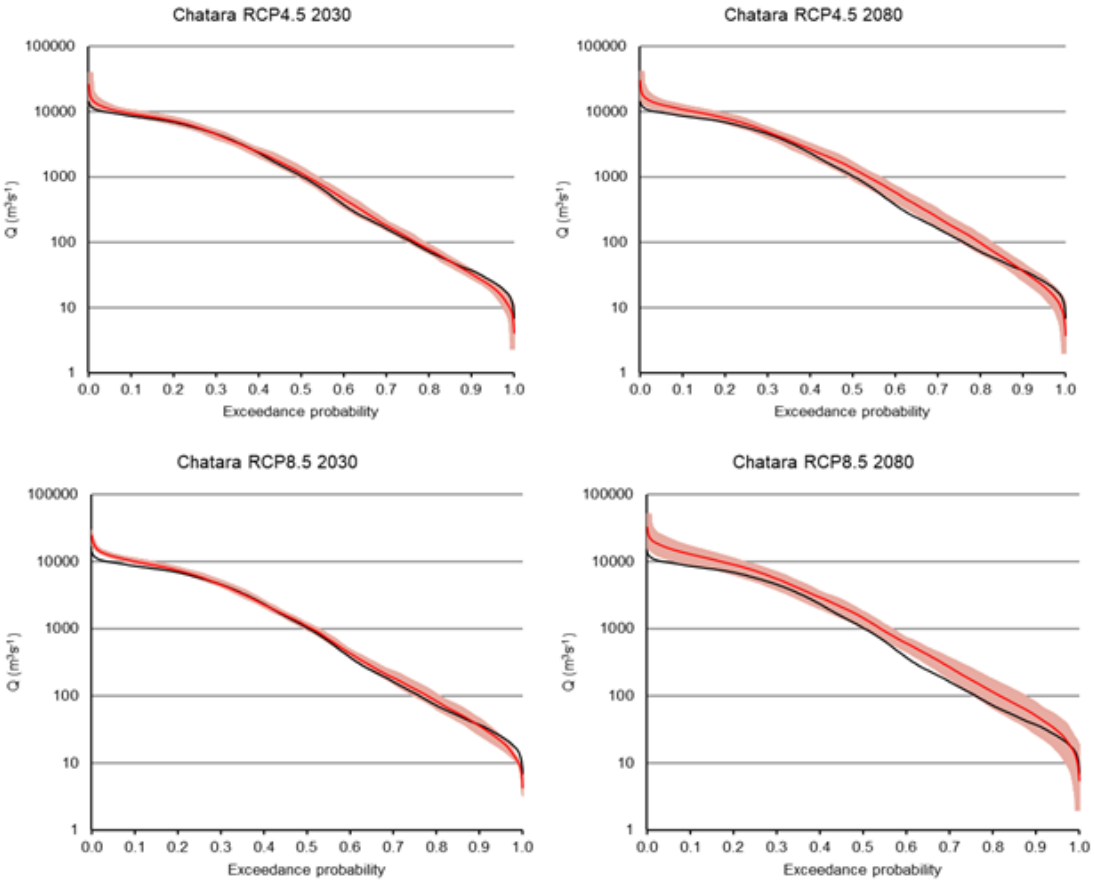

Figure 31. Flow duration curves for location Chatara. The black line indicates the flow duration curve for the historical reference (1981-2010). The red line indicates the future flow duration curve for the ensemble mean of 4 GCM runs, for the climate in 2015-2045 and 2065-2095, and RCP4.5 and RCP8.5 respectively (Data source: Wijngaard et al., (2017)).

5.1.3 Future impacts for hazards posing risk to hydropower infrastructure

The increase in temperature, extreme precipitation events, changes in glaciers, and changes in flow regimes pose risks for hydropower infrastructure. The increase in temperature accelerates ice melt processes and results in the formation of large glacial lakes. The projected increase in extreme precipitation events first leads to more frequent high flows and floods. This increases the risk of damage to hydropower infrastructure. On the other hand, an increase in extreme precipitation events leads to an increase in the number of landslides and similar natural hazards. As seen for example in the Chamoli disaster in Uttarakhand in early 2021, increases in these types of hazards can be disastrous for hydropower infrastructure. In this case, hydropower infrastructure that was still under

construction had already been destroyed. An increase in extreme precipitation events and high flows will lead to increasing sediment loads. These negatively impact hydropower infrastructure, by increased weathering of turbines, as well as filling of head ponds and reservoirs.

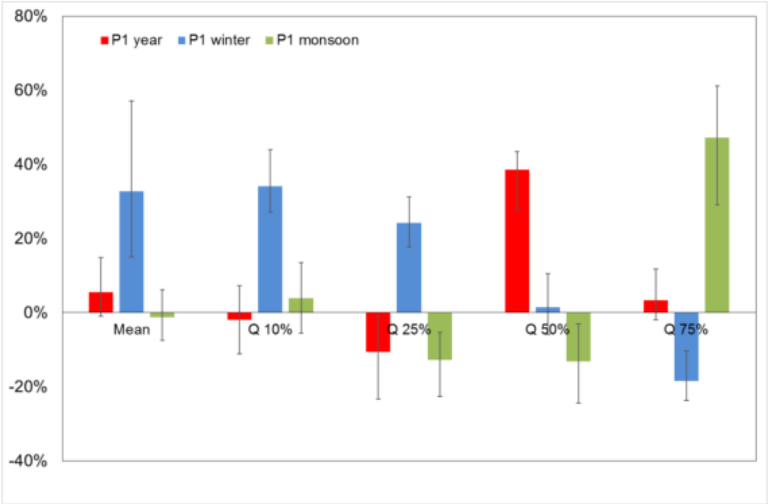

a)

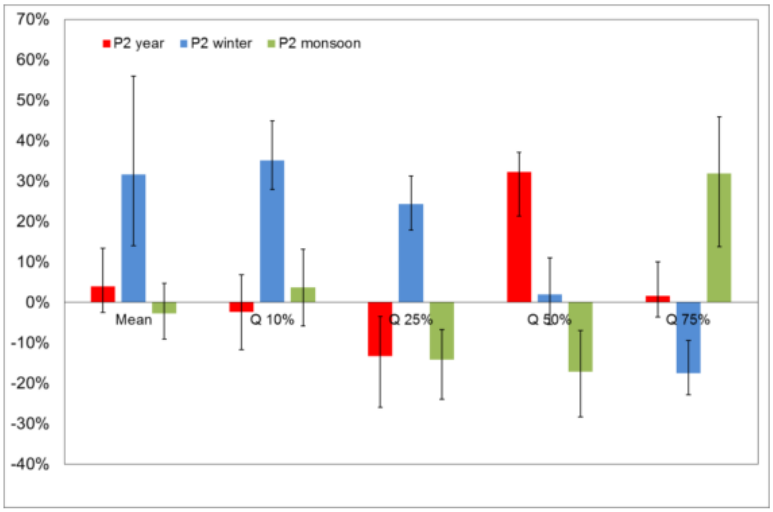

b)

Figure 32. DudhKoshi river closed at the dam site. Percentage difference of stream flow values for notable durations, mean, max/min over all the scenarios, for year, winter, and monsoon season (a) P1: 2015-2065, and (b) P2: 2066-2100 (Source: Dudhkoshi SHEP - Detailed Design - Vol. 02 - Hydrological and Meteorological Report - Jan 2020).

5.2 Identification of key hazards

To identify the relevant vulnerabilities, information gathered from the available documentation and data on the area will be used. The following potential key vulnerabilities are identified for DKSHEP.

- **Slope instability** and the likelihood of **landslides** due to heavy rainfall during the Monsoon period
- **Soil erosion** and **sedimentation** due to heavy rainfall during the Monsoon period
- **Flash flooding** due to heavy rainfall and insufficient drainage during the Monsoon period
- **GLOF** due to extreme precipitation, increased temperature, and seismic activity

- **Droughts** causing reduced generation
- **Heat Stress** causing increased losses in transmission networks
- **Reduced dry season flow** and impact on environmental flows

Based on these hazard maps and hazard levels, for each of the hazard types, the following sections discuss how the climate projections presented in the previous chapter are likely to affect the hazard level and the related potential impact to the project.

5.2.1 Slope instability and landslides

The active seismicity along the Indian and Eurasian plate boundary, steep slopes, high topographic relief, and extreme rainfall from short cloudbursts to prolonged rainfall of several days to weeks during the monsoon season is the prime cause for Nepal to be a hot spot for landslide activity (Kirschbaum et al., 2020). The prolonged period of extreme precipitation and high temperature, in addition to seismic activities and anthropogenic activities such as deforestation, irrigation, mining, road construction, etc. make such areas even more prone to landslides (Raut & Gudmestad, 2017). Due to these reasons, Nepal faces hundreds of landslides every year. The landslides in Nepal cause significant damage to infrastructure, and hundreds to thousands of fatalities annually and thus hinder economic development (Petley et al., 2007). The impact of landslide hazards can also have cascading and compound consequences, such as access to potable water, upstream floods due to temporary blockage of river flow, downstream floods damage after the landslide-induced dam break, damage to infrastructure such as hydropower, irrigation, river training work, road and electricity interruptions (W. W. Immerzeel et al., 2013; Leonard et al., 2014; Ridder et al., 2020; Shugar et al., 2021; Zscheischler et al., 2020). The heuristic fuzzy approach-based study on 1 km resolution conducted by Stanley and Kirschbaum, (2017) incorporating the most up-to-date data showed the region around DKSHEP is severely susceptible to landslide hazards (**Figure 33**). This study incorporates data on key factors including the presence of roads from OpenStreetMap, the strength of bedrock and soils, and the locations of faults from the geological map of the world.

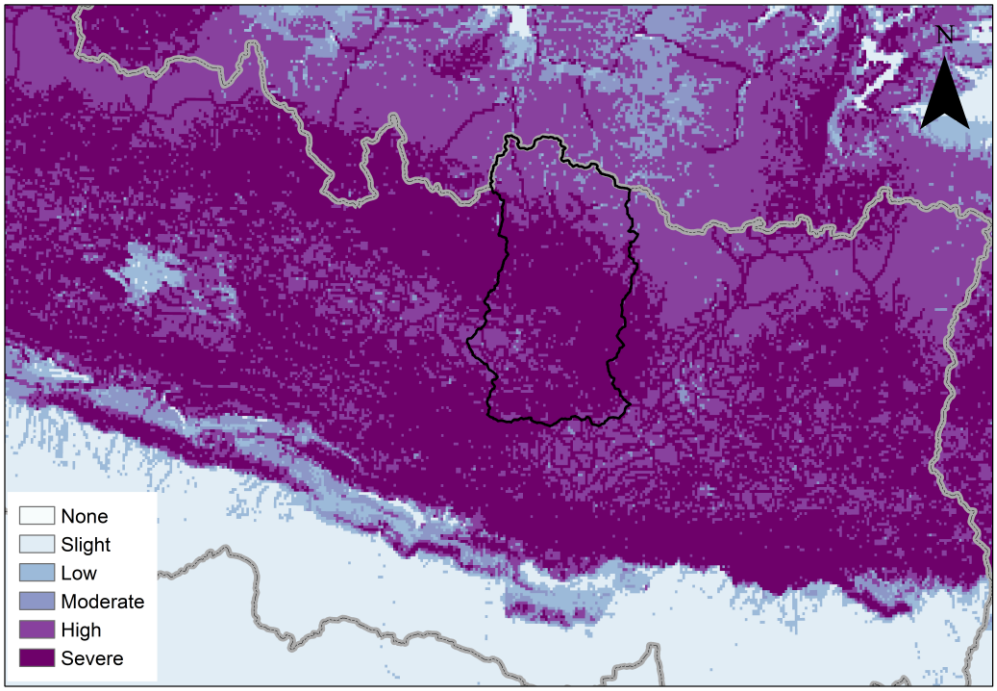

Figure 33. Landslide susceptibility map for the DKSHEP project. The black boundary represents the catchment area upstream of the proposed DKSHEP dam (Source: Stanley and Kirschbaum, (2017))

Moreover, there are large uncertainties over the estimates of landslide activity under climate change over the high mountains of Asia (Kirschbaum et al., 2020). Kirschbaum et al., (2020) found that an increase in intense precipitation will greatly affect the landslide activity over the HMA region. Furthermore, they found the largest changes to potential landslide activity are expected during the Monsoon months. Results show that within the areas of glacial lakes (131 in total), potential landslide activity is projected to increase by 20% or more for 128 (98%) of the lakes and 50% or more for 42 (32%) of the lakes (**Figure 34**).

Hazard, which involves the movement of a large amount of water, generally cascades and causes a downstream chain reaction (Shugar et al., 2021). Examples of such recent catastrophic events are the Kedarnath floods of June 2013 (Bhambri et al., 2016) and the Chamauli floods of February 2021 (Shugar et al., 2021). The lake outburst and debris flow disaster originating above Kedarnath resulted from a series of unusual hydrometeorological conditions, an unfavorable topographical disposition of the lake and watershed area, an unstable dam structure, and a lack of any stable lake outlet channel. The unprecedented heavy rainfall due to the early onset of monsoon in mid-June, immediately following a 4-week period of rapid snow cover depletion, elevated streamflow in the watershed above Kedarnath resulting in failure of saturated slope and significant run-off into the small seasonal glacial lake (Figure 35). Over more than 4000 people were killed in this event and countless buildings, roads, pilgrimage sites and infrastructures like hydropower were severely damaged and destroyed (see **Figure 36**, **Figure 37** and **Figure 38**).

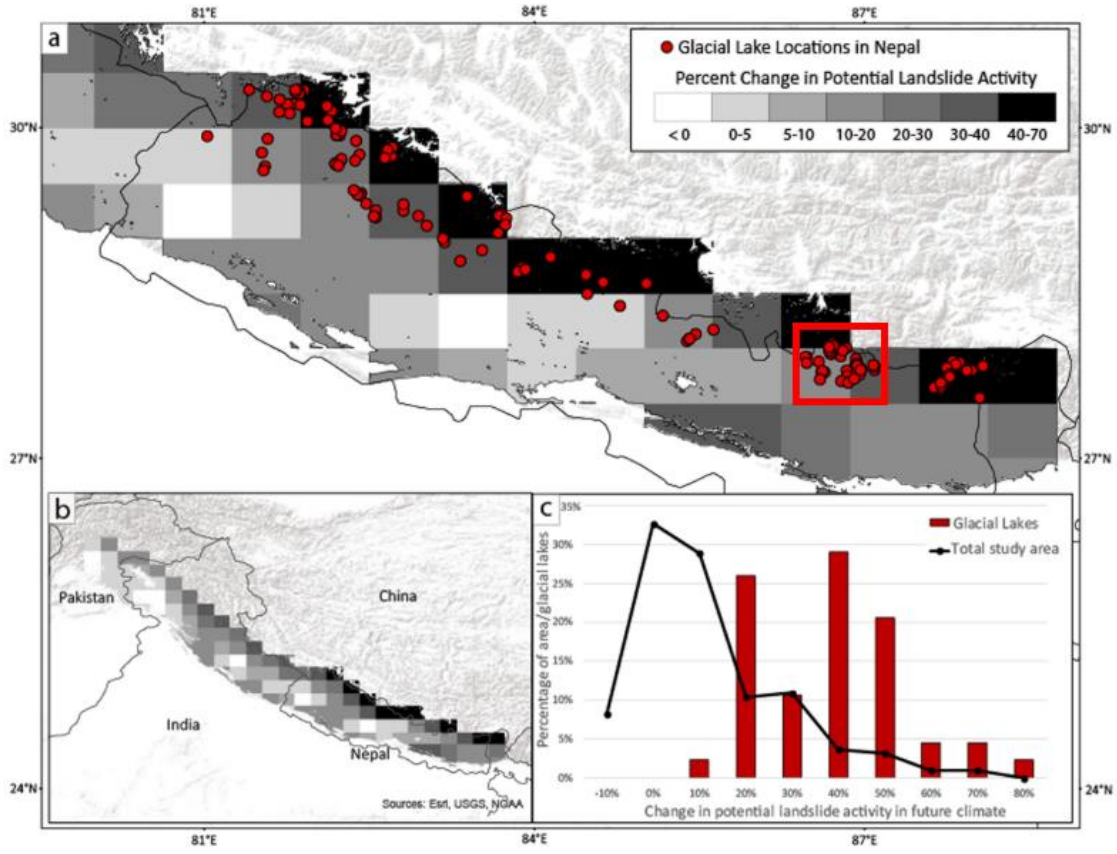

Figure 34. This figure plots the percent change in potential landslide activity comparing the present (1961–2000) and future scenarios (2061–2100), where a positive value indicates an increase in potential landslide activity toward the end of the century. Subplot (a) highlights the spatial pattern over Nepal overlaid with the current locations of 131 glacial lakes. The red box roughly indicates the region around DKSHEP, (b) shows the total study area distribution for the full year, and (c) plots the distribution of change comparing the potential landslide activity over the study area (black) and the

distribution of values at each of the glacial lake in Nepal (red). The categories of change in potential landslide activity are exclusive of the upper value such that the 0–10% bin includes all values from 0 to <10%, 20% bin includes 10% to <20%, etc.

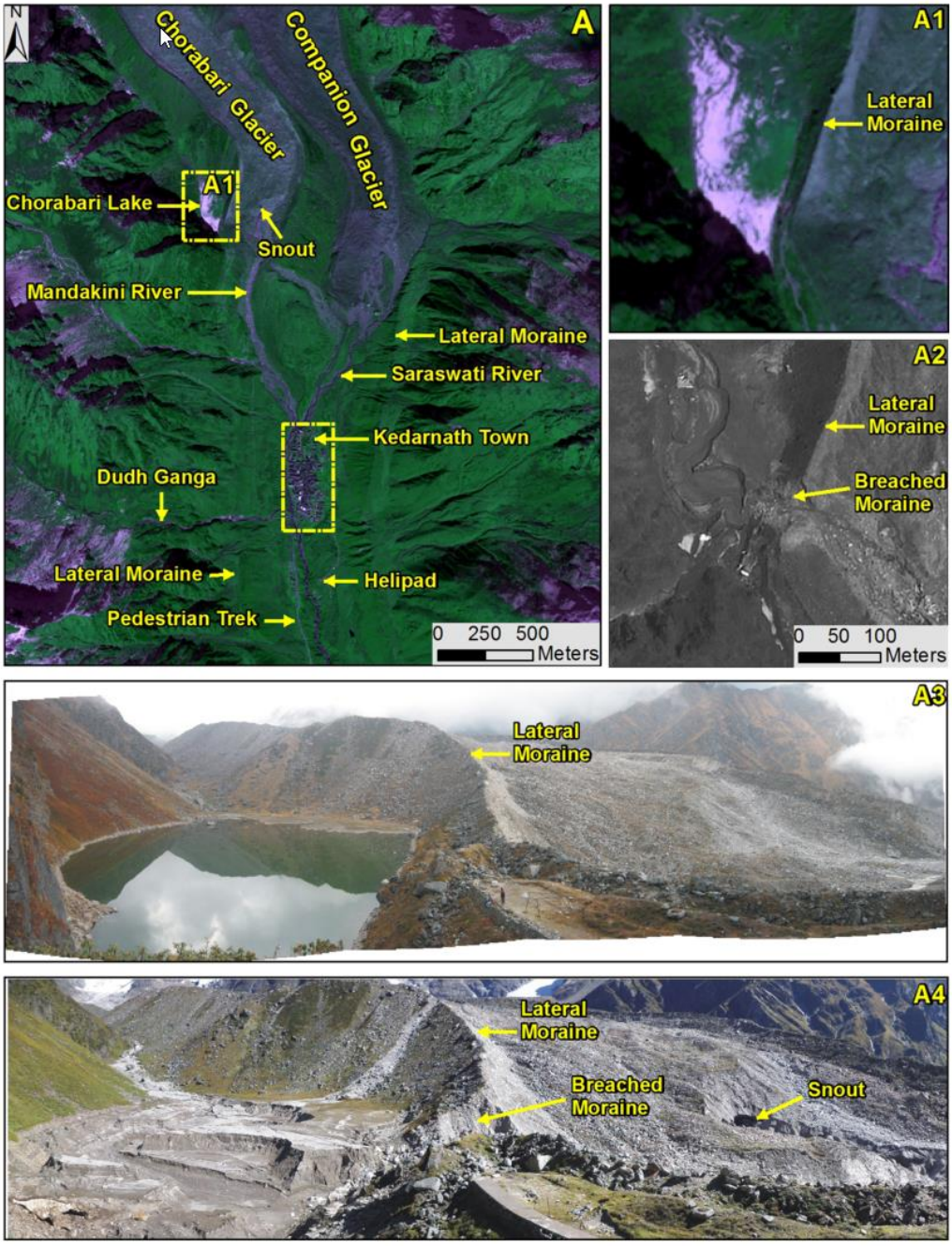

Figure 35. Ground and satellite images of Kedarnath and the surrounding area: A pre-disaster Worldview
multispectral FCC image; A1 closer view of Chorabari Lake in pre-disaster Worldview image; A2 closer view of Chorabari Lake in post-disaster Panchromatic Cartosat 2A image; A3 pre-disaster ground photograph of Chorabari Lake; and A4 post-disaster ground photograph of Chorabari Lake (Source: Bhambri et al., (2016))

Figure 36. Photographs showing the devastation between Sonprayag and Gaurikund: (a) Red arrow indicates direction of motorable road, which was completely damaged near Sonprayag; (b) power house station, which was entirely smashed; (c) broken bridge site and temporary overpass on the Songanga tributary of Mandakini River; (d) downstream flood-affected view of Sonprayag; (e) damaged road between Sonprayag and Gaurikund; red arrow shows direction to Rambara, and (f) flood level of Mandakini and damaged road near Gaurikund; red arrow shows direction to Rambara (Source: Bhambri et al., (2016)).

Figure 37. Photographs of pre-event and post-event show landscape changes between Lanchuri Dhar and Ghanurpani, 2 km downstream of Shri Kedarnath shrine (Source: Bhambri et al., (2016)).

Figure 38. The Uttarakhand flood exceeded every previous high-end boundary of water surge, infrastructure failure, and survivability. At the Vishnuprayag Hydroelectric Project on the Alaknanda River, floodwaters surged over the 55-feet tall dam and boulders buried it in 60 feet of rubble. (top). Mud and silt still lie in piles on the top of the dam. The cracked and ruptured concrete, and exposed steel reinforcing bars on the dam's walls, are evidence of the beating the dam took from the Uttarakhand flood in mid-June 2013 (bottom) (Source: https://www.circleofblue.org/).

A heavy rainfall-induced landslide on August 2, 2014 about 16 km downstream of the powerhouse on the Sunkoshi River at Jure, Nepal significantly impacted several hydropower structures (**Figure 39**). The soil and rock mass flowed downslope and across the valley and up onto the opposite bank, damming the river. The landslide dam created was about 400 m long (east-west), 105 m at the base and 30 to 35 m high, which created a lake 3 km long and about 200 m in width, with a volume of 8.6 million m^3. The catastrophic event caused by the landslide and damming of the river led to at least 200 fatalities. Significant impacts to the infrastructure were recorded including the submerged powerhouse of the 2MW Sanima Hydropower Project, two gates at the 10 MW Sun Koshi Hydroelectric project were washed away, and damage to a 2-km-long section of the Arniko Highway. Three of the transmission line towers failed and power from 45 MW Upper Bhote Koshi was interrupted for six months as new towers needed to be constructed. Nearly 10% of the nation's hydropower capacity was impacted by this landslide event (Bhatt, 2017).

Figure 39. Jure landslide on the Sunkoshi River (left). Damages to Sunkoshi hydropower and Araniko highway after the breach of the landslide dam (right) (Source: Retrieved from Google on 15th July 2021).

5.2.2 Floods

Fluvial floods are among the most common and devastating natural disasters worldwide (Yukiko Hirabayashi et al., 2021). Fluvial flood is common in the rainy season in Nepal and has been the most frequent, highly damaging, and widespread natural hazard (**Figure 40** and **Figure 41**). Among Himalayan countries, Nepal accounts for significant upstream portions of the Himalayan region that has steep and rugged topography, diverse land cover patterns, and biodiversity (Shin et al., 2021). South Asian monsoon strongly modulates the seasonality of the river flows in Nepal as it brings 80% of the annual precipitation from June to September (Bookhagen & Burbank, 2006). The intense monsoon precipitation produces a typical unimodal hydrograph (**Figure 42**) with a sharp rise in flow volumes, often causing widespread flooding. Most flood-related disaster occur in Nepal during the monsoon season (**Figure 41**). The change in historical annual flow is found to vary according to the basin locations (**Figure 42**). The Koshi river basin shows a wet period only above the 50th quantile during 1990-2005 and a relatively dry period after 2010 (**Figure 42** right sub plot).

Flood risk has changed drastically over the years could be attributed to factors such as socioeconomic growth and climate change (Yukiko Hirabayashi et al., 2021). The climate models predict significant changes in extreme precipitation and temperature compared across Nepal (Chhetri et al., 2021). Many studies confirm that the rain is becoming more erratic, leading to extremes, such as floods. Moreover, the likely escalations in hydrological extremes like floods, and flash flood floods will have strong social and economic consequences.

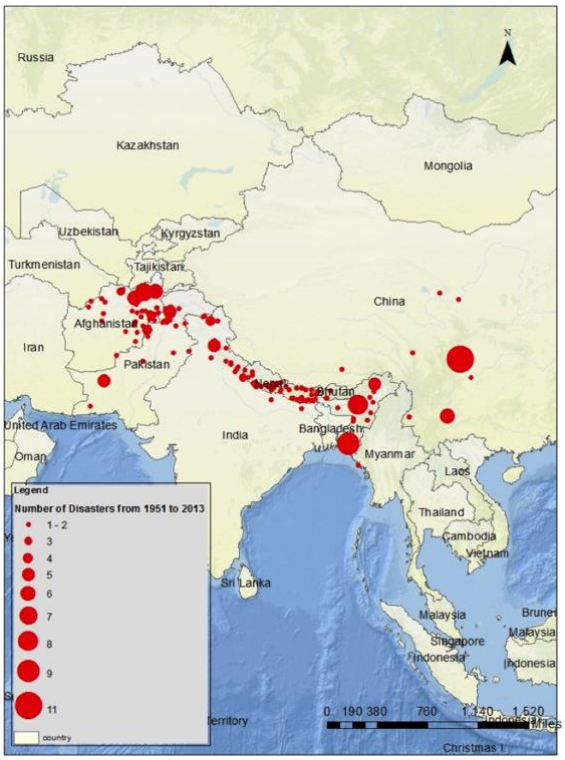

Figure 40. Spatio-temporal patterns of frequency of "reported" flooding disasters over 1951–2013 (Source: Elalem and Pal, (2015)).

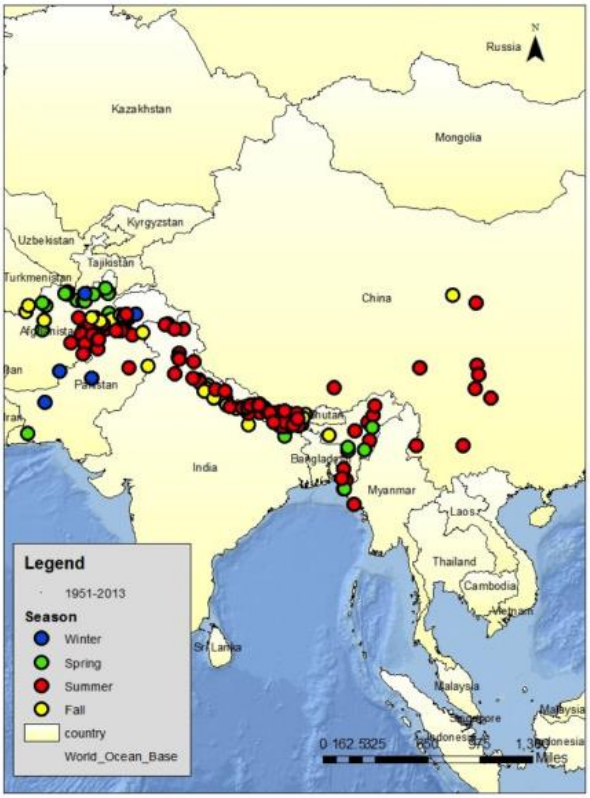

Figure 41. Timing of flooding disasters over the HKH region as per historical record; winter is Dec—Feb, spring is Mar—May, summer or monsoon is Jun—Aug, and autumn is Sep—Nov. (Source: (Source: Elalem and Pal, (2015)).

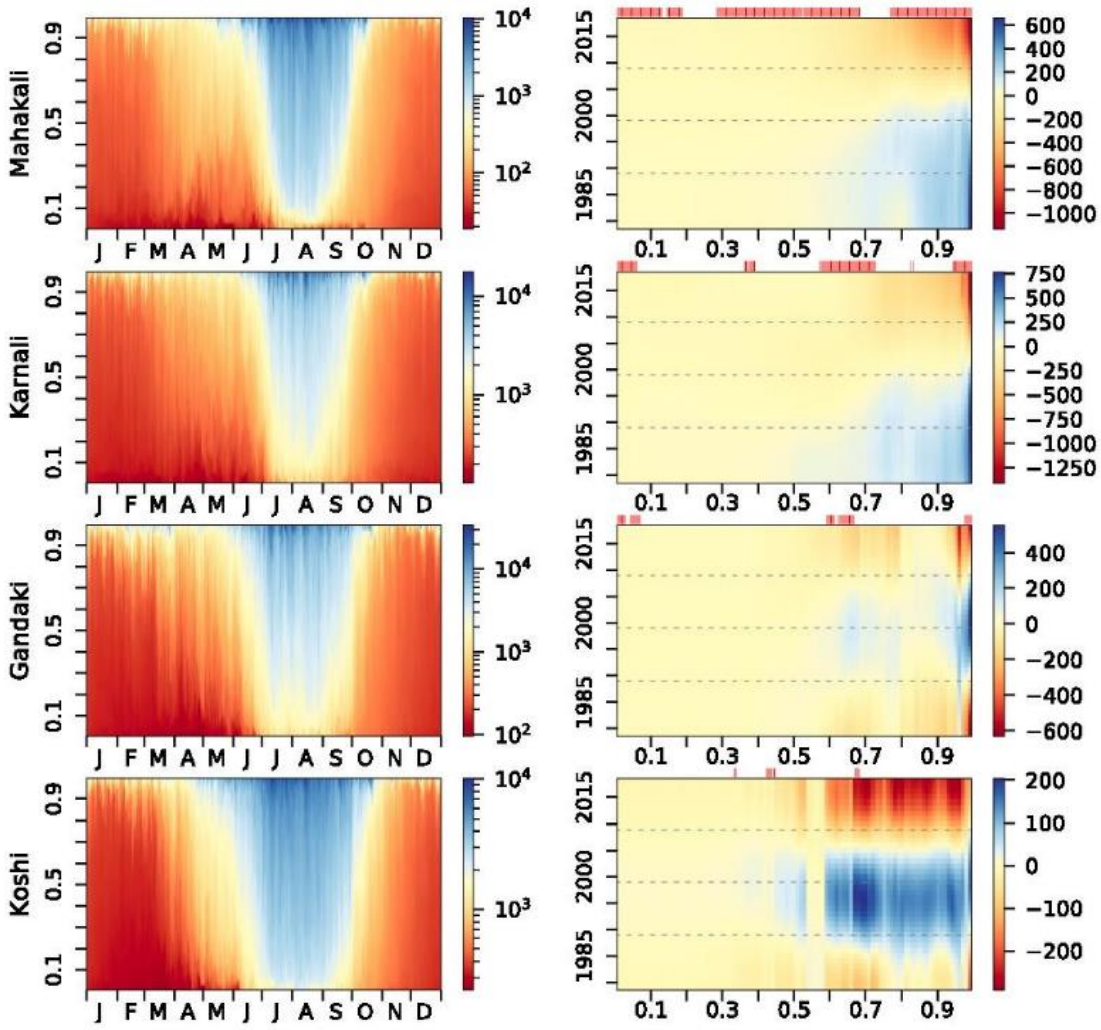

Figure 42. Evolution of river discharge at the outlets of four major river basins in Nepal over the 1979–2018 period. Long-term seasonality (left) and changes in annual discharge in cumecs (right). Red and blue bars on top of the subplots in the right plot indicate significant monotonic decrease and increase, respectively, over the 40-year period at a given DOY (day of year). Gray dash lines in the left subplot indicate decadal periods from 1979 to 2018 (Source: Shin et al., (2021)).

5.2.3 GLOF

Glaciers are the headwater of many river systems in HMA (W. W. Immerzeel et al., 2020). Global warming is causing the excess retreat of the glaciers in this region (Kraaijenbrink et al., 2017). The wasting of glacier is further associated with the rapid expansion and formation ice-dammed, moraine-dammed lakes. The sudden release or outburst of water due to the breaching of these moraine dams and lakes, create a GLOF, causing damage to lives, livelihoods, assets, and infrastructure locally and up to hundreds of kilometers downstream of their source (Cook et al., 2018). With the retreat of glaciers, frequently proglacial lakes are formed between the former moraines and the retreating glacier front, filled with meltwater. These can become unstable and burst, resulting in extreme flooding downstream (Allen et al., 2016; Harrison et al., 2018; A. B. Shrestha et al., 2010; Zaginaev et al., 2016).

The impact of a GLOF can cascade and extend across international boundaries, creating severe challenges for early warning and other risk reduction strategies. Outburst floods from moraine-dammed glacial lakes can be triggered by various mechanisms, including intense precipitation and snowmelt

and most commonly, from the impact of ice and/or rock avalanches into a lake (N. R. Khanal et al., 2015). Zheng et al., (2021) found that 6.8 ± 0.1% in the glacial lake area and 5.9% in lake number across the Third Pole between 1990 and 2015. The authors also found that at least 296 GLOF events from 109 glacial lakes occurred over the Third Pole since 1560. As per the results from their study, GLOFs in the central Himalayas are primarily from the failures of moraine-dammed glacial lakes (**Figure 43**). This study suggested that there is notable regional variation in projected glacial lake development from east to west, with a region such as central Himalaya (the region where DKSHEP is located) already revealing close to their maximum lake area by 2050, for RCP 8.5 scenario (**Figure 44**). The authors also provide the quantitative assessment of potential GLOF hazard and risk for a total of 6,958 existing moraine-dammed glacial lakes across the Third Pole and provide hierarchical classifications (**Figure 45**). It has been found that the GLOF hazard and risk are higher for the central Himalayan region (where the DKSHEP is located, **Figure 45**) and the total risk value in future under RCP8.5 is approaching a state of 'peak risk' by the end of the twenty-first century (**Figure 46**). The border region between PRC and Nepal will remain a major hotspot (~42% of all these future dangerous glacial lakes).

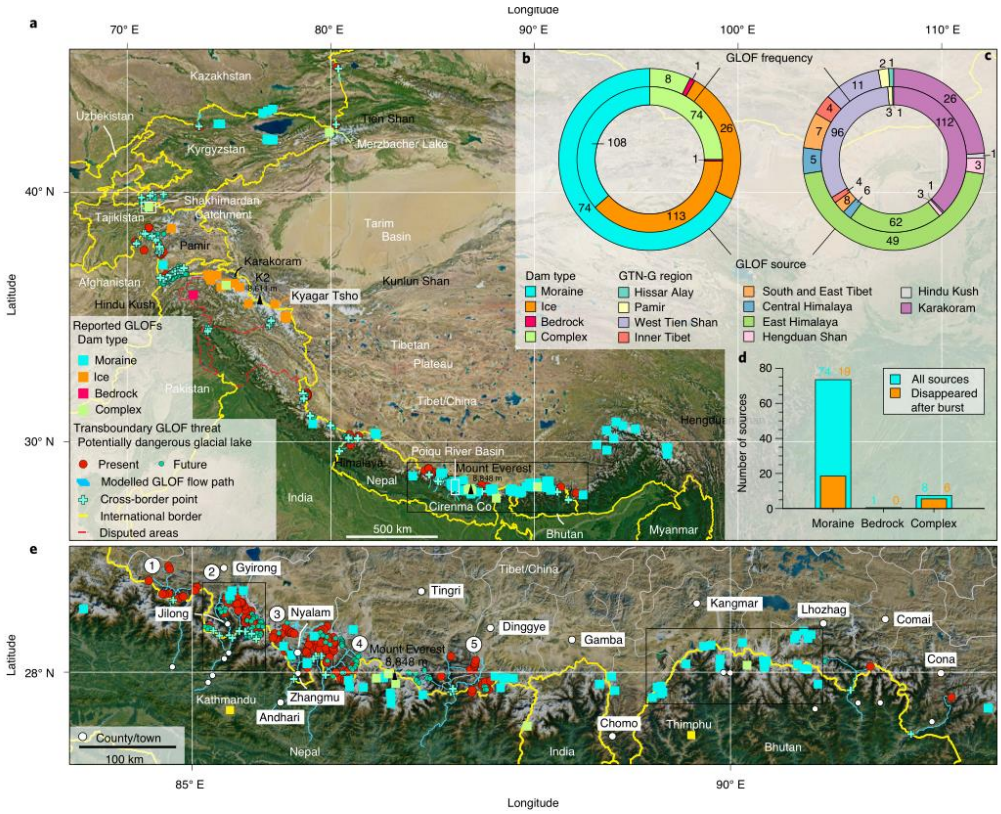

Figure 43. Reported historical GLOFs and potential transboundary threats on the Third Pole. (a) Map showing the spatial distribution of recorded GLOF sources by lake dam type as well as present and projected (ice-free scenario) glacial lakes with possible transboundary GLOF threats across the Third Pole. For ice-dammed GLOF sources, only those with known geographic coordinates are shown. The black box near the bottom of the panel is the location of (e). (b) Double doughnut chart representing the number of past GLOF sources and flood frequency by lake dam type. (c) Double doughnut chart showing the number of past GLOF sources and flood frequency per region. (d) Statistics of GLOF sources by lake dam type. Ice-dammed cases were not counted owing to their repetitive nature. e, Amplified map showing a hotspot of potential transboundary GLOF threat between PRC and Nepal, and a historical GLOF hotspot in the eastern Himalayas. The circled numbers represent five concentrated regions with potential transboundary GLOF threats. The capital cities of Nepal and

Bhutan are indicated with yellow squares. Base maps: Google, Europa Technologies. (Source: Zheng et al., (2021)).

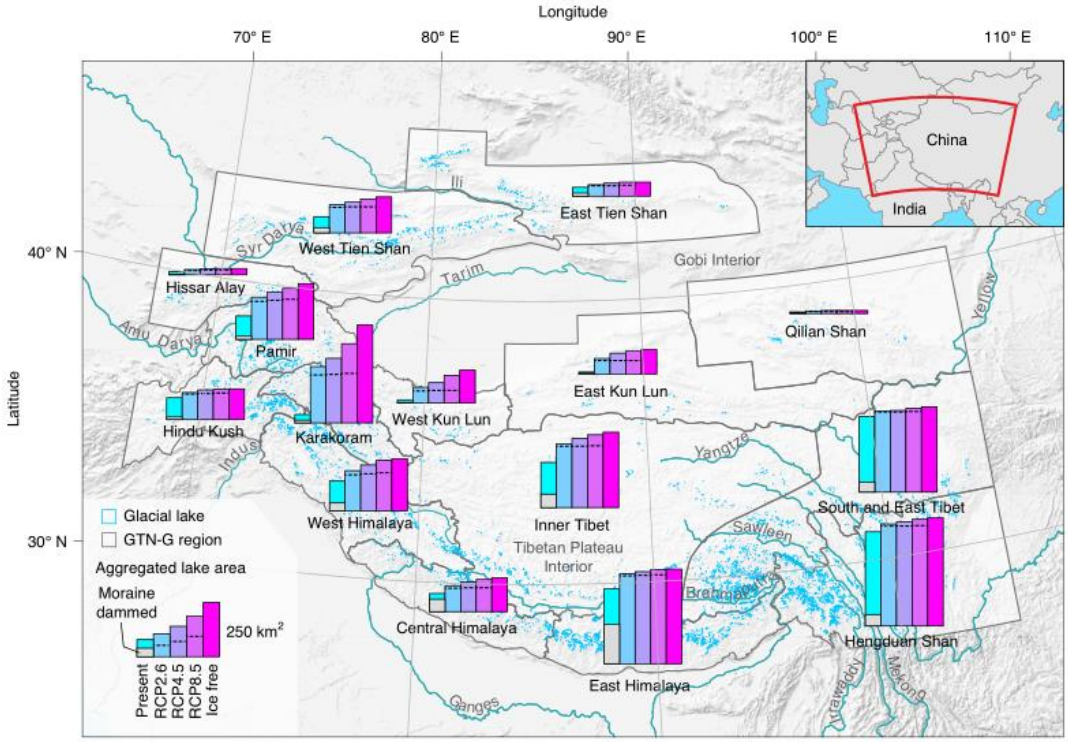

Figure 44. Region-wide present and projected glacial lakes to 2050, 2100 and on an ice-free Third Pole. Map showing the geographical extent of the Third Pole and the spatial distribution of its present glacial lakes. Bar charts in different colors denote the present and potential future glacial lake areas (present plus projected results under three RCPs, and under the ice-free scenario) that were aggregated into the Global Terrestrial Network for Glaciers (GTN-G) regions, respectively. The proportional area of present moraine-dammed glacial lakes to all present glacial lakes is shown in grey. Dashed lines show estimated changes in 2050 (Source: Zheng et al., (2021)).

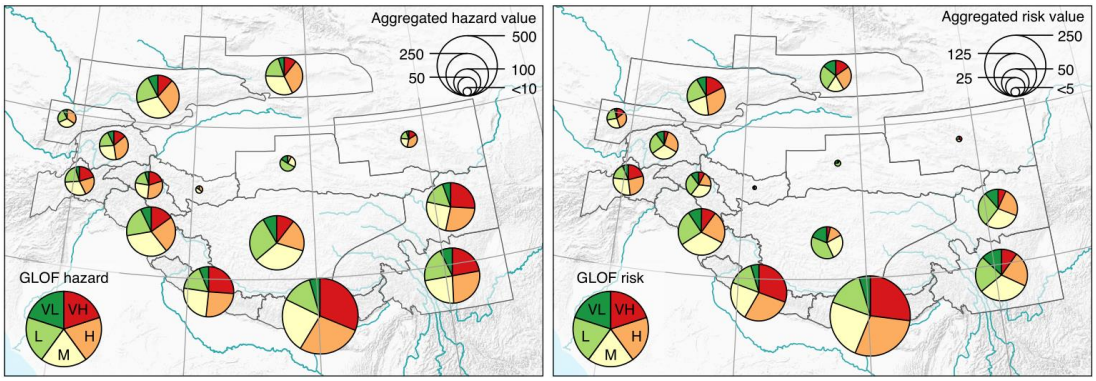

Figure 45. Region-wide present GLOF hazard and risk across the Third Pole. Pie charts showing the proportion of different GLOF hazard (a) and risk (b) levels per region. VL, very low; L, low; M, medium; H, high; VH, very high. Aggregated hazard and risk values are the total sums of normalized values within each region (Source: Zheng et al., (2021)).

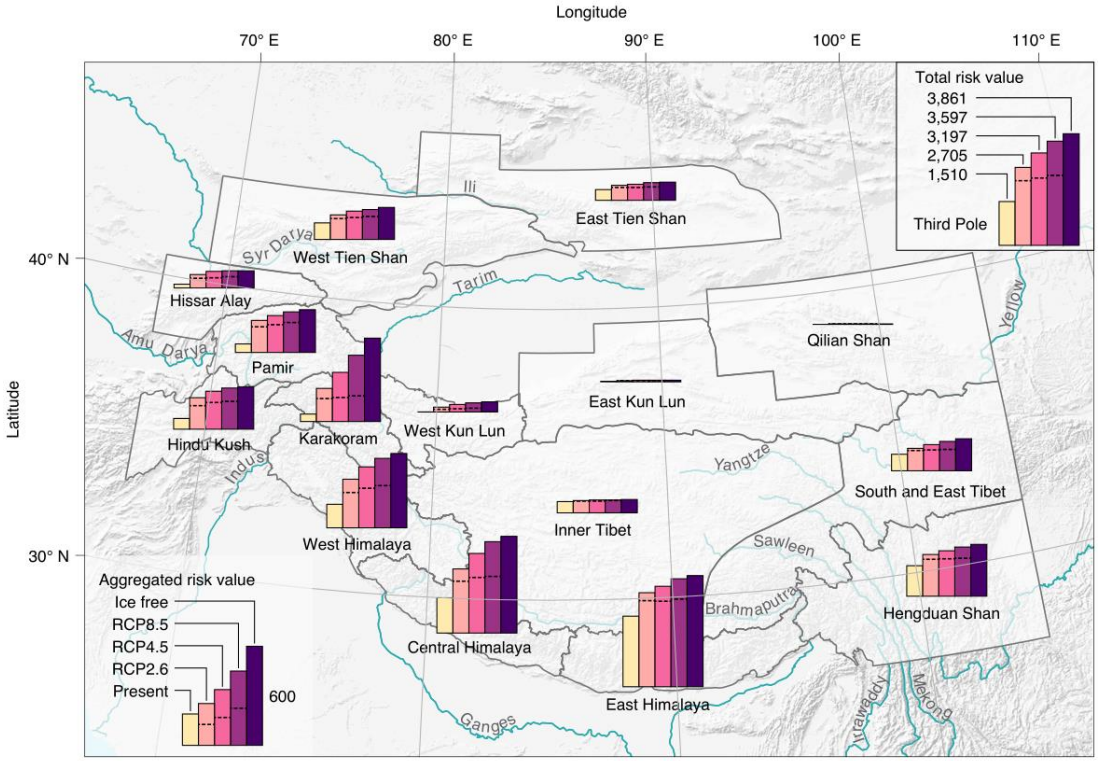

Figure 46. Region-wide future changes in GLOF risk to 2050, 2100 and on an ice-free Third Pole. Bar plots indicate projected changes in GLOF risk per region from the present to 2050 and 2100 (under three RCPs) as well as under the ice-free scenario. Dashed lines show estimated changes to 2050. The future GLOF risk was estimated based on currently known infrastructures that are exposed to modeled flood flow paths from potential future lakes and includes the assessed risk from present moraine-dammed glacial lakes (that is, these lakes are assumed to remain in the future). Inset: changes in GLOF risk over the whole Third Pole; note that the scale differs from the regional risk values. (Source: Zheng et al., (2021)).

DudhKoshi basin is the most densely glacierized region of Nepal. Almost all the glaciers are retreating at a rate of 10–59 m a^{-1} and the retreat rate has been accelerated in the last half-decade (Bajracharya & Mool, 2009). There are 473 glacial lakes in the Dudhkoshi basin and the largest one is Imja Tsho with an area of about 0.95 km^2 is recorded as one of the fastest-growing lakes in the entire Himalayas. The other important lakes in the Dudhkoshi basin are Lumding Tsho, Dig Tsho, Imja Tsho, Tam Pokhari, Dudh Pokhari, Hungu and Chamiang. Amongst the numerous glaciers and glacial lakes, the Dudhkoshi basin includes 12 potentially dangerous glacial lakes, the largest number in any sub-basin of Nepal. All of these potentially dangerous glacial lakes, except lake 444, are dammed by loose and unstable moraine (Bajracharya & Mool, 2009).

At least 24 GLOF events (**Figure 47**), 12 originating in the Nepal Himalayas, are known to have had an impact on Nepal (ICIMOD, 2011). Three GLOF events are recorded in the Dudhkoshi region in the past (**Table 12**). The first event was recorded on September 3, 1977. The event is caused by the rapid inflow of water into Lake Nare, situated below Mt Ama Dablam, leading to the overtopping of the end-moraine of the lake and water is discharged to Imja river in the Dudhkoshi valley. About 4-5 $x10^5$ cubic meters (cumecs) of water is released from Nare Lake with a peak of 800 cumecs. The second event recorded in the Dudhkoshi region was on August 4, 1985. The glacial meltwater from Dig Tsho lake, located at the end moraine of Langoche Glacier in the western section of Sagarmatha National Park, drains to Bhotekoshi and then to Dudhkoshi river. Langoche is a ‘clean-ice’ glacier, with little or no surface debris, surrounded by precipitous mountain walls and hanging glaciers. The GLOF event

appears to have been triggered by an ice avalanche (possibly accompanied by rock fall) that hit the steep glacier surface and fell suddenly into the lake. It is estimated that 6–10 million cumecs of water drained from the lake in about four hours, making the average rate of discharge about 500 and the instantaneous peak around 2000 cumecs. This event affected the Namche Small Hydel facility located 11 km from the breach. After August 1985 drainage of Dig Tsho was improved using a low-level outlet and the lake is no longer considered to be dangerous after the reformation. The third GLOF event was recorded on September 3, 1998. This GLOF was triggered when an ice avalanche hit the frontal lake (Tam Pokhari) and induced a surge wave that overtopped the end moraine dam. It is estimated that NRs 156 million in damage was incurred in this event.

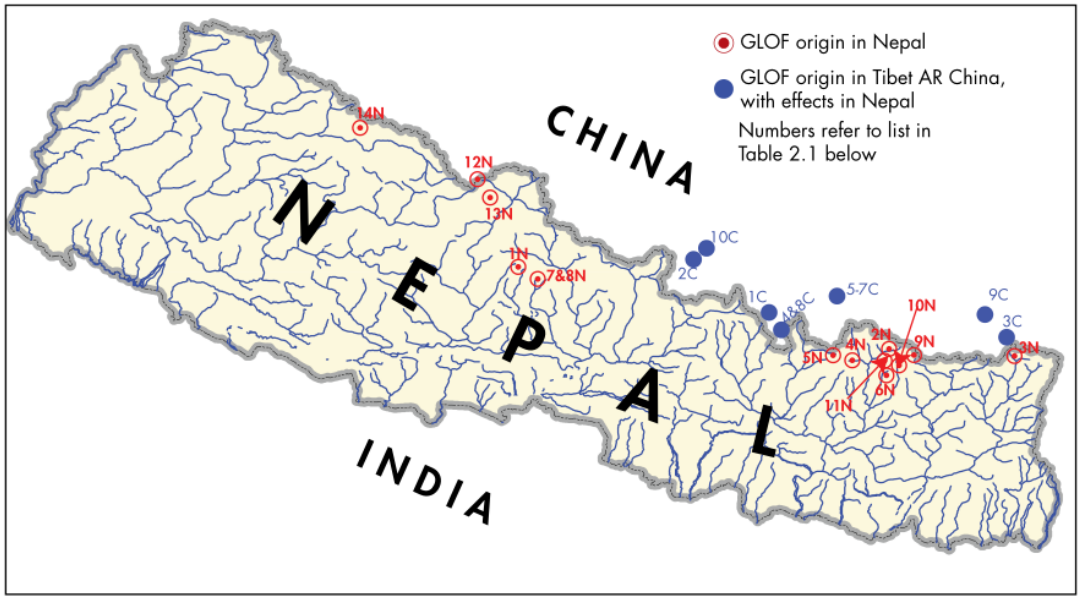

Figure 47. Location of GLOF events recorded in Nepal, and in Tibet AR, People's Republic of China, that caused damage in Nepal (Source: ICIMOD, (2011)).

Table 12. GLOF events recorded in Nepal (Source: ICIMOD, (2011)).

	Date	River basin	Lake	Cause	Losses
Entirely within Nepal					
1N	450 years ago	Seti Khola	Machhapuchchhre	Moraine collapse	Pokhara valley covered by 50–60m deep debris
2N	3 Sep 77	Dudh Koshi	Nare	Moraine collapse	Human lives, bridges, others
3N	23 Jun 80	Tamor	Nagma Pokhari	Moraine collapse	Villages destroyed 71 km from source
4N	4 Aug 85	Dudh Koshi	Dig Tsho	Ice avalanche	Human lives, hydropower station, 14 bridges, etc
5N	12 Jul 91	Tama Koshi	Chubung	Moraine collapse	Houses, farmland, etc.
6N	3 Sep 98	Dudh Koshi	Tam Pokhari	Ice avalanche	Human lives and more than NRs 156 million
7N	15 Aug 03	Madi River	Kabache Lake	Moraine collapse	Not known
8N	8 Aug 04	Madi River	Kabache Lake	Moraine collapse	Not known
9N	Unknown	Arun	Barun Khola	Moraine collapse	Not known
10N	Unknown	Arun	Barun Khola	Moraine collapse	Not known
11N	Unknown	Dudh Koshi	Chokarma Cho	Moraine collapse	Not known
12N	Unknown	Kali Gandaki	Unnamed (Mustang)	Moraine collapse	Not known
13N	Unknown	Kali Gandaki	Unnamed (Mustang)	Moraine collapse	Not known
14N	Unknown	Mugu Karnali	Unnamed (Mugu Karnali)	Moraine collapse	Not known
Originated in TAR/China and caused damage in Nepal					
1C	Aug 1935	Sun Koshi	Tara-Cho	Piping	66,700 sq.m of wheat fields, livestock, etc
2C	25 Aug 64	Trishuli	Longda	Not known	Not known
3C	21 Sep 64	Arun	Gelhaipuco	Glacier surge	Highway and 12 trucks
4C	1964	Sun Koshi	Zhangzangbo	Piping	No remarkable damage
5C	1968	Arun	Ayaco	Not known	Road, bridges, etc
6C	1969	Arun	Ayaco	Not known	Not known
7C	1970	Arun	Ayaco	Not known	Not known
8C	11 Jul 81	Sun Koshi	Zhangzangbo	Ice Avalanche	Hydropower station
9C	27 Aug 82	Arun	Jinco	Glacier surge	Livestock, farmland
10C	6 Jun 95	Trishuli	Zanaco	Not known	Not known

One of the recent examples where GLOF originated in PRC-impacted hydropower facilities in Nepal was the Bhotekoshi flood of June 2016. The Upper Bhotekoshi Project (45 MW) sustained significant damage to the headworks and powerhouse from a moraine-dammed lake outburst in the Zhangzangbo River basin, a primary tributary of the Poiqu/Bhote Koshi River in PRC, about 24 km upstream of the dam. The intense precipitation (above-average rainfall for June) over the previous week saturated the Bhotekoshi watershed and consequently, the flows are above the danger level in the river. At the time of the flood, the Bhotekoshi River peaked at about 3.5 m above the top of the dam and about 1.7 m above the powerhouse yard (Bruen et al., 2017). Flood debris including large boulders, up to 8 m in diameter was carried up by flood water and struck the dam and headworks. Damage included a complete failure of the riverside wall, two bridge support piers, and the deflector wall in the desanding basin and localized damage of the base slab. Flood debris accumulated upstream of the structures, obstructing river flow and blocking the spillway and river intake. In addition, river erosion associated with the high river flows destroyed about a 100-m-long section of the left bank guide wall downstream of the powerhouse, causing instability of a section of the powerhouse backslope. The control room on the erection bay floor was completely destroyed by flooding the powerhouse (**Figure 49**). At the downstream facilities, the impacts of the debris-laden flood were largely associated with the flooding and submergence of the powerhouse equipment and transformers.

Figure 48. Damaged dam of the Upper Bhotekoshi Hydropower Project (45 MW) before (left) and after (right) flooding on 5 July 2016 on the Bhotekoshi River in Sindhupalchowk district, Nepal (Source: Bruen et al., (2017))

Figure 49. The control room on the erection bay floor was completely destroyed by flooding of the powerhouse (Source: Bruen et al., (2017))

5.2.4 Sedimentation

The reservoirs are used for many purposes, among them to provide reliable irrigation, water supply, hydropower, flood mitigation, and recreational activity and for providing downstream minimum flows for navigation. Reservoir sedimentation is a process of erosion, entrainment, transportation, deposition, and compaction of sediment carried into reservoirs formed and contained by dams. In an unregulated river, with stable catchments, sediment processes are relatively balanced. Construction of a dam decreases flow velocities, initiating or accelerating sedimentation, resulting in the deposition of earth materials such as rocks, cobble, gravel, sand, silt, and clay. The storage capacity of the reservoir decreases due to the accumulation of sediments. Moreover, the river downstream starts to erode, also known as the 'hungry water condition', due to the disturbance of the sediment balance and such processes have a big influence on the river morphology. Sedimentation in reservoirs is a considerable

and severe problem that results in undesirable side effects for the environment and costly counter-measurements (Bronsvoort, 2013). Sustainable hydropower requires dealing with the important issue of reservoir sedimentation (Kondolf et al., 2014). Many reservoirs were designed by estimating sedimentation rates in order to provide a pool with sufficient volume to achieve a specified design life. Without sustainable management, over the period of years, the sediments gradually displace the volume that was previously used for water storage, until eventually the reservoir becomes filled with sediment. Thus, the design life of the reservoir is typically far less than what is actually achievable.

Reservoir sediment comes from upland and in-channel sources which may include fields, gullies, and vegetated and forested areas, or disturbed areas where vegetation may have been cleared in preparation for a land use change. Changes in sediment yield over time will depend on watershed management, land use, sediment control measures, hydraulic structures, hydrology, and other factors, such as changes in hydrologic variability. Wildfires, landslides, volcanic eruptions, and other phenomena will affect sediment yield. Glacial retreat and melting of permafrost create new sediment sources, which may increase sediment loads. Reservoir sedimentation has impacts on the generation, and stability of the dam impacts the flushing capability of outlets and causes damage to turbines and other mechanical equipment.

Developing regions of the world that stand to benefit most from hydroelectricity are often those with the highest sediment yields (**Figure 50**). Sustainable hydropower development must involve consideration of sediment management techniques during design, construction, and operation (Annandale et al., 2016; Pradhan, 2004).

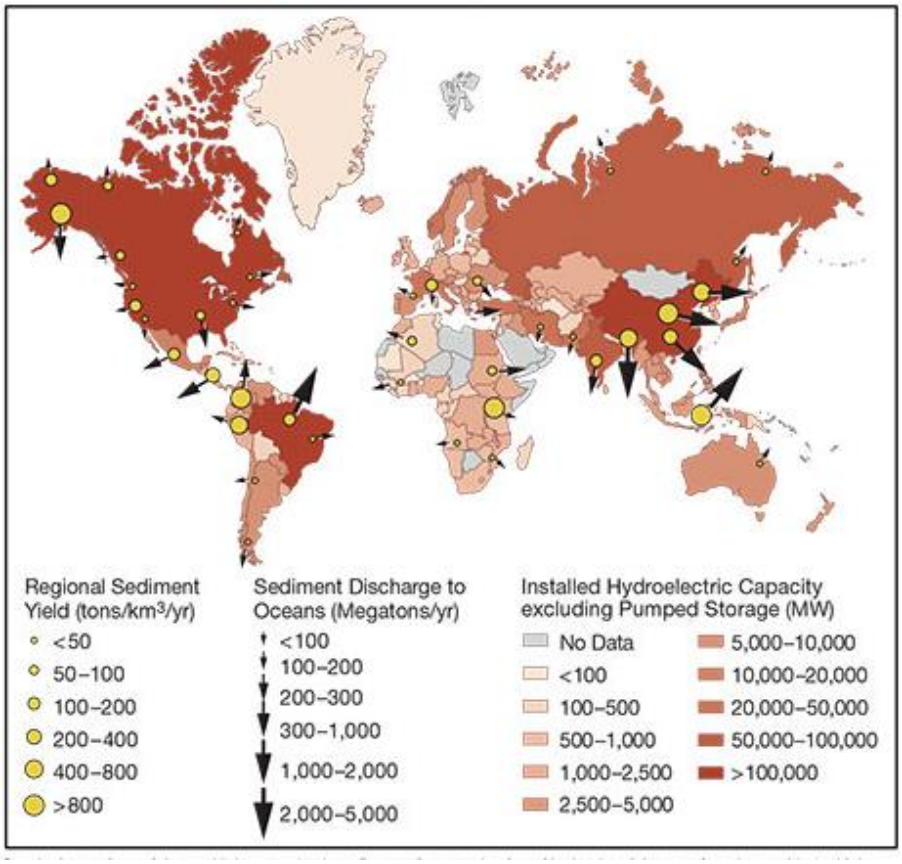

Figure 50. Comparison of Hydroelectric Potential and Sediment Production (Source: Bruen et al., (2017)).

In Nepal, sustainability of peaking run-of-river hydropower (PROR) projects, such as Kaligandaki 'A' (144 MW) and Middle Marsyangdi (70 MW), is a key issue (D. P. Sangroula, 2009). Kaligandaki 'A' has

3 units with a capacity of 48 MW each. It is a six-hour peaking run-of-river type power station with an annual design generation of 842 GWh (NEA, 2019, 2020a). A concrete gravity dam with radial crest gates stores about 3.5 million m3 (Mm^3) for peaking power generation. The power plant is shut down during major flood events (> 2000 m3/s) and the gates are opened to pass the flood through the reservoir at maximum velocity. Kaligandaki river generates a suspended sediment load of 43 Mt/yr (of which around 25 percent is sand) and about 95 % of this suspended sediment load is transported during monsoon season. This transported sand has a high concentration of highly abrasive angular quartz. The sediment transport during monsoon in Kaligandaki river is enough to completely fill the reservoir in a single season. The headworks of this project has been experiencing problems in dealing with floating debris and suspended sediment which has resulted in increased turbine erosion (**Figure 52**) problems since its operation in the year 2002 (Bishwakarma, 2012; Chhetry & Rana, 2015; Koirala et al., 2016; World Bank, 2019). The Kaligandaki A has lost 51% of the total volume and 6.7% of live storage due to sedimentation (H. S. Shrestha, 2012). The Middle Marsyangdi is a peaking runoff river facility with an annual design generation of 398 GWh and a daily peaking capacity of 5 hours at maximum river discharge. The region around intake has patches of sediment deposition mainly caused due to meandering nature of Marsyangdi river (**Figure 53**). The Middle Marsyangdi reservoir has lost 65% of its total volume due to sedimentation (H. S. Shrestha, 2012). The total losses for the live storage capacity are about 14.1 %.

Figure 51. Sediment deposition in the reservoir (left) and forebay (right) of the Kaligandaki 'A' reservoir (Source: Shrestha, (2012)).

Figure 52. Photos of damage of runner and facing plates of Unit No: 2 of Kaligandaki 'A' hydropower (Source: Chhetry and Rana, (2015))

Figure 53. Areas of high sediment deposit upstream of the reservoir (red marked areas) and location of intake (blue marked area) (Source: NDRI, (2016))

Another storage project that has been impacted by the sedimentation issue is Kulekhani I HEP. Catastrophic floods and the landslide due to a cloud burst event in the year 1993 severely impacted this project. The debris flow and landslide (over 300) during this event killed 1500 people in the Kulekhani and an immense sediment load was deposited in the reservoir (Dhital, 2003). Kulekhani I (60 MW) has lost 21.7 (more than 25 %) million m3 in total (out of 85.3 million m3) and 14 million m3 in its live storage capacity (Karky & Joshi, 2009; D. Sangroula, 2007; D. P. Sangroula, 2009). The average annual loss rate is about 1.14% of the total original volume. This project was designed in 1977 to be the only peaking hydropower that acts as an emergency standby station during peak load demand. The expected annual energy generation capacity of this plant is 165 GWH as primary energy and 46 GWH as secondary energy (NEA, 2020a). The loss of reservoir capacity has severely impacted the generation of electricity (**Figure 54**). The sedimentation load in the rivers is highly correlated with the river discharge. It is well established that the frequency and magnitude of extreme precipitation will increase in the future (see Section 4.2) and thus will also increase the chances of landslides and floods. The increase in sediment influx in the reservoir will decrease energy generation. In the future, under different scenarios, it is expected energy generation in Kulekhani I will decrease by at least 30% (**Table 13**).

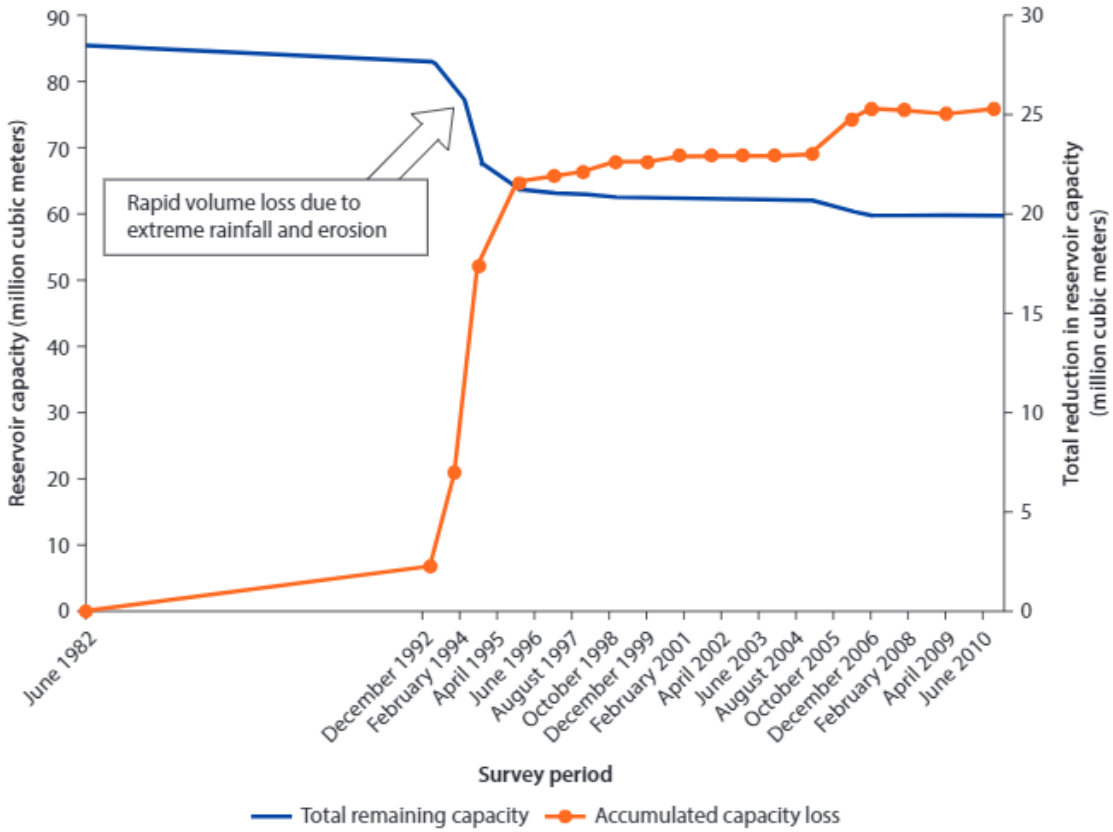

Figure 54. Loss of storage capacity in Kulekhani reservoir, Nepal, resulting from the extreme monsoon of 1993 (Source: (Annandale et al., 2016))

Table 13. Annual total energy generation by the power plant for future timeframes with A2 and B2 scenarios for different reservoir operation times and their percentage change (% ch.) as compared with baseline average annual energy generation (Source: Shrestha et al., (2014)).

Total Annual Energy Generation (GWh)												
	A2						B2					
Operating Time	2020s	% ch.	2050s	% ch.	2080s	% ch.	2020s	% ch.	2050s	% ch.	2080s	% ch.
Baseline Average Annual Energy Generation (1982–2009)=143 GWh												
3 h	54	−62	54	−62	54	−62	54	−62	54	−62	54	−62
4 h	72	−50	72	−50	71	−50	72	−50	73	−49	73	−49
6 h	92	−36	92	−36	92	−36	92	−35	93	−35	93	−35
7 h	95	−33	97	−32	95	−34	97	−32	100	−30	99	−31
8 h	101	−29	102	−29	101	−29	102	−29	113	−21	102	−28
10 h	113	−21	114	−21	112	−22	113	−21	115	−20	114	−20
12 h	113	−21	114	−20	112	−21	113	−21	117	−18	115	−20
10 h in dry and 3 h wet season	126	−12	127	−11	125	−13	127	−12	131	−8	128	−11

5.2.5 Droughts

Drought is one of the most complex and least understood extreme climatic events which may result in significant water shortages, reduced hydropower generation, crop yield reduction, economic losses, and adverse impacts on the society and environment (IPCC, 2019b; Trenberth et al., 2013, 2015; Wilhite, 2000). Droughts have become more prevalent in recent decades and are expected to intensify in the future (Dai, 2013; Mishra & Singh, 2010). Among others, droughts are dependent on meteorological, hydrological, and physiographic characteristics such as precipitation, temperature, wind, soil moisture, and topography. Four types of droughts are recognized in the scientific literature-agricultural; hydrological; meteorological; socioeconomic (Mishra & Singh, 2010).

Nepal is experiencing frequent droughts over the last few years (Ghimire et al., 2010; Khatiwada & Pandey, 2019; Miyan, 2015; Sharma et al., 2021). Several drought events, due to low precipitation, were recorded in Nepal in 1992, 1994, 2005, 2006, 2008-2009, and 2015 (Adhikari, 2018; Dahal et al., 2016). Most importantly, climate variability has induced and accelerated drought conditions in Nepal (Wang et al., 2013). The authors have found more frequent and intense droughts in the dry season over the past decade in the Western parts of Nepal. The droughts had a significant impact on crop production across Nepal (Hamal et al., 2020). For instance, the severe drought in 2008-2009 decreased the national wheat and barley production (WFP, 2009). The droughts in 2005-06 and 2006-07 decreased the overall agricultural production by 21,553 and 179,910 metric tons (WECS, 2011). Moreover, the severe drought in 2015 caused food insecurity in western Nepal, affecting more than 80% of the population (Gyanwali, 2016).

Sharma et al., (2021) investigated the national-scale drought characteristics from the standardized precipitation index (SPI) using monthly data from 220-gauge stations over Nepal for about four decades (i.e. 1980–2016). Based on the observed data authors found major drought events in 1982, 1985, 1991–1992, 1994, 2005–2006, 2008–2009, 2012, 2013, and 2015. The authors found that 1992 and 2015 were extreme drought (SPI ≤ −2) years, which occurred from the SPI1 to SPI12 timescales (**Figure 55**).

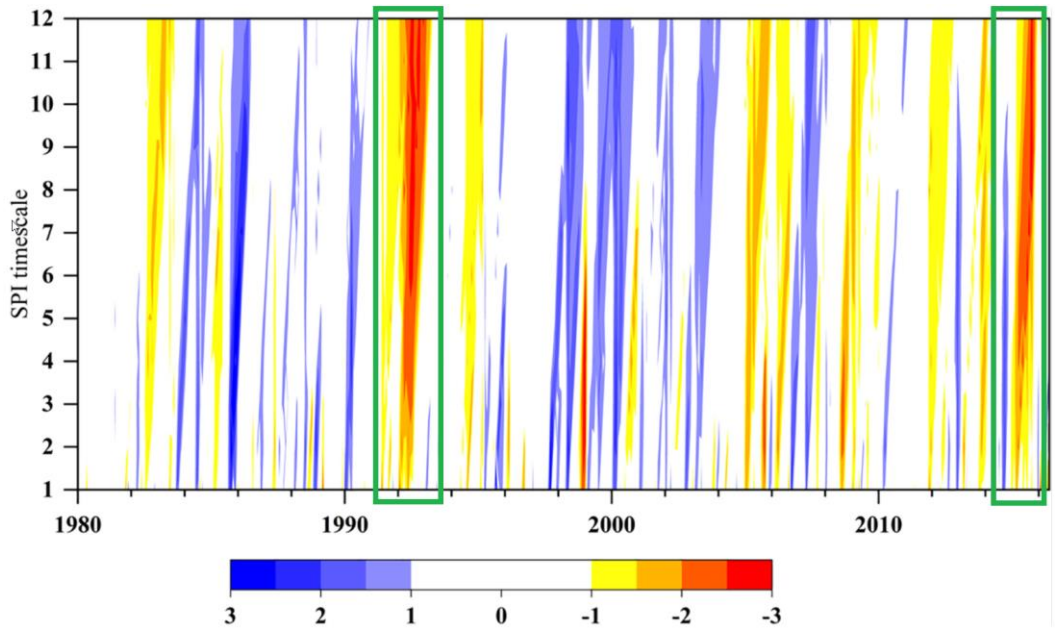

Figure 55. Temporal evolution of the standardized precipitation index (SPI) at different timescales over Nepal, 1980–2016. The yellow to red and blue values in the colour bar represent dryness and wetness, respectively. The year 1992 and 2015 are marked by green rectangles (Source: Sharma et al., (2021)).

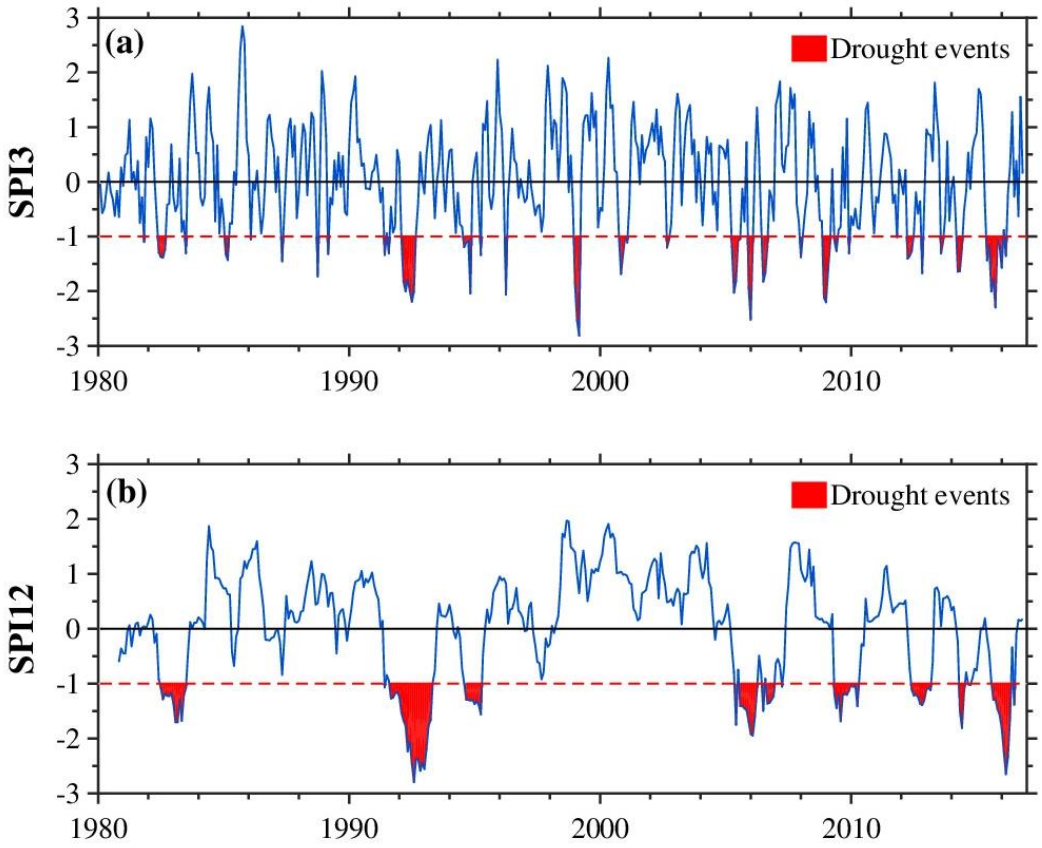

Figure 56. Temporal variation of (a) SPI3 and (b) SPI12 over Nepal, 1980–2016. The red dotted line represents the threshold level of drought (Source: Sharma et al., (2021))

Authors have found that Nepal experienced extreme short-term drought (SPI3 ≤ −2) events in 1992, 1998, 2005–2006, 2009, and 2015. A total of eight long-term drought events (SPI12 ≤ −1) in 1982–1983, 1991–1993, 1994–1995, 2005–2006, 2008–2009, 2012–2013, 2014, and 2015–2016 were also observed by authors during the study period. Moreover, most of the yearly drought events mainly occurred after 2005, suggesting that drought has increased in recent decades.

Koshi basin showed increasing frequency and intensity of drought events (Hamal et al., 2020; N. K. Shrestha et al., 2017). Joshi and Dongol, (2018) found that the severe drought in Ramechhap, the mid-hill districts in the Koshi river basin, has resulted in the drying of major spring and river sources. This has led to the migration of the community to places with better water security. Nepal et al., (2021) investigated the soil moisture deficit index (SMDI) by applying the process-based J2000 hydrological model in the transboundary Koshi River basin. The authors found the most severe drought was observed in 1992 throughout the Koshi River basin, followed by 1994. The other prominent drought years in the period under study (1997-2006) are 2006 and 2002 in the trans-Himalaya region, 1992 and 1991 in the mountains, and 1995 and 1994 in the plains of the Koshi river basin (**Table 14**). The frequency of these events has increased in the later years of the study period and is most evident in the premonsoon season (**Figure 57**).

Table 14. Average annual SMDI values, from 1980 to 2007, for trans-Himalaya, mountains, and plains and for the whole Koshi basin. Thered and blue bars show the negative and positive SMDI values; the average SMDI values for each year are given in the respective rows (Source: Nepal et al., (2021)).

Year	Trans-Himalaya	Mountains	Plains	Koshi basin
1980	1.49	0.21	0.57	0.72
1981	1.26	-0.20	0.28	0.4
1982	-0.66	-0.23	-0.32	-0.39
1983	-1.21	0.45	-0.04	-0.21
1984	-0.45	0.07	0.31	-0.02
1985	-0.39	0.15	0.51	0.09
1986	-0.29	0.96	0.18	0.33
1987	-0.33	0.55	0.65	0.31
1988	0.35	0.09	0.11	0.18
1989	-0.29	0.04	-0.17	-0.13
1990	-0.50	0.35	0.01	-0.02
1991	-0.49	-0.57	-0.42	-0.5
1992	-1.08	-0.78	-0.91	-0.91
1993	-0.24	0.34	-0.24	-0.02
1994	-1.11	-0.31	-0.97	-0.76
1995	-1.00	-0.30	-0.98	-0.72
1996	1.06	0.41	-0.01	0.49
1997	0.12	0.00	-0.17	-0.02
1998	0.92	0.71	0.87	0.82
1999	1.18	-0.11	0.36	0.43
2000	1.29	0.00	0.22	0.47
2001	-0.84	-0.09	-0.28	-0.38
2002	-1.23	0.35	0.41	-0.12
2003	-0.79	0.25	1.01	0.16
2004	-0.87	0.43	0.24	-0.03
2005	-1.05	-0.23	-0.72	-0.63
2006	-1.35	-0.26	-0.41	-0.64
2007	-0.28	0.62	0.39	0.27

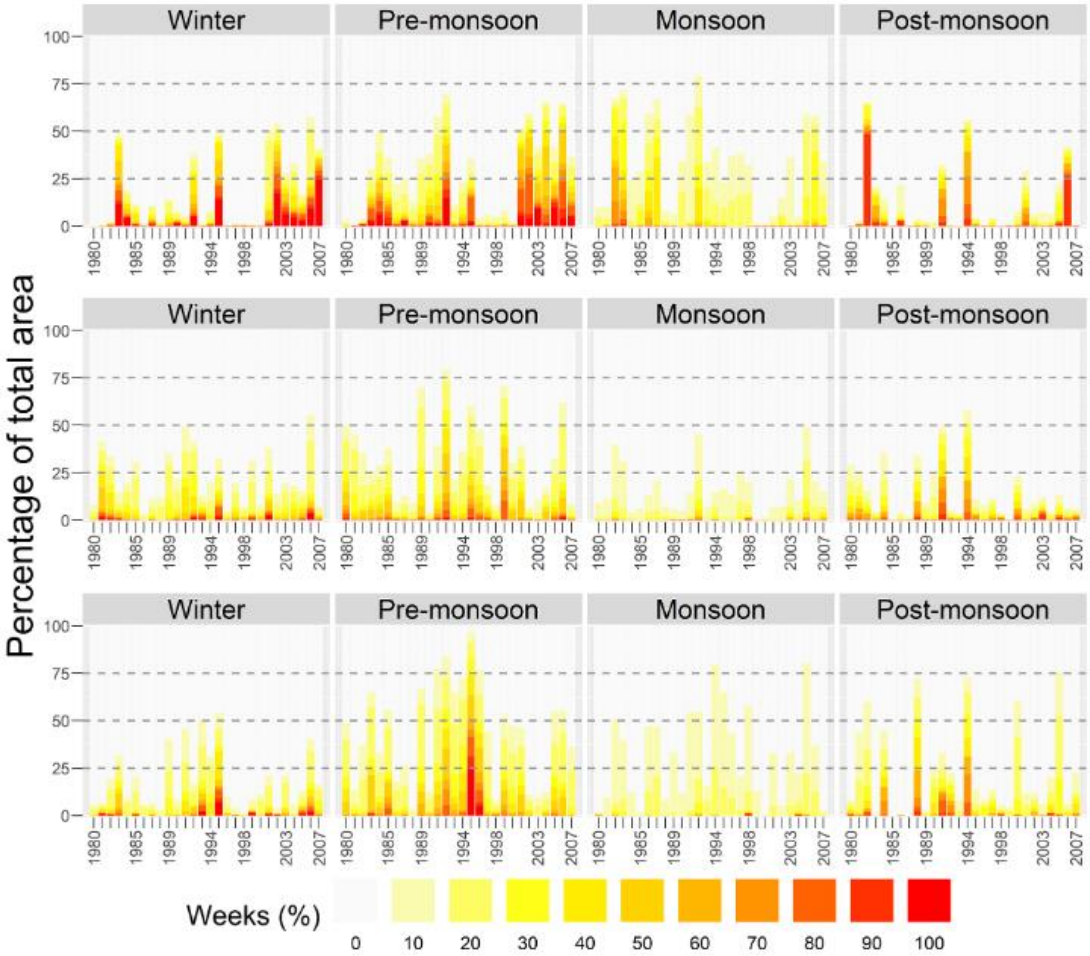

Figure 57. Percentage of weeks with severe drought in the trans-Himalaya (top row), the mountains (middle row), and the plains (bottom-row) (Source: Nepal et al., (2021)).

5.2.6 Heat Stress

In RCP 4.5 scenario, which reflects medium warming, the CMIP5 projects a temperature rise of between 1.2°C and 2.4°C for the 2015–2045 and 2065-2080 time period (see section 4.2.3). In the RCP 8.5 scenario, which represents high warming, the models project a temperature increase of between 2.4°C and 3.9°C for the same time period. Rising temperatures will affect snow hydrology and glacier melt, and may affect hydro plants with substantial catchments above the snow line (Basnyat & Watkiss, 2017). As per the authors, the changes in the hydrological regime will have a large impact on the plants at higher elevations compared to those at lower elevations. With an ever-increasing temperature, evaporation losses from dams and reservoirs will increase. This will significantly impact the reservoir operation strategy and thus reduces the overall power generation.

The steep increase in temperature and heat stress may constrain future electricity supply adequacy by reducing electric transmission capacity and increasing electricity demand (Bartos et al., 2016). With the increase in atmospheric carbon concentrations, higher ambient air temperatures may strain power infrastructure by simultaneously reducing the rated capacity of electric transmission lines and increasing peak electricity load.

5.2.7 Reduced low flows and impacts on environmental flows

Changes in precipitation and streamflow may have important implications for overall water resources planning, management, and development. Sectors such as irrigation, agriculture hydropower, fisheries, recreation, and navigation, could be most directly affected by the decrease in water amount (IPCC, 2019b). Changes in water volume together with changes in frequency, timing, and duration of both dry and wet season flow are also important aspects (L. Bharati et al., 2016).

Bharati et al., (2016) used weather data at a spatial resolution of 0.5° × 0.5° (~50 km × 50 km) and applied Soil and Water Assessment Tool (SWAT) to understand the impact of climate change on the flow regime of the Koshi basin. The authors divided the entire Koshi basin until Chatara into about 80 sub-basins and assess the variability in flows under A2 and B1 climate scenarios from the IPCC Special Report on Emission Scenarios (IPCC-SRES). Based on the results authors suggest premonsoon and winter flows, important for energy generation in dry seasons, are decreasing significantly in the DKSHEP and Koshi basin (**Figure 58** and **Figure 59**).

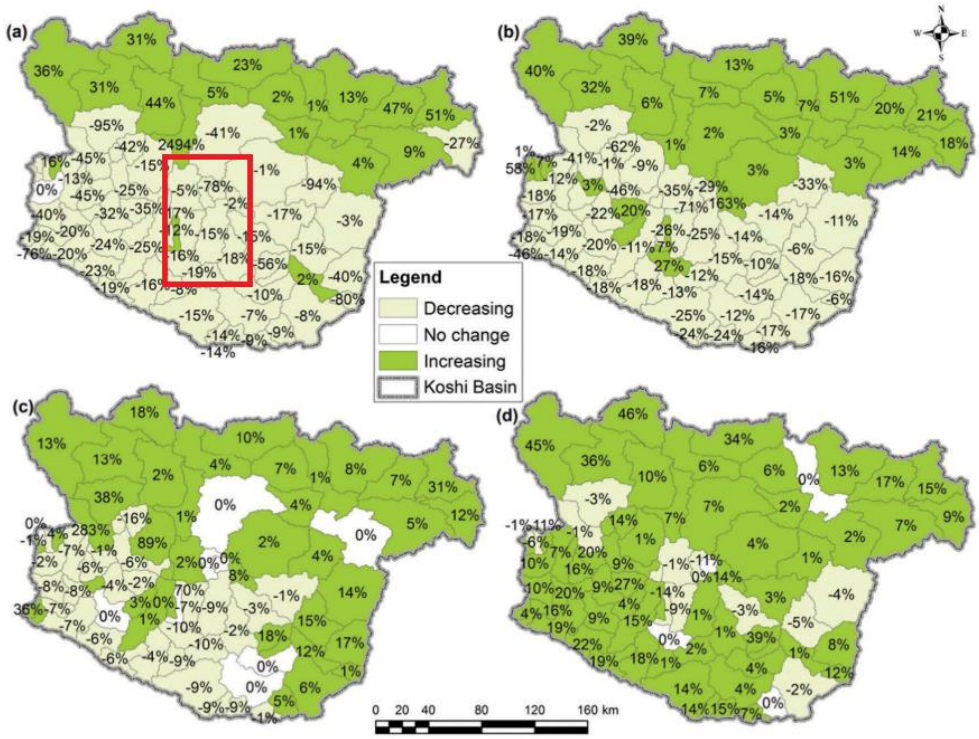

Figure 58. Percentage change in flow volume during the (a) winter, (b) pre-monsoon, (c) monsoon and (d) post-monsoon seasons under the A2 climate projections for the 2030s. The red rectangle indicates the DKSHEP (Source: Bharati et al., (2016)).

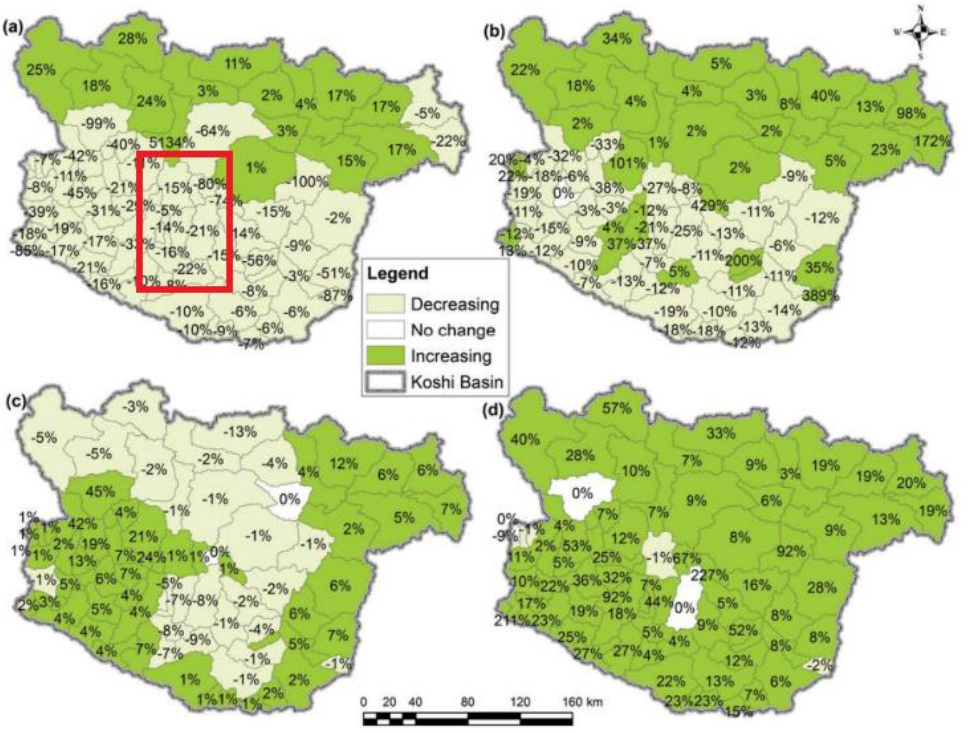

Figure 59. Percentage change in flow volume during the (a) winter, (b) pre-monsoon, (c) monsoon and (d) post-monsoon seasons under the B1 climate projections for the 2030s. The red rectangle indicates the DKSHEP (Source: Bharati et al., (2016)).

Devkota and Gyawali, (2015) also projected a decrease in mean water availability in the region (**Table 15**). Though the changes in mean water availability are not significant, the daily and monthly variations in flow are significantly high. The authors found a slight decrease in low flows compared to the baseline. Based on the results authors suggest storage facilities such as the Koshi High Dam (1) to fulfill the downstream water requirements for irrigation, domestic and industrial uses, (2) to generate stipulated hydropower and (3) for flood control. **Table 15.** Comparison of flow statistics of historical and projected flow series (Source: Devkota and Gyawali, (2015))

Variables	Observed		Projected ECHAM05		Projected HADCM3	
	1987–1996 (baseline)	1997–2006	2041–2050	2051–2060	2041–2050	2051–2060
Q_{avg}	1654	1471	1429	1717	1448	1500
CV	0.97	1.07	1.15	1.29	1.17	1.2
Q_{avg} + Sdv $(\mu + \sigma)$	3257					
Min daily	255	201	219	247	230	245
Max daily	9610	9480	23,780	36,020	15,000	19,830
Min monthly	299	231	257	256	237	261
Max monthly	6089	6181	5620	8614	4673	6844
Annual min	1354	1251	1135	1247	1280	1296
Annual max	1795	2055	1713	2088	1757	1881
Q_{90}	378	315	289	290	272	284
Q_{95}	350	294	275	268	256	265
Q_1	6230	6470	7625	9752	8443	8148
$Q_{0.1}$	7730	8300	14,530	26,450	12,700	15,760

Nepal, (2016) used J2000 hydrological model in the Dudhkoshi river (unital Rabuwa bazar) basin to understand the climate change impacts on the hydrological regime. The authors found the total discharge is projected to increase by 13% by mid-century and decrease slightly thereafter. Authors also predict the decrease in the winter and pre-monsoon flows for future climate change scenarios.

Bharati et al., (2019) also found an increase in mean water availability for both RCP4.5 and RCP8.5 scenarios. The lower range for the projected average monthly discharge was found to be within the range of the discharge in the reference period for all the months which suggests no changes in future low flows. Recently, Kaini et al., (2020) suggested that for the Koshi basin, the minimum monthly flow for the winter season will increase in the future (Table 16). There will be a significant shift in the hydrological regime as a shift in peak flow towards August and September is expected under the future climate change scenarios (**Figure 60**).

Table 16. Change in average minimum monthly flow relative to the measured river flow discharge (1982–2010). All values are in m3/s (Source: Kaini et al., (2020)).

Study period / climate change scenario flow rates (m^3/s)		Jan.	Feb.	Mar.	Apr.	May	June	July	Aug.	Sept.	Oct.	Nov.	Dec.
Short term	RCP4.5	88	69	46	−60	−445	−1530	−604	192	723	480	327	147
	RCP8.5	37	31	25	22	297	−344	561	545	236	287	77	42
Midcentury	RCP4.5	71	52	59	224	946	−612	−259	192	457	379	225	112
	RCP8.5	74	65	63	−30	−186	−1530	43	1122	944	333	194	100
End-of-century	RCP4.5	57	34	25	142	1095	−803	−302	641	693	441	189	104
	RCP8.5	122	89	68	0	−686	−1989	86	1507	1239	821	271	181

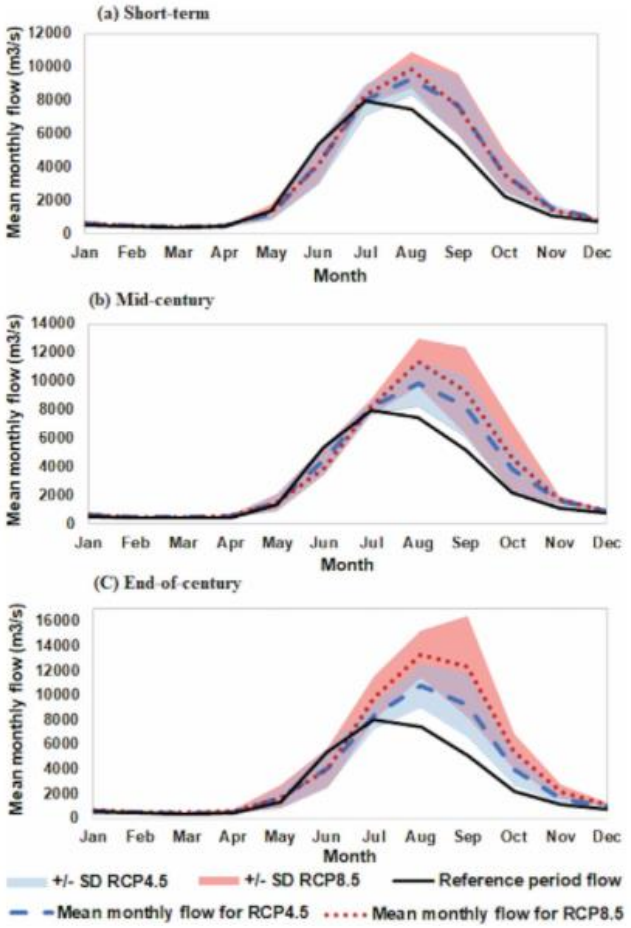

Figure 60. Projected average monthly river flow (ensemble mean) with standard deviation for the Koshi River at Chatara for the short-term, midcentury and end-of-century periods. Projections are relative to the reference data for 1981–2010 (Source: Kaini et al., (2020)).

Over 90% of Nepal's existing hydropower plants are the ROR and PROR types, which are generally designed based on the dry season flows. Due to the reduction in dry season flows in recent decades only about 30% of electricity (of the total installed capacity) is generated in low-flow seasons (Bhatt, 2017).

5.3 Overall risk classification matrix

The main variables that were considered are slope instability, soil erosion, sedimentation, flash flooding, GLOF, droughts, and heat stress. Expected changes in these climate variables may have an impact on the project components and should thus be considered in the design. Considering the climate hazard analysis in the project area, and the area-specific climate change projections, the following risks are considered most relevant:

- The projected increase in extreme precipitation and temperature events, changes in glaciers, and changes in flow regimes pose risks for hydropower infrastructure. With declining glacier mass and snow cover, the seasonality of flow will become more erratic when the hydrological system shifts towards a more rainfall-dominated system. This can imply more frequent hydrologic droughts and periods of low flows outside the monsoon season, as well as more frequent extremely high flows or floods during the monsoon season. Flooding will increase the risk of damage to hydropower infrastructure such as dam, intake, powerhouse and transmission line whereas droughts will reduce the hydropower generation and will significantly impact the environmental flow.
- An increase in intense precipitation will greatly surge the landslide activity over the DKSHEP region. The landslide and landslide-dam breach induce floods will greatly affect the key project infrastructures including the transmission lines. The resulting debris and mudflow event pose a serious risk to the stability of the dam and the efficiency of sediment operation. The deposition of sediments into the reservoir will greatly reduce the live water storage capacity of the DKSHEP reservoir thus affecting the overall power generation.
- An increase in extreme precipitation events and high flows will increase hillslope erosion which will lead to increased sediment loads. These negatively impact hydropower infrastructure, by increasing weathering of turbines, as well as the filling of head ponds and reservoirs.
- The Dudhkoshi basin includes 12 potentially dangerous glacial lakes, the largest number in any sub-basin of Nepal. In past, three catastrophic GLOF events were recorded in (or in adjacent basins) the Dudhkoshi region. The GLOF events are associated with immense damage and are highly likely to cascade and cause a downstream chain reaction.
- The projected increase in temperature extremes may put significant strain on the electricity transmission lines and transformers, potentially leading to system faults, reduced power supply, and power outages.

The climate vulnerability and risk analysis process has gathered several datasets in the public domain, together with local information, associated with each risk to determine the most important risks associated with the project area. **Table 17** summarizes this and provides an expert judgment of the risk for the project components and indicates possible adaptation measures.

Table 17. Screening of most important climate risks and vulnerable project components

Climate Hazard	Vulnerable Project Components	Expected Change in Climate Variables	Risk	Potential adaptation options
Erosion of catchment and command areas	Reservoir, intake and dam	Increase in maximum 1-day rainfall, precipitation intensity predicted by climate model ensemble	**High**	• Sediment management upstream regions of the reservoir • Efficient sediment flushing operation scheme for the reservoir • Increase the flushing capacity of bottom outlets
Fluvial and Flash flooding	Reservoir, intake and dam	Increase in rainfall extremes	**High**	• Establishment of an early warning system in the upstream regions of the reservoir. • Provision for the effective passage of the probable maximum flood through the reservoir without affecting its stability. • Increase in the capacity of the main and emergency spillway.
Seismic events, landslides and slope failures	Reservoir, intake dam and transmission line	Increase in maximum 1-day rainfall, precipitation intensity and erosion	**High**	• Identification and management of landslides in the DKSHEP region. • Efficient sediment management and operation scheme for the reservoir. • Careful investigation of the potential landslide location and avoiding the substations and transmission line.
Increased Drought Occurrence	Environmental flow	Increase in Consecutive Dry Days, increase in temperatures predicted by climate model ensemble	**Medium**	• Optimal adaptive reservoir operation rules that consider the reduced inflows into the reservoir. • Increasing the size of bottom outlets to ensure the minimum environmental flow downstream.
GLOF	Reservoir, dam, powerhouse and transmission line	Increase in extreme precipitation, temperature leading to snow melt, glacier retreat and ice and rock avalanches.	**High**	• Adequate monitoring of the retreat rate of glaciers and stability of the lakes. • Provision for the effective passage of the probable maximum flood through the reservoir without affecting its stability.

Heat stress	Transmission line	Increase in maximum temperature	Medium	• Construction of cooling towers • Improvement in energy transmission facilities and technology.

6 Recommendations for adaptation measures

The climate risks assessed in the previous chapter for DKSHEP urge climate adaptation-related activities that make sure that the project development objectives are not compromised by climate change. These climate adaptation activities complement the “Business as Usual” activities of the project, which are the project activities that did not originate with an explicit intent to address climate change impacts. Without the climate adaptation activities proposed here, the project will most likely not achieve its development objectives due to the adverse impacts of climate change on the medium- (next decades) and long-term (second half of the century). This section describes the climate adaptation activities proposed for the project.

In general, robust design specifications could allow structures to withstand more extreme conditions (such as floods and landslides). In some circumstances, it may also be necessary to consider redesigning extremely vulnerable existing infrastructure. All recommendations for this project have been considered based on critical site parameters such as topography, slope, minimum and maximum temperature, rainfall and soil conditions, etc. The adaptation activities target the climate risks to the hydropower systems that were classified as “medium” or “high” in the climate risk assessment (see previous section). In short, these risks are:

- **Increased Flooding**. Due to the increase in magnitude and frequency of rainfall, flooding will likely increase in the future. Climate adaptation measures are required that specifically reduce flood risk, to the extent possible through a catchment management approach and the use of bioengineering techniques.
- Increased erosion. Due to the scarce vegetation cover in the catchment areas, the erodible soil type (loess), steep slopes, and likely increase in extreme weather events that drive erosion (rainfall extremes), it is concluded that the climate risk for increased erosion and consequent yield loss is high. Climate adaptation measures are required that specifically reduce erosion risk, to the extent possible through Nature-based Solutions.
- **Frequent landslides**. The combination of erosion and earthquake hazard causes a high risk of landslides and slope failures in the upstream regions of the DKSEHP project. Climate adaptation activities are required which can cope with earthquake risk and makes the infrastructure less vulnerable to extreme weather.
- **higher GLOF risk**. Due to global warming, the increase in magnitude and frequency of rainfall, and recent seismic activity, the GLOF risk is higher for the central Himalayan region. Adequate monitoring of the retreat rate of glaciers and the stability of the lakes are thus required to cope with it.
- **Increased drought** risk due to erratic precipitation and changes in the seasonality of the precipitation in the future. This could impact the overall project including the environmental flow requirements downstream.
- **Increased heat stress**. Expected increases in temperature and frequency and duration of heat waves in the project area can reduce the electricity-carrying capacity of the transmission lines.

As such, climate adaptation activities have been incorporated into the project, and have been divided into the following components of the project:
- Engineering interventions
- Non-engineering interventions

6.1 Engineering interventions

To make sure that climate change impacts will not compromise the infrastructural and engineering interventions of the project, climate adaptation is required to reduce the risk of failure. For example, the probable maximum flood (QPMF) for the detailed design of the project is calculated based on the basin average of eight precipitation stations within the catchment. However, existing hydro-meteorological stations, mostly located in valleys lower than 4000m (except two stations: Periche 4260 m and Pyramid 5035 m), are sparsely distributed in the region. Therefore, the extreme climate signals are biased towards these station observations at lower elevations. Also, the assessment of climate change impacts in the detailed design report is based on the three GCM outputs and doesn't represent the full distribution of projected impacts.

There are many examples of infrastructure and facility failures in recent years in Nepal and the Himalayan region. For instance; the Melamchi flood event in June 2021 resulted from the breach of a landslide dam upstream, releasing a torrential debris flow and flood that struck the settlements and water supply project; the Chamoli floods in February 2021 caused by the rock and ice avalanche which eventually transformed into an extraordinarily large and mobile debris flow that transported boulders >20 m in diameter, and scoured the valley walls up to 220 m above the valley floor; the Kedarnath floods in June 2013 primarily due to cloudburst event which instigated numerous landslide and flash floods at big spatial scales; June 2016 GLOF induced floods in the Bhotekoshi river which significantly damaged the headworks and powerhouse of the Upper Bhotekoshi HEP. There is substantial damage to the critically important water resources infrastructures in all these events. Major infrastructure projects are being built in the Himalayas without a proper understanding of the risks of these devastating landslides (Shugar et al., 2021). It highlights the perils of building infrastructure at great cost in areas subject to these events without understanding them properly. So, the detailed design should incorporate the findings of this CRA study.

The cost estimate of adaptation measures is a challenging task and requires a detailed assessment. The exact adaptation cost requires the collaboration of the CRA expert and the design team. **Table 18** provides a qualitative cost estimate relative to the total cost of the project. For instance, the spillway costs about 17.5%, the third highest cost after the dam (19 %) and main powerhouse (18.3 %), of the total project cost. So, the potential adaptation cost associated with spillway will be higher compared to other components of DKSHEP.

Table 18. Potential adaptation activity recommended by this study.

Potential Adaptation Activity	***Target Climate Risk***	***Relative Cost***	***Justification of the adaptation finance***
(A) Project infrastructure related			
Increase the flood passing capacity of the main and emergency spillway by modifying the design	Extreme weather events, seismic events, GLOF events and increased occurrence of landslides	**High**	Due to the increase in magnitude and frequency of rainfall flooding will likely increase in the future. To ensure that the engineering and non-engineering interventions of the project are not compromised by the effects of climate change and geophysical hazards, it is necessary to enhance the flood-passing capacity of the main and emergency spillway.

Increase the size of the bottom outlet of the reservoir to avoid sedimentation.	Soil erosion, slope failure, seismic events, GLOF events and increased occurrence of landslides	**Low**	The DKSHEP project is at risk of experiencing reservoir sedimentation due to several factors, including scarce vegetation cover in the catchment area, erodible soil, steep slopes, slope failure, landslide, earthquakes, and the probable increase in extreme weather events that drive erosion. The sedimentation could potentially impact the downstream release of environmental flow. Therefore, it is recommended that the flushing capacity of the bottom outlets be increased to facilitate the removal of sediments.
Shifting the location of key DKSHEP components	Slope failure, landslide activity and flooding	**Low**	Due to fragile geology, steep slopes seismic activity and extreme weather conditions, landslides are likely to increase in the DKSHEP project. So, it is recommended to identify locations with stable topography for the key components of the project and transmission lines.
(B) Project region related			
Upstream sediment trapping by constructing check dams in the upstream regions of the reservoir	Soil erosion, slope failure and landslide	**Medium**	The DKSHEP region is highly vulnerable to erosion and landslide activity. The increase in frequency and magnitude of weather and climate-related extremes and anthropogenic activities will likely increase the number of landslides and soil erosion. So, sediment trapping upstream of the hydropower reservoir is recommended.
Identification of the potential landslide	Soil erosion and landslide	**Medium**	It is recommended to identify the potential landslide sites in the DKSHEP region and apply slope stabilization techniques to mitigate the risk.

6.2 Non-engineering measures

6.2.1 Bio-engineering solution for key project components

To improve slope stability and maintain ecological balance, bioengineering techniques are deployed in developing countries as they are cost-effective and also ecosystem-friendly (Raut & Gudmestad, 2017). The application of suitable bioengineering techniques in hydropower projects can reduce the risks associated with erosion, slope failure, and landslides and help in increasing the lifetime of the project. Suitable bioengineering techniques can be adopted by analyzing the physical and geographical conditions (DSCW, 2016). Examples of bio-engineering methods applied in Nepal are, grass lines, grass seeding, shrub and tree planting, bush layering, palisades, wattling, stone pitching, check dams, and bamboo crib walls. These techniques reduce the runoff speed, strengthen the soil, prevent formation of rills and gully and block the movement of debris consequently helping to reduce

the erosion and stabilize the slope. The suitable bioengineering techniques should be applied around the key components of DKSHEP projects such as dam, settling basin, forebay and powerplant.

6.2.2 Nature-based Solutions for upstream command area

Nature-based solutions are actions undertaken to protect, sustainably manage and restore natural and modified ecosystems in ways that address challenges like climate change, disaster risk reduction, food and water security, health and economic development effectively and adaptively, to provide both human well-being and biodiversity benefits (IUCN, 2019; OECD, 2020). These include sustainable upstream land use management techniques.

6.2.3 Early warning system

As per United Nations Office for Disaster Risk Reduction (UNDRR) early warning system (EWS) is an integrated part of hazard monitoring forecasting, prediction, assessment, and communication (Meechaiya et al., 2019). Dissemination and communication of GLOF, landslide, and flood risk information and early warnings to the operators and managers of HEP could help in risk management and adaptation.

7 Carbon footprint

A carbon footprint is the total greenhouse gas (GHG) emissions caused by an individual, event, organization, service, place, product, or project, expressed as carbon dioxide equivalent. The global temperature is increasing rapidly due to increasing annual emission rates of carbon dioxide and methane (Smith et al., 2015). There are huge gaps between the reality and the actions that need to be to achieve the Paris Climate Agreement goal to cut carbon emissions to limit global warming to 1.5° C this century. Global estimates from the period of 1850-2011 show that two-thirds of the earth's carbon emissions were contributed by the United States, the European Union, Japan, the Russian Federation, and the People's Republic of China (PRC) together (**Figure 61**). Although the relative contribution of emissions is insignificant for underdeveloped and developing nations, countries like Nepal are at higher risk of changing climate.

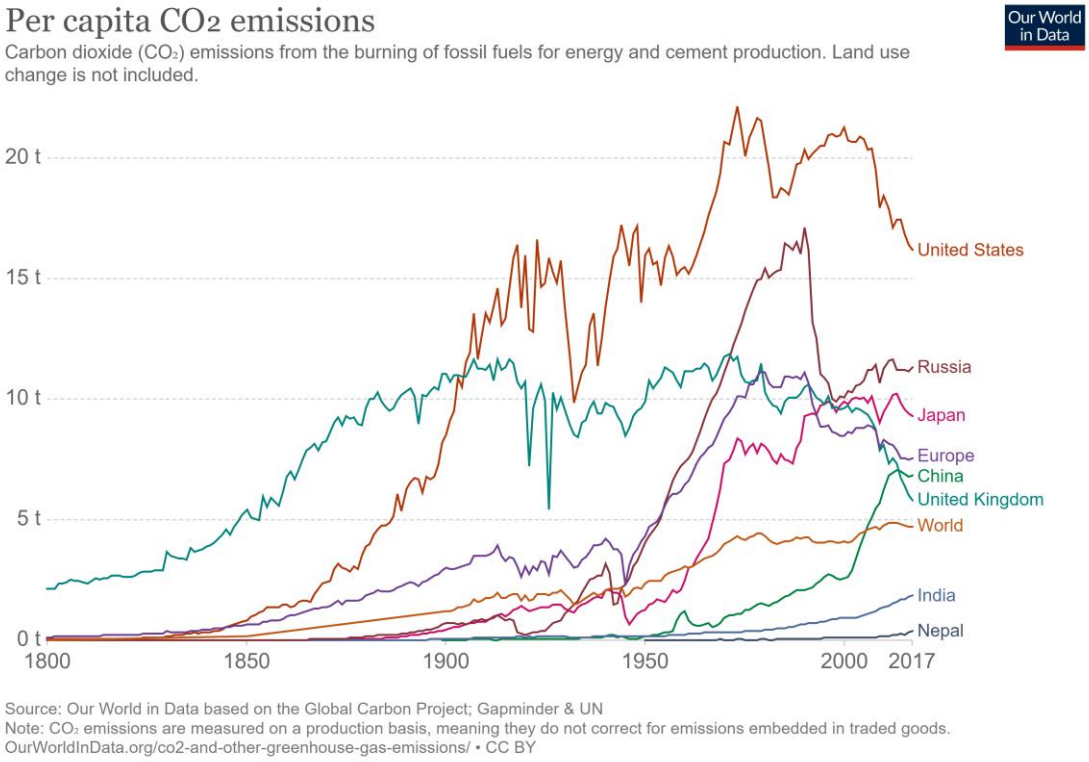

Figure 61. Per capita carbon emissions of Nepal compared to several countries and regions around the world (Source: https://ourworldindata.org/co2/country/nepal)

Most of the carbon emissions in Nepal is contributed by the transportation and industrial sector (**Figure 62**). Due to rapid population growth and development in recent decades, carbon emissions have been alarmingly increasing in Nepal (**Figure 63**).

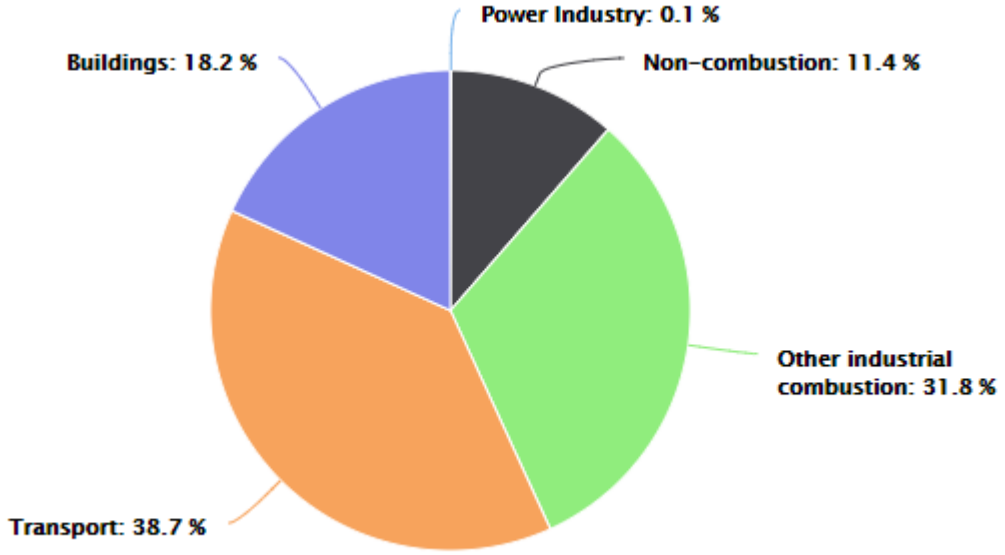

Figure 62. Overall carbon emissions by sectors in Nepal (Source: https://www.worldometers.info/co2-emissions/nepal-co2-emissions/).

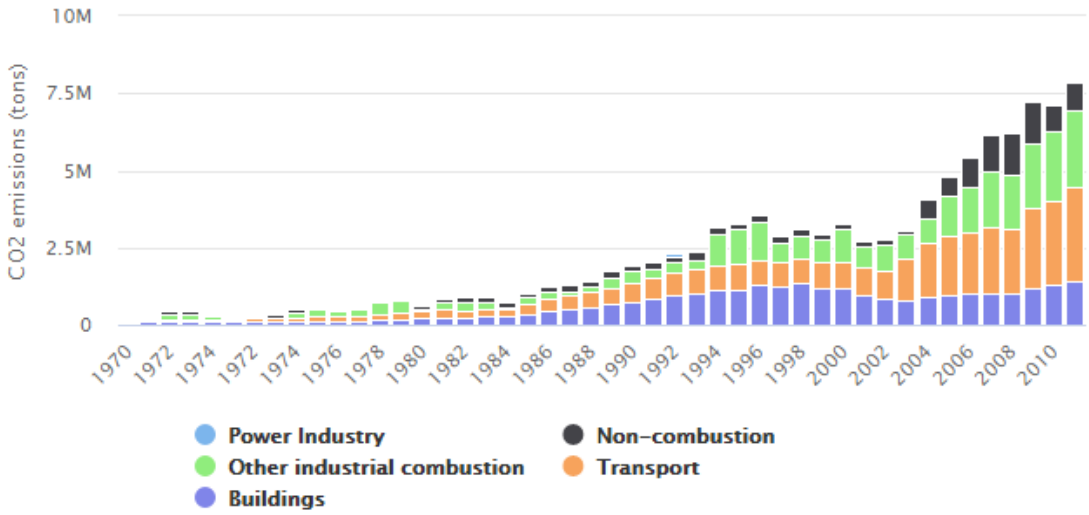

Figure 63. Annual contribution of carbon emissions by sectors in Nepal (Source: https://www.worldometers.info/co2-emissions/nepal-co2-emissions/).

International financial institutions (IFIs) need an estimate and it is mandatory to report it for their climate-related investment-specifically, on the gross GHG emissions and GHG emission reduction attributable to their projects. ADB also complies with the policies and practices where GHG emission estimates are needed. ADB provides two harmonized guidance documents on GHG accounting: one for energy efficiency projects and another for renewable energy projects (Source: ADB, (2017)).

In order to limit the emission, several portfolios of strategies such as energy efficiency increases, carbon capture and storage (CSS), alternative (nuclear and renewable) energy sources, and forest and agricultural conservation, are coined. Among others, hydropower is considered to be a low-carbon technology (Fearnside & Pueyo, 2012). Mostly, the emissions from hydroelectric reservoirs arise from the decomposition of organic matter that was either flooded, transferred to the reservoir, grown in the reservoir such as by algal production, or grown in newly created marshes in the reservoir area. The real impact of the reservoir on GHG emission is therefore calculated as the difference between GHG emissions before and after reservoir construction (**Figure 64**). ADB requires that GHG emissions from projects emitting 100,000 tons of carbon dioxide or more be monitored (ADB, 2009).

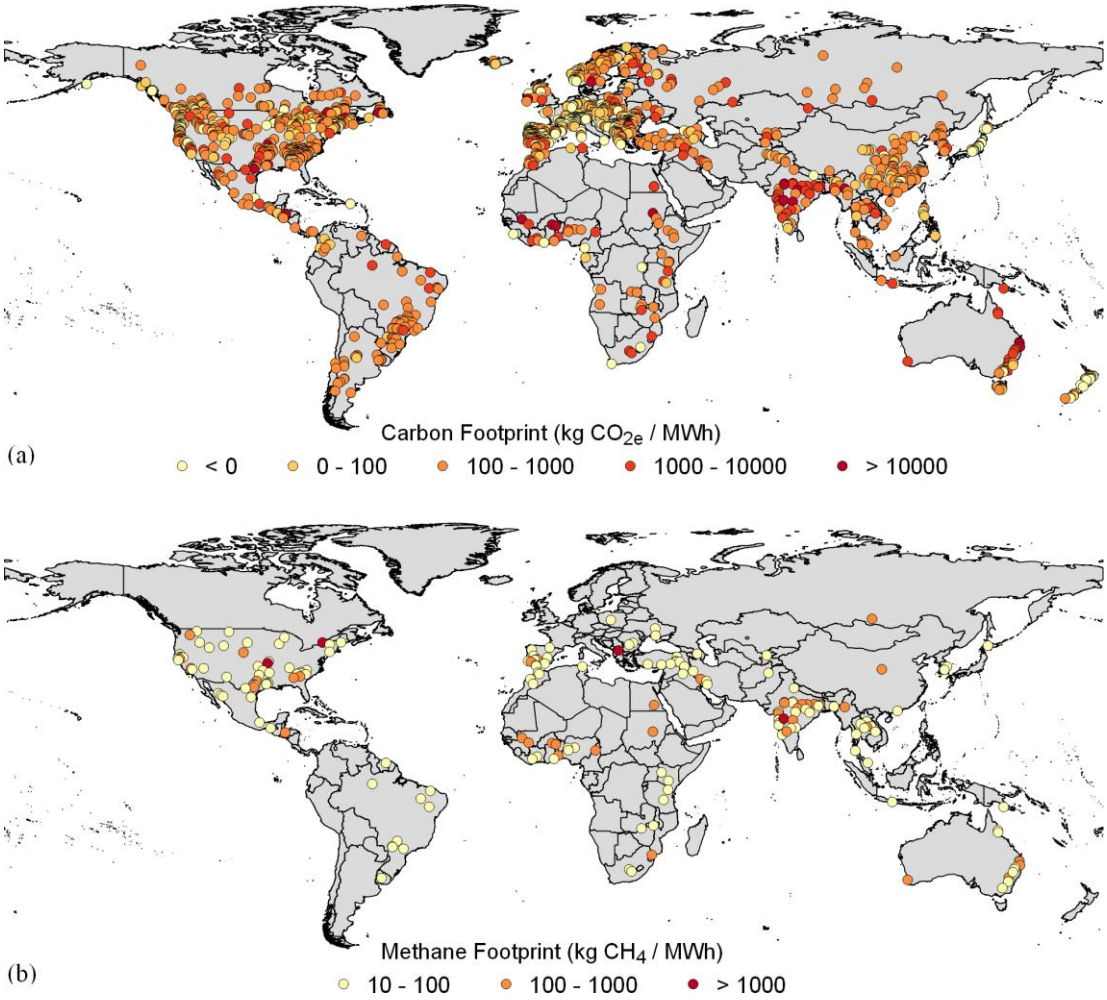

Figure 64. (a) Carbon footprints of hydropower plants across the world. (b)Hydropower plants with high methane emissions (>10 kg CH4/MWh) and a large share of methane emissions (> 50% of the carbon footprint). Source: (Scherer & Pfister, 2016)

7.1 Methods

The GHG emission is calculated as per the method described in ADB, (2017).

Emission Reduction (ER)
Emission reduction is the difference between baseline and project emissions when generating the same amount of power

ER = BE – PE
BE = baseline emission
PE = project emission

Baseline Emission (BE)
BE is the amount of emissions generated by grid-connected power plants when generating the same amount of power as the large hydropower plants.

BE = EG × EF grid
EG = annual electricity generation by the large hydro project, MWh/year
EF grid = combined emission factor for the grid, tCO_2 /MWh

Project emission (PE)
BE = EG × EF hydro
EG = annual electricity generation by the large hydro project, MWh/year
EF hydro = Emission factor for the large hydropower to account for methane emission from the dam

7.2 Results

7.2.1 Scenario A: DKSHEP replaces locally generated electricity

Assumptions: -
Installed capacity (IC): 635 MW
Load factor (LF): 88% (based on the range used in Table 10.2 of Vol. 1 - Main report)
Baseline grid emission factor (GE): 0.019 tCO_2/MWh (For Nepal based on Append C of ADB, (2017) report)
Dam emission factor (DE): 0.09 tCO_2/MWh (based on Eq 30 of ADB, (2017) report)

Table 19. Carbon emission calculation from the DKSHEP project for scenario A.

Emission	***Equation***	***Value***	***Units***
Total generation (TG)	IC × 8760 × LF	4,895,088	MWh/yr
Baseline Emission (BE)	TG × GE	93,007	tCo2/yr
Project Emission (PE)	TG × DE	440,558	tCo2/yr
Emission Reduction (ER)	BE - PE	-347,551	tCo2/yr

7.2.2 Scenario B: DKSHEP partially replaces locally generated electricity and rest being imported by India

Assumptions: -
Installed capacity (IC): 635 MW
Load factor (LF): 88% (based on the range used in Table 10.2 of Vol. 1 - Main report)
Baseline grid emission factor (GE): 0.754 tCO_2/MWh for India and 0.019 for Nepal (based on Append C of ADB, (2017) report)

Dam emission factor (DE): 0.09 tCO_2/MWh (based on Eq 30 of ADB, (2017) report)

Table 20. Carbon emission calculation from the DKSHEP project for scenario B.

Emission	***Equation***	***Value***	***Units***
Total generation (TG)	IC × 8760 × LF	4,895,088	MWh/yr
Energy imported from India in 2019/2020		1,729,000	MWh/yr
Energy replaced in Nepal		3,166,088	MWh/yr
Baseline Emission (BE)	TG (India) × GE (India) + TG (Nepal) × GE (Nepal)	1,363,822	tCo2/yr
Project Emission (PE)	TG × DE	440,558	tCo2/yr
Emission Reduction (ER)	BE - PE	923,264	tCo2/yr

In scenario A, it is assumed that the energy in the baseline scenario is already generated in Nepal. Under this assumption, 347,551 tCo2 per year will be contributed instead of a reduction. In scenario B, it is assumed that a fraction of energy is currently imported from India and the rest is generated locally. This assumption is based on NEA, (2020b) which states that 22.3% of energy is currently imported from India. The total baseline emission based on this assumption is found to be 1,363,822 tCO_2/yr. The project emission regardless of the scenario is found to be 440,558[1] tCO_2/yr. The DKSHEP as per scenario B will reduce 923,264 tCO_2 emissions every year compared to baseline conditions.

[1] As per IPCC Good Practice Guidance for LULUCF, 2003 Table 3A.3.5 under Tropical, wet climate, the total CO_2 emission will be around 43,592 tCO_2/yr and 9,526 tCO2/yr assuming the warm temperature, wet climate condition. These emission estimates are calculated only for the reservoir area of the DKSHEP.

8 Conclusion

The present Climate Risk Assessment (CRA) reviewed the Dudhkoshi Storage Hydro-electric project (DKSHEP), in the context of expected climate change till the end of the century. The analysis was done based on the NASA-NEX ensemble of downscaled General Circulation Models (GCMs). The consideration based on the full ensemble for a medium stabilization scenario (RCP4.5) and a business-as-usual scenario (RCP8.5) allows for the inclusion of the uncertainty in future climate in the assessment. The climate model analysis yields the following conclusions for the project area:

- The DKSHEP will reduce 923,264 tCO2 every year compared to the baseline condition.
- The annual daily maximum temperature is expected to increase on average by about 1.2 and 1.3 degrees under the RCP 4.5 scenario for T1 (2015–2045) and T2 (2065–2095) time horizon and 2.4 and 3.9 degrees under the RCP 8.5 scenario for the T1 and T2 time horizon.
- Extremes related to temperatures (e.g. warm spells, extremely warm days) are likely to increase in frequency and intensity.
- On average the precipitation is expected to increase by 9.1 and 9.3% for the T1 and T2 time horizon under the RCP4.5 scenario; 22.8 and 37.4% for the T1 and T2 time horizon under the RCP8.5 scenario.
- The GCMs show a large range of uncertainty for seasonal changes under both RCP 4.5 and RCP 8.5.
- Precipitation extremes are likely to increase in frequency and intensity. Maximum 1-day precipitation is expected to increase by about 9% for both the T1 and T2 time horizon under the RCP4.5 scenario; 20 and 31% for the T1 and T2 time horizon under the RCP8.5 scenario.
- There is no significant change in the number of consecutive dry days per year. However, the model uncertainty increases over the end of the century time horizon.

Considering the type of climate hazards and risks in the project area, and the area-specific climate change projections, overall, the most serious threat comes from the expected increase in precipitation and temperature extremes. Due to the increase in magnitude and frequency of precipitation, erosion, and landslide activity will likely increase in the future. In addition, while the hazard exposure is constricted to upstream parts of the project area, the expected increase in extreme precipitation events may cascade and lead to more frequent and powerful flooding events over the larger regions. Seismic activity and warming-induced GLOF events in the upstream part of DKSHEP may have a significant impact on the project infrastructure. Higher extreme discharges may also lead to more frequent landslides and more powerful mudflows, posing a serious risk of damaging reservoir and transmission towers which may lead to power outages. Heat-related stresses may put significant strain on the electricity system, leading to system faults, reduced power supply, and power outages.

For adaptation and climate proofing the main recommendation is to use a full ensemble of future projections rather than three as currently used in the detailed design report. Including more GCM outputs in the analysis will help to quantify the uncertainty and the upper bound of the probable maximum flood. This is highly relevant to the DKSHEP as there are many instances in the Himalayan region, such as the Melamchi flood event in June 2021, the Chamoli flood in February 2021, the Kedarnath flood in June 2013 and the Bhotekoshi flood in June 2016, which resulted in significant damage to the critical water resources infrastructures, especially hydropower, and the livelihood of the communities downstream. The second high-priority recommendation is to increase the flood passage capacity through the reservoir. The extreme events in the recent past have increased significantly and more extremes are likely on the way. The third recommendation is to increase the sediment flushing capacity of the reservoir. The project region is highly vulnerable to seismic, GLOF, and landslide

activity. All of these catastrophic events are associated with the transport of large amounts of debris and sediments. Sediment concentration under normal dry and wet conditions will not be representative of extreme conditions. A number of catastrophic and cascading GLOF and landslide events in a single monsoon season may entirely fill the water storage capacity of the reservoir so it is highly recommended to increase the sediment flushing capacity to cope with unprecedented situations. The final recommendation is to implement bioengineering techniques, nature-based solutions, and an early warning system for the mitigation of flood and landslide-related hazards in the project region.

This CRA relies on climate model projections and therefore is prone to uncertainties. The downscaled climate models used in this study have a spatial resolution of about 25 km, whereas climate change signals may vary strongly over short distances and particularly in mountainous terrain. There is often also a large spread in the climate model projections. Therefore, the full ensemble of models has been analyzed and the uncertainty range is displayed in all figures in this report.

9 References

ADB. (2009). Safeguard Policy Statement, (June), 97.

ADB. (2012). *Climate Risk and Adaptation in the Electric Power Sector*. Manila, Philippines.

ADB. (2013). *Guidelines for climate proofing investment in the energy sector*. Manila, Philippines.

ADB. (2014). *Climate Risk Management in ADB projects*. Manila.

ADB. (2016). *Guidelines for Climate Proofing Investment in the Water Sector - Water Supply and Sanitation*. Manila.

ADB. (2017). *Guidelines for Estimating Greenhouse Gas Emissions of ADB Projects: Asian Development Bank*. Retrieved from https://www.adb.org/documents/guidelines-estimating-ghg-energy-projects

Adhikari, S. (2018). Drought impact and adaptation strategies in the mid-hill farming system of western nepal. *Environments - MDPI*, *5*(9), 1–12. https://doi.org/10.3390/environments5090101

Allen, S. K., Linsbauer, A., Randhawa, S. S., Huggel, C., Rana, P., & Kumari, A. (2016). Glacial lake outburst flood risk in Himachal Pradesh, India: an integrative and anticipatory approach considering current and future threats. *Natural Hazards*, *84*(3), 1741–1763. https://doi.org/10.1007/s11069-016-2511-x

Annandale, G., Morris, G., & Karki, P. (2016). *Extending the Life of Reservoirs*. *Concrete International*.

Bajracharya, S. R., & Mool, P. (2009). Glaciers, glacial lakes and glacial lake outburst floods in the Mount Everest region, Nepal. *Annals of Glaciology*, *50*(53), 81–86. https://doi.org/10.3189/172756410790595895

Bartos, M., Chester, M., Johnson, N., Gorman, B., Eisenberg, D., Linkov, I., & Bates, M. (2016). Impacts of rising air temperatures on electric transmission ampacity and peak electricity load in the United States. *Environmental Research Letters*, *11*(11). https://doi.org/10.1088/1748-9326/11/11/114008

Basnyat, D. B., & Watkiss, P. (2017). Policy Brief: Adaptation to climate change in the hydro-electricity sector in Nepal, 12. Retrieved from https://cdkn.org/wp-content/uploads/2017/05/policy-brief-12-page-version.pdf

Bhambri, R., Mehta, M., Dobhal, D. P., Gupta, A. K., Pratap, B., Kesarwani, K., & Verma, A. (2016). Devastation in the Kedarnath (Mandakini) Valley, Garhwal Himalaya, during 16–17 June 2013: a remote sensing and ground-based assessment. *Natural Hazards*, *80*(3), 1801–1822. https://doi.org/10.1007/s11069-015-2033-y

Bharati, L., Gurung, P., Maharjan, L., & Bhattarai, U. (2016). Past and future variability in the hydrological regime of the Koshi Basin, Nepal. *Hydrological Sciences Journal*, *61*(1), 79–93. https://doi.org/10.1080/02626667.2014.952639

Bharati, Luna, Bhattarai, U., Khadka, A., Gurung, P., Neumann, L. E., Penton, D. J., et al. (2019). *From the mountains to the plains: Impact of climate change on water resources in the Koshi River Basin*. *IWMI Working Papers* (Vol. 187). https://doi.org/10.5337/2019.205

Bhatt, R. P. (2017). Hydropower Development in Nepal - Climate Change, Impacts and Implications. *Renewable Hydropower Technologies*, (December). https://doi.org/10.5772/66253

Bishwakarma, M. B. (2012). Performance improvement of headworks: a case of Kalignadaki A Hydropweor Project through physical hydraulic modelling.

Bolch, T., Shea, J. M., Liu, S., Azam, F. M., Gao, Y., Gruber, S., et al. (2019). Status and Change of the Cryosphere in the Extended Hindu Kush Himalaya Region. *The Hindu Kush Himalaya Assessment*, 209–255. https://doi.org/10.1007/978-3-319-92288-1_7

Bookhagen, B., & Burbank, D. W. (2006). Topography, relief, and TRMM-derived rainfall variations along the Himalaya. *Geophysical Research Letters*, *33*(8), 1–5. https://doi.org/10.1029/2006GL026037

Bookhagen, B., & Burbank, D. W. (2010). Toward a complete Himalayan hydrological budget: Spatiotemporal distribution of snowmelt and rainfall and their impact on river discharge. *Journal of Geophysical Research: Earth Surface*, *115*(3), 1–25. https://doi.org/10.1029/2009JF001426

Boulange, J., Hanasaki, N., Yamazaki, D., & Pokhrel, Y. (2021). Role of dams in reducing global flood exposure under climate change. *Nature Communications*, *12*(1), 1–7. https://doi.org/10.1038/s41467-020-20704-0

Bronsvoort, K. (2013). Sedimentation in reservoirs: Investigating reservoir preservation options and the possibility of implementing Water Injection Dredging in reservoirs, 142. Retrieved from https://repository.tudelft.nl/islandora/object/uuid%3A191323c1-b2ec-4d3e-9e28-2958c1ee287c

Bruen, M., Witnik, J., & Sthapit, B. (2017). Three Strikes: Natural Hazards Impact Nepal Hydropower Project. *Proceedings of HydroVision International 2017*. Retrieved from https://www.hydroreview.com/world-regions/surviving-three-natural-disasters-lessons-learned-at-upper-bhote-koshi-in-nepal/

Brun, F., Berthier, E., Wagnon, P., Kääb, A., & Treichler, D. (2017). A spatially resolved estimate of High Mountain Asia glacier mass balances from 2000 to 2016. *Nature Geoscience*, *10*, 668. Retrieved from https://doi.org/10.1038/ngeo2999

Byers, L., Friedrich, J., Hennig, R., Kressig, A., Li, X., Mccormick, C., & Valeri, L. M. (2019). Technical Note a

Global Database of Power Plants, (x), 1–18.
Chhetri, R., Pandey, V. P., Talchabhadel, R., & Thapa, B. R. (2021). How do CMIP6 models project changes in precipitation extremes over seasons and locations across the mid hills of Nepal? *Theoretical and Applied Climatology*, (0123456789). https://doi.org/10.1007/s00704-021-03698-7
Chhetry, B., & Rana, K. (2015). Effect of Sand Erosion on Turbine Components: A Case Study of Kali Gandaki "A" Hydroelectric Project (144 MW), Nepal. *Hydro Nepal: Journal of Water, Energy and Environment*, *17*(August 2015), 24–33. https://doi.org/10.3126/hn.v17i0.13270
Cook, K. L., Andermann, C., Gimbert, F., Adhikari, B. R., & Hovius, N. (2018). Glacial lake outburst floods as drivers of fluvial erosion in the Himalaya. *Science*, *362*(6410), 53–57. https://doi.org/10.1126/science.aat4981
Dahal, P., Shrestha, N. S., Shrestha, M. L., Krakauer, N. Y., Panthi, J., Pradhanang, S. M., et al. (2016). Drought risk assessment in central Nepal: temporal and spatial analysis. *Natural Hazards*, *80*(3), 1913–1932. https://doi.org/10.1007/s11069-015-2055-5
Dai, A. (2013). Increasing drought under global warming in observations and models. *Nature Climate Change*, *3*(1), 52–58. https://doi.org/10.1038/nclimate1633
Devkota, L. P., & Gyawali, D. R. (2015). Impacts of climate change on hydrological regime and water resources management of the Koshi River Basin, Nepal. *Journal of Hydrology: Regional Studies*, *4*, 502–515. https://doi.org/10.1016/j.ejrh.2015.06.023
Dhital, M. R. (2003). Causes and consequences of the 1993 debris flows and landslides in the Kulekhani watershed, central Nepal. *International Conference on Debris-Flow Hazards Mitigation: Mechanics, Prediction, and Assessment, Proceedings*, *2*(October), 931–942.
DSCW. (2016). *Guideline on Landslide Treatment and Mitigation.Department of soil Conservation and Watershed Management, Kathmandu, Nepal.* (Vol. 2016).
Elalem, S., & Pal, I. (2015). Mapping the vulnerability hotspots over Hindu-Kush Himalaya region to flooding disasters. *Weather and Climate Extremes*, *8*, 46–58. https://doi.org/10.1016/j.wace.2014.12.001
Fearnside, P. M., & Pueyo, S. (2012, June 25). Greenhouse-gas emissions from tropical dams. *Nature Climate Change*. Nature Publishing Group. https://doi.org/10.1038/nclimate1540
Ghimire, Y. N., Shivakoti, G. P., & Perret, S. R. (2010). Household-level vulnerability to drought in hill agriculture of Nepal: implications for adaptation planning. *Http://Dx.Doi.Org/10.1080/13504501003737500*, *17*(3), 225–230. https://doi.org/10.1080/13504501003737500
Gyanwali, S. (2016). In west Nepal, a river basin is home to drought and poverty. Retrieved July 16, 2021, from https://scroll.in/article/814642/in-west-nepal-a-river-basin-is-the-home-to-drought-and-poverty
Hamal, K., Sharma, S., Khadka, N., Haile, G. G., Joshi, B. B., Xu, T., & Dawadi, B. (2020). Assessment of drought impacts on crop yields across Nepal during 1987–2017. *Meteorological Applications*, *27*(5), 1–18. https://doi.org/10.1002/met.1950
Harrison, S., Kargel, J. S., Huggel, C., Reynolds, J., Shugar, D. H., Betts, R. A., et al. (2018). Climate change and the global pattern of moraine-dammed glacial lake outburst floods. *Cryosphere*, *12*(4), 1195–1209. https://doi.org/10.5194/tc-12-1195-2018
Hirabayashi, Y., Mahendran, R., Koirala, S., Konoshima, L., Yamazaki, D., Watanabe, S., et al. (2013). Global flood risk under climate change. *Nature Climate Change*, *3*(9), 816–821. https://doi.org/10.1038/nclimate1911
Hirabayashi, Yukiko, Tanoue, M., Sasaki, O., Zhou, X., & Yamazaki, D. (2021). Global exposure to flooding from the new CMIP6 climate model projections. *Scientific Reports*, *11*(1), 1–7. https://doi.org/10.1038/s41598-021-83279-w
Hock, R., Rasul, G., Adler, C., Cáceres, B., Gruber, S., Hirabayashi, Y., et al. (2019). Chapter 2: High Mountain Areas. IPCC Special Report on the Ocean and Cryosphere in a Changing Climate. *IPCC Special Report on the Ocean and Cryosphere in a Changing Climate*, 131–202.
Huss, M., & Hock, R. (2018). Global-scale hydrological response to future glacier mass loss. *Nature Climate Change*, 1. https://doi.org/10.1038/s41558-017-0049-x
ICIMOD. (2011). Glacial lakes and glacial lake outburst floods in Nepal. *Kathmandu: ICIMOD*.
Immerzeel, W. W., Pellicciotti, F., & Bierkens, M. F. P. (2013). Rising river flows throughout the twenty-first century in two Himalayan glacierized watersheds. *Nature Geoscience*, *6*(9), 742–745. https://doi.org/10.1038/ngeo1896
Immerzeel, W. W., Lutz, A. F., Andrade, M., Bahl, A., Biemans, H., Bolch, T., et al. (2020). Importance and vulnerability of the world's water towers. *Nature*, *577*(7790), 364–369. https://doi.org/10.1038/s41586-019-1822-y
Immerzeel, W.W., Droogers, P., de Jong, S. M., & Bierkens, M. F. P. (2009). Large-scale monitoring of snow cover and runoff simulation in Himalayan river basins using remote sensing. *Remote Sensing of Environment*, *113*(1), 40–49. https://doi.org/10.1016/j.rse.2008.08.010
Immerzeel, W W, Wanders, N., Lutz, A. F., Shea, J. M., & Bierkens, M. F. P. (2015). Reconciling high-altitude precipitation in the upper Indus basin with glacier mass balances and runoff. *Hydrology and Earth System Sciences*, *19*(11), 4673–4687. https://doi.org/10.5194/hess-19-4673-2015
Immerzeel, Walter W. (2010). Climate change will effect the asian water tower. *Science*, *1382*.

https://doi.org/10.1126/science.1183188
Immerzeel, Walter Willem, Pellicciotti, F., & Shrestha, A. B. (2012). Glaciers as a Proxy to Quantify the Spatial Distribution of Precipitation in the Hunza Basin. *Mountain Research and Development*, *32*(1), 30–38. https://doi.org/10.1659/MRD-JOURNAL-D-11-00097.1
IPCC. (2019a). *Special Report: The Ocean and Cryosphere in a Changing Climate*. https://doi.org/https://www.ipcc.ch/report/srocc/
IPCC. (2019b). Summary for Policymakers — Special Report on Climate Change and Land. Retrieved July 16, 2021, from https://www.ipcc.ch/srccl/chapter/summary-for-policymakers/
IUCN. (2019). International union for conservation of nature. *ANNUAL REPORT 2019*, 953–968. https://doi.org/10.1163/ej.9789004163300.i-1081.832
Joshi, N., & Dongol, R. (2018). Severity of climate induced drought and its impact on migration: a study of Ramechhap District, Nepal. *Tropical Agricultural Research*, *29*(2), 194. https://doi.org/10.4038/tar.v29i2.8289
Kaini, S., Nepal, S., Pradhananga, S., Gardner, T., & Sharma, A. K. (2020). Impacts of climate change on the flow of the transboundary Koshi River, with implications for local irrigation. *International Journal of Water Resources Development*, *00*(00), 1–26. https://doi.org/10.1080/07900627.2020.1826292
Karky, B. S., & Joshi, L. (2009). Payment for Environmental Services - an approach to enhancing water storage capacity. *Water Storage: A Strategy for Climate Change Adaptation in the Himalayas. Sustainable Mountain Development. ICIMOD*, *56*(56), 31–33.
Khanal, N. R., Mool, P. K., Shrestha, A. B., Rasul, G., Ghimire, P. K., Shrestha, R. B., & Joshi, S. P. (2015). A comprehensive approach and methods for glacial lake outburst flood risk assessment, with examples from Nepal and the transboundary area. *International Journal of Water Resources Development*. https://doi.org/10.1080/07900627.2014.994116
Khanal, S., Lutz, A. F., Kraaijenbrink, P. D. A., van den Hurk, B., Yao, T., & Immerzeel, W. W. (2021). Variable 21st Century Climate Change Response for Rivers in High Mountain Asia at Seasonal to Decadal Time Scales. *Water Resources Research*, *57*(5), e2020WR029266. https://doi.org/10.1029/2020wr029266
Khatiwada, K. R., & Pandey, V. P. (2019). Characterization of hydro-meteorological drought in Nepal Himalaya: A case of Karnali River Basin. *Weather and Climate Extremes*, *26*(November 2018), 100239. https://doi.org/10.1016/j.wace.2019.100239
Kirschbaum, D., Kapnick, S. B., Stanley, T., & Pascale, S. (2020). Changes in Extreme Precipitation and Landslides Over High Mountain Asia. *Geophysical Research Letters*, *47*(4), 1–9. https://doi.org/10.1029/2019GL085347
Koirala, R., Thapa, B., Neopane, H. P., Zhu, B., & Chhetry, B. (2016). Sediment erosion in guide vanes of Francis turbine: A case study of Kaligandaki Hydropower Plant, Nepal. *Wear*, *362–363*, 53–60. https://doi.org/10.1016/j.wear.2016.05.013
Kondolf, G. M., Gao, Y., Annandale, G. W., Morris, G. L., Jiang, E., Zhang, J., et al. (2014). Sustainable sediment management in reservoirs and regulated rivers: Experiences from five continents. *Earth's Future*, *2*(5), 256–280. https://doi.org/10.1002/2013ef000184
Kraaijenbrink, P. D. A., Bierkens, M. F. P., Lutz, A. F., & Immerzeel, W. W. (2017). Impact of a 1.5 °C global temperature rise on Asia's glaciers. *Nature*, *549*(7671), 257–260. https://doi.org/10.1038/nature23878
Lehner, B., & Grill, G. (2013). Global river hydrography and network routing: Baseline data and new approaches to study the world's large river systems. *Hydrological Processes*, *27*(15), 2171–2186. https://doi.org/10.1002/hyp.9740
Leonard, M., Westra, S., Phatak, A., Lambert, M., van den Hurk, B., Mcinnes, K., et al. (2014). A compound event framework for understanding extreme impacts. *Wiley Interdisciplinary Reviews: Climate Change*, *5*(1), 113–128. https://doi.org/10.1002/wcc.252
Lutz, A. F., Immerzeel, W. W., Shrestha, A. B., & Bierkens, M. F. P. (2014). Consistent increase in High Asia's runoff due to increasing glacier melt and precipitation. *Nature Climate Change*, *4*(7), 587–592. https://doi.org/10.1038/nclimate2237
Meechaiya, C., Wilkinson, E., Lovell, E., Brown, S., & Budimir, M. (2019). the Governance of Warning System Opportunities Under Federalism, 48.
Mishra, A. K., & Singh, V. P. (2010). A review of drought concepts. *Journal of Hydrology*, *391*(1–2), 202–216. https://doi.org/10.1016/j.jhydrol.2010.07.012
Miyan, M. A. (2015). Droughts in asian least developed countries: Vulnerability and sustainability. *Weather and Climate Extremes*, *7*, 8–23. https://doi.org/10.1016/j.wace.2014.06.003
NASA. (2015). *NEX-GDDP: Global Daily Downscaled Projections for Studies of Climate Change Impacts*.
NDRI. (2016). Adaptation to Climate Change in the Hydro-electricity Sector in Nepal Final Report, *2016*(December 2016).
NEA. (2019). Generation Directorate Fiscal year 2018/19, *2019*(August). Retrieved from https://nea.org.np/admin/assets/uploads/annual_publications/Generation_2076.pdf
NEA. (2020a). Generation Directorate Fiscal year 2019/20. *Nepal Electrcicity Authority*, (12), 14 to 42. Retrieved from https://www.nea.org.np/admin/assets/uploads/annual_publications/Generation_NEA_Final_book_2077.pdf

NEA. (2020b). *NEPAL ELECTRICITY AUTHORITY: A YEAR IN REVIEW-FISCAL YEAR-2019/2020*. Kathmandu, Nepal.
Nepal, S. (2016). Impacts of climate change on the hydrological regime of the Koshi river basin in the Himalayan region. *Journal of Hydro-Environment Research*, *10*(December 2015), 76–89. https://doi.org/10.1016/j.jher.2015.12.001
Nepal, S., Pradhananga, S., Kumar Shrestha, N., Kralisch, S., Shrestha, J. P., & Fink, M. (2021). Space-time variability in soil moisture droughts in the Himalayan region. *Hydrology and Earth System Sciences*, *25*(4), 1761–1783. https://doi.org/10.5194/hess-25-1761-2021
OECD. (2020). *Nature-based solutions for adapting to water-related climate risks*. *OECD Environment Policy Papers*.
Petley, D. N., Hearn, G. J., Hart, A., Rosser, N. J., Dunning, S. A., Oven, K., & Mitchell, W. A. (2007). Trends in landslide occurrence in Nepal. *Natural Hazards*, *43*(1), 23–44. https://doi.org/10.1007/s11069-006-9100-3
Pradhan, P. M. S. (2004). Improving Sediment Handling in the Himalayas. *OSH Research*, (October), 1–6.
Pritchard, H. D. (2019). Asia's shrinking glaciers protect large populations from drought stress. *Nature*, *569*(7758), 649–654. https://doi.org/10.1038/s41586-019-1240-1
Raut, R., & Gudmestad, O. T. (2017). *Use of bioengineering techniques to prevent landslides in Nepal for hydropower development*. *International Journal of Design and Nature and Ecodynamics* (Vol. 12). https://doi.org/10.2495/DNE-V12-N4-418-427
RGI Consortium. (2017). GLIMS: Global Land Ice Measurements from Space. https://doi.org/https://doi.org/10.7265/N5-RGI-60
Ridder, N. N., Pitman, A. J., Westra, S., Ukkola, A., Hong, X. Do, Bador, M., et al. (2020). Global hotspots for the occurrence of compound events. *Nature Communications*, *11*(1). https://doi.org/10.1038/s41467-020-19639-3
Rounce, D. R., Hock, R., & Shean, D. E. (2020). Glacier Mass Change in High Mountain Asia Through 2100 Using the Open-Source Python Glacier Evolution Model (PyGEM). *Frontiers in Earth Science*, *7*(January), 1–20. https://doi.org/10.3389/feart.2019.00331
Sangroula, D. (2007). Sediment Management for Sustainability of Storage Projects in Himalayas-A case study of the Kulekhani Reservoir in Nepal. *International Conference on Small Hydropower-Hydro*, (October), 22–24. Retrieved from http://ahec.org.in/links/International conference on SHP Kandy Srilanka All Details/Papers/Technical Aspects-A/A6.pdf
Sangroula, D. P. (2009). Hydropower Development and Its Sustainability With Respect to Sedimentation in Nepal. *Journal of the Institute of Engineering*, *7*(1), 56–64. https://doi.org/10.3126/jie.v7i1.2063
Scherer, L., & Pfister, S. (2016). Hydropower's biogenic carbon footprint. *PLoS ONE*, *11*(9). https://doi.org/10.1371/journal.pone.0161947
Sharma, S., Hamal, K., Khadka, N., Shrestha, D., Aryal, D., & Thakuri, S. (2021). Drought characteristics over Nepal Himalaya and their relationship with climatic indices. *Meteorological Applications*, *28*(2), 1–15. https://doi.org/10.1002/met.1988
Shean, D. E., Bhushan, S., Montesano, P., Rounce, D. R., Arendt, A., & Osmanoglu, B. (2020). A Systematic , Regional Assessment of High Mountain Asia Glacier Mass Balance, *7*(January), 1–19. https://doi.org/10.3389/feart.2019.00363
Shin, S., Pokhrel, Y., Talchabhadel, R., & Panthi, J. (2021). Spatio-temporal dynamics of hydrologic changes in the Himalayan river basins of Nepal using high-resolution hydrological-hydrodynamic modeling. *Journal of Hydrology*, *598*(January), 126209. https://doi.org/10.1016/j.jhydrol.2021.126209
Shrestha, A. B., Eriksson, M., Mool, P., Ghimire, P., Mishra, B., & Khanal, N. R. (2010). Glacial lake outburst flood risk assessment of Sun Koshi basin, Nepal. *Geomatics, Natural Hazards and Risk*, *1*(2), 157–169. https://doi.org/10.1080/19475701003668968
Shrestha, H. S. (2012). Application of Hydrosuction Sediment Removal System (HSRS) on Peaking Ponds. *Hydro Nepal: Journal of Water, Energy and Environment*, *11*, 43–48. https://doi.org/10.3126/hn.v11i0.7162
Shrestha, N. K., Qamer, F. M., Pedreros, D., Murthy, M. S. R., Wahid, S. M., & Shrestha, M. (2017). Evaluating the accuracy of Climate Hazard Group (CHG) satellite rainfall estimates for precipitation based drought monitoring in Koshi basin, Nepal. *Journal of Hydrology: Regional Studies*, *13*(September), 138–151. https://doi.org/10.1016/j.ejrh.2017.08.004
Shrestha, S., Khatiwada, M., Babel, M. S., & Parajuli, K. (2014). Impact of Climate Change on River Flow and Hydropower Production in Kulekhani Hydropower Project of Nepal. *Environmental Processes*, *1*(3), 231–250. https://doi.org/10.1007/s40710-014-0020-z
Shugar, D. H., Jacquemart, M., Shean, D., Bhushan, S., Upadhyay, K., Sattar, A., et al. (2021). A massive rock and ice avalanche caused the 2021 disaster at Chamoli, Indian Himalaya. *Science*, eabh4455. https://doi.org/10.1126/SCIENCE.ABH4455
Smith, S. J., Edmonds, J., Hartin, C. A., Mundra, A., & Calvin, K. (2015). Near-term acceleration in the rate of temperature change. *Nature Climate Change*, *5*(4), 333–336. https://doi.org/10.1038/nclimate2552
Stanley, T., & Kirschbaum, D. B. (2017). A heuristic approach to global landslide susceptibility mapping. *Natural Hazards*, *87*(1), 145–164. https://doi.org/10.1007/s11069-017-2757-y

Trenberth, K. E., Dai, A., Schrier, G. van der, Jones, P. D., Barichivich, J., Briffa, K. R., & Sheffield, J. (2013). Global warming and changes in drought. *Nature Climate Change 2014 4:1*, *4*(1), 17–22. https://doi.org/10.1038/nclimate2067
Trenberth, K. E., Fasullo, J. T., & Shepherd, T. G. (2015). Attribution of climate extreme events. *Nature Climate Change*, *5*(8), 725–730. https://doi.org/10.1038/nclimate2657
Viviroli, D., Weingartner, R., & Messerli, B. (2003). Assessing the Hydrological Significance of the World's Mountains. *Mountain Research and Development*, *23*(1), 32–40. https://doi.org/10.1659/0276-4741(2003)023[0032:ATHSOT]2.0.CO;2
Wang, S. Y., Yoon, J. H., Gillies, R. R., & Cho, C. (2013). What caused the winter drought in western nepal during recent years? *Journal of Climate*, *26*(21), 8241–8256. https://doi.org/10.1175/JCLI-D-12-00800.1
Watkiss, P., Wilby, R., & Rodgers, C. A. (2020). Principles of Climate Risk Management for Climate Proofing Projects. *Asian Development Bank, 2020*, *July*(No. 69), 50. Retrieved from https://www.adb.org/publications/climate-risk-management-climate-proofing-projects
WB and ADB. (2021). *Climate Risk Country Profile - Nepal*. Retrieved from www.worldbank.org
WECS. (2011). (Water and Energy Commission Secretariat). Water resources of Nepal in the context of climate change, 68. Retrieved from https://wwfeu.awsassets.panda.org/downloads/water_resources_of_nepal_final_press_design.pdf
WECS. (2019). Assessment of Hydropower Potential of Nepal, 134. Retrieved from http://www.wecs.gov.np/storage/listies/February2021/final-report-july-2019-on-hydropower-potential.pdf
WFP. (2009). *Crop and food security assessment: Joint assessment report*. *WFP*.
WHO. (2015). CLIMATE AND HEALTH COUNTRY PROFILE – 2015 NEPAL, 6.
Wijngaard, R.R., Lutz, A. F., Nepal, S., Khanal, S., Pradhananga, S., Shrestha, A. B., & Immerzeel, W. W. (2017). Future changes in hydro-climatic extremes in the Upper Indus, Ganges, and Brahmaputra River basins. *PLoS ONE*, *12*(12), 26. https://doi.org/10.1371/journal.pone.0190224
Wijngaard, René R, Lutz, A. F., Nepal, S., Khanal, S., Pradhananga, S., Shrestha, A. B., & Immerzeel, W. W. (2017). Future changes in hydro-climatic extremes in the Upper Indus, Ganges, and Brahmaputra River basins. *PloS One*, *12*(12), e0190224.
Wilhite, D. A. (2000). Drought As a Natural Hazard: Concepts and Definitions. *Droughts*, 33–33. https://doi.org/10.4324/9781315830896-24
World Bank. (2019). *Valuing Green Infrastructure*. *Valuing Green Infrastructure*. https://doi.org/10.1596/32757
Zaginaev, V., Ballesteros-Cánovas, J. A., Erokhin, S., Matov, E., Petrakov, D., & Stoffel, M. (2016). Reconstruction of glacial lake outburst floods in northern Tien Shan: Implications for hazard assessment. *Geomorphology*, *269*, 75–84. https://doi.org/10.1016/j.geomorph.2016.06.028
Zheng, G., Allen, S. K., Bao, A., Ballesteros-Cánovas, J. A., Huss, M., Zhang, G., et al. (2021). Increasing risk of glacial lake outburst floods from future Third Pole deglaciation. *Nature Climate Change*, *11*(5), 411–417. https://doi.org/10.1038/s41558-021-01028-3
Zscheischler, J., Martius, O., Westra, S., Bevacqua, E., Raymond, C., Horton, R. M., et al. (2020). A typology of compound weather and climate events. *Nature Reviews Earth & Environment*, (June), 1–15. https://doi.org/10.1038/s43017-020-0060-z

Appendix A: Detailed task and deliverables

1. Proactively liaise with the ADB project officer and environment specialists to obtain project information required.
2. Review the feasibility study and other background information to understand the design of the project.
3. Collate and review existing legislation, policies, and institutional arrangements in relation to climate change mitigation and adaptation in Nepal.
4. Calculate the carbon footprint of the project following ADB's Guidelines for Estimating GHG of ADB Projects but factoring in GHG emissions from this being a HEP with large storage reservoir with reference to IPCC Good Practice Guidance for LULUCF, 2003 Table 3A.3.5.
5. Collate and review existing information on current and future climate vulnerability at the scale of Nepal, the Koshi river basin and the Dudh Koshi river basin, as well as HEP and transmission line specific climate vulnerability including ADB's energy sector guidance.
6. Collate and review existing information to identify the existing climate and climate change projections for the project area, paying particular attention to changes in the hydrological/ glacial conditions.
7. Develop detailed scenarios of climate change variables for future time horizons pertinent to the project, including documentation of scenario methods, data sources, uncertainties, and caveats.
8. If there are any uncertainties, identify whether and how remaining gaps in the knowledge base could be easily filled.
9. Informed by tasks 5-8 and the current project design, undertake climate change risk assessment to identify the potential climate change impacts on the different project components and the technical, economic, social and environment implications for the design and operation of the project e.g., water availability for continued power generation, environmental flows, downstream flood risks, storms affecting transmission towers etc.
10. Initially the assessment is to use a simple methodological approach; but the expert will make recommendations for any detailed modelling of high-risk climate change impacts on relevant aspects of the project if it could benefit project design and operation.
11. Identify potential options for climate resilience measures to incorporate in the project design and operation to address the risks identified with an initial indication of their anticipated cost, and any technical, economic, social and environment implications.
12. Prepare a comprehensive draft and final draft climate change impact report on the above tasks and respond to any comments on the draft deliverables from ADB in producing the final draft version to be shared with NEA. This report is to include (i) introduction, (ii) methodologies, (iii) carbon footprint, (iv) climate change vulnerabilities of project components, (v) climate trends in the project area, (vi) climate change impacts, and (vii) climate resilience measures/next steps.
13. In case of any gaps or further assessment requirements identified these must be flagged early since window for its completion is July – December 2021 with clear guidance on scope of works to ensure no misunderstanding of exactly what is required to make the climate change reporting final. Finalization of the report will be separately contracted once ADB has discussed the findings of the final draft report with NEA and the scope of works has been agreed.
14. Share GIS map files produced in undertaking the above tasks with the ADB environment specialist for record purposes and for sharing with the project for use in their documentation